Fall 2016

Potential applications for halloysite nanotubes based drug delivery systems

Lin Sun

POTENTIAL APPLICATIONS FOR HALLOYSITE NANOTUBES

BASED DRUG DELIVERY SYSTEMS

by

Lin Sun, M.D.

A Dissertation Presented in Partial Fulfillment
of the Requirements of the Degree
Doctor of Philosophy

COLLEGE OF APPLIED AND NATURAL SCIENCES
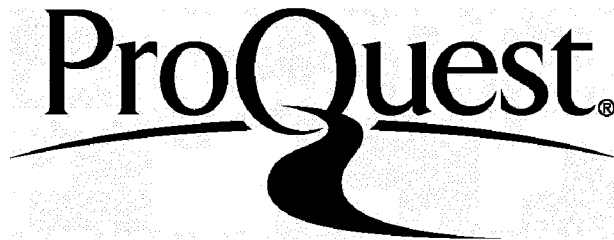LOUISIANA TECH UNIVERSITY

November 2016

ProQuest Number: 10307869

ProQuest 10307869

LOUISIANA TECH UNIVERSITY

THE GRADUATE SCHOOL

April 27, 2016
_____
Date

We hereby recommend that the dissertation prepared under our supervision by

Lin Sun, M.D.
_____

entitled   **Potential Applications for Halloysite Nanotubes**
_____

Based Drug Delivery Systems
_____

_____

be accepted in partial fulfillment of the requirements for the Degree of

Doctor of Philosophy in Molecular Sciences and Nanotechnology
_____

_____
Supervisor of Dissertation Research

_____
Head of Department

School of Biological Sciences
_____
Department

Recommendation concurred in:

Advisory Committee

Approved:

_____
Director of Graduate Studies

_____
Dean of the College

Approved:

_____
Dean of the Graduate School

ABSTRACT

Drug delivery refers to approaches, formulations, technologies, and systems for transporting a drug in the body. The purpose is to enhance the drug efficacy and to reduce side reactions, which can significantly improve treatment outcomes. Halloysite is a naturally occurred alumino-silicate clay with a tubular structure. It is a biocompatible material with a big surface area which can be used for attachment of targeted molecules. Besides, loaded molecules can present a sustained release manner in solution. These properties make halloysite nanotubes (HNTs) a good option for drug delivery.

In this study, a drug delivery system was built based on halloysite via three different fabrication methods: physical adsorption, vacuum loading and layer-by-layer coating. Methotrexate was used as the model drug. Factors that may affect performance in both drug loading and release were tested. Results showed that methotrexate could be incorporated within the HNTs system and released in a sustained manner. Layer-by-layer coating showed a better potential than the other two methods in both MTX loading and release. Besides, lower pH could greatly improve MTX loading and release while the increased number of polyelectrolytes bilayers had a limited impact.

Osteosarcoma is the most common primary bone malignancy in children and adolescents. Postoperative recurrence and metastasis has become one of the leading causes for patient death after surgical remove of the tumor mass. A strategy could be a sustained release of chemotherapeutics directly at the primary tumor sites where

recurrence would mostly occur. Then, this HNTs based system was tested with osteosarcoma cells *in vitro* to show the potential of delivering chemotherapeutics in the treatment of osteosarcoma. Methotrexate was incorporated within HNTs with a layer-by-layer coating technique, and drug coated HNTs were filled into nylon-6 which is a common material for surgical sutures in industry. Results showed that (1) methotrexate could be released in a sustained manner; (2) cytotoxicity test confirmed the biocompatibility of HNTs and methotrexate coated HNTs; (3) proliferation test confirmed the growth inhibition of released methotrexate on osteosarcoma cells; and (4) nylon-6 could prolong the sustained release of methotrexate from polyelectrolytes coated HNTs.

Another application comes from the prevention of surgical site infection. It is a common complication in surgery, which may prolong hospital stay, increase mortality rate, and cause additional financial burden for patients. By directly releasing antibiotics at the surgical site, it is supposed to enhance the drug efficacy and improve the treatment outcome. Therefore, the same HNTs based system was tested with *E. coli in vitro* to show the potential of delivering antibiotics to enhance the prevention of surgical site infection. Nitrofurantoin was incorporated within HNTs using the layer-by-layer coating technique, and the drug coated HNTs were filled into nylon-6 again. Results showed that (1) nitrofurantoin could be incorporated with this HNTs based drug delivery system, and released in a sustained manner; (2) nylon-6 could prolong the sustained release of nitrofurantoin from polyelectrolytes coated HNTs; and (3) released nitrofurantoin could severely inhibit *E. coli* growth.

Therefore, a tunable drug delivery system based on HNTs was developed, and a great potential of medical application in drug delivery was shown.

APPROVAL FOR SCHOLARLY DISSEMINATION

The author grants to the Prescott Memorial Library of Louisiana Tech University

the right to reproduce, by appropriate methods, upon request, any or all portions of this

Dissertation. It is understood that "proper request" consists of the agreement, on the part

of the requesting party, that said reproduction is for his personal use and that subsequent

reproduction will not occur without written approval of the author of this Dissertation.

Further, any portions of the Dissertation used in books, papers, and other works must be

appropriately referenced to this Dissertation.

Finally, the author of this Dissertation reserves the right to publish freely, in the

literature, at any time, any or all portions of this Dissertation.

Author _____Lin Sun_____

Date _____8/1/2016_____

DEDICATION

To my mother, Yinghui Liu, and father, Qingbo Sun. I appreciate their support and encouragement all the time. No matter what happens, we were, are and will be together.

TABLE OF CONTENTS

LIST OF TABLES

LIST OF FIGURES

ACKNOWLEDGMENTS

CHAPTER 1

INTRODUCTION

1.1   Objective

This dissertation introduces a newly formed drug delivery system based on

halloysite nanotubes (HNTs). By applying several fabrication methods, biologically

functional molecules (such as DNA, RNA, proteins, and drugs) could be loaded within

this nano-vehicle, and released in a sustained/controlled manner at the sites of action.

Subsequently, these released molecules could act on the surrounding tissues or cells. In

this way, biomolecules can be directly delivered to their action sites, which would

increase their efficacy and safety, and avoid potential side reactions as well.

1.2   Background

1.2.1   Nanotechnology

In the 21st Century, nanotechnology has become one of the leading elements

advancing technology, and nanotech-based products have impacted almost everything we

touch in life, such as medicines, chemicals, biologics, and pharmaceuticals [1]. In

particular, the breakthroughs of nano-engineering made in the field of drug delivery and

formulation development have contributed significantly to the growth of

nanopharmaceuticals [2]. Because of the inherent potential of nanopharmaceutical

products to overcome solubility and stability issues, localized drug delivery, enhanced

drug efficacy, the need to avoid unwanted side reactions, and assistance in diagnosis via *in vivo* imaging, increased research efforts have been focused on the specific fields of drug delivery and formulation.

1.2.2 Drug Delivery

During the past few years, an increased number of researchers have realized the importance of effective drug delivery, which is a fundamental part of drug development. Many drug delivery systems have been developed and have entered the market, such as liposomes and nanoparticles. Theoretically speaking, an ideal drug delivery system should improve the stability, absorption, and therapeutic concentration of the drug within the target environment, as well as the long-term release of the drug at the target site. Additionally, it should help reduce the frequency of drug administration and improve patient comfort [1].

1.2.3 Market Need

In the pharmaceutical industry, the field of drug delivery offers a new direction for expanding drug markets, because newly developed nanotechnology could assist in making current drugs more efficacious and improve their competition against other counterparts. In 2012, it was estimated that about 13% of the global pharmaceutical market was related to the sale of products based on a drug delivery system [3].

1.3 Specific Aims

In this dissertation, a halloysite-based drug delivery system was developed with different fabrication methods. Factors that could affect the loading and releasing process were tested to obtain more control over the newly formed nano-vehicle. Three fabrication methods were compared in the performance of both loading and release results. The best

method was used in subsequent experiments. Two individual *in vitro* tests were used to verify the potential of using an HNT based system for drug delivery. Methotrexate (MTX) and nitrofurantoin (NFT) were used as model drugs, and osteosarcoma cells and *Escherichia coli* (*E. coli*) were used for tested targets to individually show the feasibility in the treatment of osteosarcoma and surgical site infection.

1.4   Projects and Hypotheses

1.4.1   Project 1

Three fabrication methods were used to dope methotrexate with HNTs. By comparing the loading and release results, we may be able to identify the impact of loading and release processes, such as the pH, temperature, concentration, spatial structure, polyelectrolytes, etc. In this way, information on the loading and release processes with the HNTs based drug delivery system may be used to improve the delivery system.

1.4.2   Project 2

In the first *in vitro* test, osteosarcoma cells were used as the disease model, because metastasis and recurrence are still the most common causes leading to patient death after surgical remove of the primary tumor mass. MTX is a commonly used drug in the treatment of osteosarcoma and was used as the model drug for delivery. MTX was supposed to be loaded within the HNTs based drug delivery system, and could be released subsequently in a sustained manner. Besides, released MTX could keep its biological function intact during the whole process, and act on the osteosarcoma cells. In this way, the HNTs based drug delivery system showed a potential to deliver

chemotherapeutics to target sites of the tumor to prevent postoperative metastasis and/or recurrence.

1.4.3 Project 3

In the second *in vitro* test, surgical site infection was the targeted disease model, as it is a common complication in surgery. It causes unnecessary direct health problems and indirect social cost to patients, and increases the financial burden on society. Nitrofurantoin was selected as the model drug, and *E. coli* was used as the target pathogen. NFT was supposed to be loaded within the HNTs based drug delivery system, and could be released in a sustained manner in bacterial broth with its biological function intact. Then, it could subsequently act on the bacteria and inhibit its growth. The same result should be achieved when NFT coated HNTs were filled within nylon-6 which is a routine material for sutures. In this way, antibiotics could be delivered to the surgical site and be released locally to prevent the potential infection.

1.5   Exclusions

In this dissertation, all of the work was focused on passive drug delivery. Active drug delivery is more complicated and would become the next step if results from preliminary experiment are satisfied.

1.6   Outline of Dissertation

Chapter 1 introduces the objective and general background for this dissertation. It also describes the specific projects and associated hypotheses which will be discussed in subsequent chapters, and presents the organization of this dissertation.

Chapter 2 gives a brief literature review concerning the main concepts and technologies related to this dissertation: nanotechnology, drug delivery, halloysite nanotubes, layer-by-layer technique, osteosarcoma, and surgical site infection.

Chapter 3 describes the methods and instruments used in the experiment.

Chapter 4 introduces current fabrication methods which can be applied to prepare the HNTs based drug delivery system. By comparing the loading and release results, factors which may affect the loading and release process were discussed, such as pH, concentration, spatial structure, and polyelectrolytes. Besides, advantages and limitations were compared among the studied fabrication methods, and the appropriate method could be selected for subsequent projects.

Chapter 5 presents the application of using HNTs based drug delivery system to deliver MTX to osteosarcoma cells *in vitro* showing its potential in the treatment of postoperative recurrence.

Chapter 6 describes the application of using HNTs based drug delivery system to deliver NFT to *E. coli in vitro* showing its potential to prevent postoperative surgical site infection.

Chapter 7 concludes the results of the dissertation, and recommends direction for future study.

CHAPTER 2

LITERATURE REVIEW

2.1 Nanomedicine

2.1.1 Nanotechnology and Medicine

The emerging trends and development of nanotechnology have been attracting more and more attention, especially in medical fields. A specific term called nanomedicine is used to describe the application of nanotechnology in medicine. There have been many promising applications of nanomedicine including, but not limited to, drug delivery, *in vitro* diagnosis, *in vivo* imaging, therapy techniques, biomaterials, and tissue engineering, which are summarized in **Table 2-1** [4]. Some of them have been realized and their products have entered the marketplace, while others are still under active research. Experts estimated that the global market of nanotechnology-based products in medical fields would grow to $ 70-160 billion by 2015 [5-6].

Table 2-1: Nanoscale application in medicine [4].

Submedical Field	Application
Drug Delivery	Nanotechnology based drug delivery systems can (1) enhance the therapeutic efficacy and minimize adversities associated with available drugs; (2) enable new classes of therapeutics; and (3) encourage the re-investigation of pharmaceutically suboptimal but biologically active new molecular entities that were previously considered undeveloped.

In Vitro Diagnostics	Nanoscale sensors (e.g., nanowires, nanotubes, nanoparticles, cantilevers, and micro/nanoarrays) can enable fast and high throughput detection of disease biomarkers with higher sensitivity and lower sample consumption. Nanotechnology also offers hope for the early detection of viruses, bacteria, and circulating tumor cells, as well as for single cell analysis.
In Vivo Imaging	Targeted imaging nanoprobes (e.g., magnetic nanoparticles, quantum dots, and carbon nanotubes) could provide a faster, less invasive, and more accurate way to diagnose diseases (e.g., cancer) at their earliest stages and monitor disease progression. Some other possible opportunities include reporting *in vivo* efficacy of therapeutics and tracking nanocarrier biodistribution in the body. In addition, imaging nanoprobes could help surgeons to locate tumors and their margins, identify important adjacent structures, and map sentinel lymph nodes.
Therapy Techniques	Certain nanomaterials have unique therapeutic properties that differ from conventional drugs, and can, therefore, be directly used to treat diseases. For example, hafnium oxide- and gold-based nanoparticles can greatly enhance X-ray therapy; gold nanoshells/nanorods carbon nanotubes, magnetic nanoparticles can induce hypothermia to kill cancer cells; and nanocrystalline silver is being used as an antimicrobial agent.
Biomaterials	Biocompatible nanomaterials that have optimal mechanical properties can be used as medical implants, such as dental restoratives and bone substitutes (also categorized as hard-tissue engineering.). Nanocoatings or nanostructured surfaces can also improve the biocompatibility and adhesion of biomaterials.
Tissue Engineering	Nanotechnology can enable the design and fabrication of biocompatible scaffolds at the nanoscale and control the spatiotemporal release of biological factors, resembling native extracellular matrix, to direct cell behaviors, and eventually lead to the creation of implantable tissues.

2.1.2   Nanotechnology and Drug Development

Drug discovery and development is one of the many fields in medicine that benefit from nanotechnology. In the pharmaceutical industry, an ideal candidate of new

molecular entity (NME) for potential drug development should demonstrate potent

biological activity, appropriate water solubility, and enough circulating half-life.

Actually, some NMEs have adequate bioactivity but show poor water solubility or short

half-life period in circulation, while others have good solubility and half-life period but

weak biological function. In either case, there is always a degree of compromise, and the

drug developmental potential is less ideal than expected. Fortunately, breakthroughs in

nanotechnology make it possible to address some of these shortcomings associated with

potential NMEs. For example, nanotechnology can significantly improve the

pharmacological properties (like water solubility and circulating half-life in blood) of

such NMEs, leading to the discovery of optimally safe and effective drug candidates [4].

In this way, nanotechnology could revolutionize the rules and possibilities of developing

new drugs. In fact, many current nanotechnology-based therapeutic products have been

validated through the improvement of previously approved drugs, and some novel classes

of nano-therapeutics are now underway [7-9].

2.2   Drug Delivery

2.2.1   Nanomaterials for Drug Delivery

Nowadays, more and more papers are published every day about drug delivery

based on nanomaterials that show an increasing attention to the research of

nanomaterials. Obviously, nanomaterials offer many advantages (**Table 2-2**) as drug

delivery vehicles. Drug particles are expected to go through a long route inside the

human body to reach scheduled sites and act on targeted tissues and cells. However, there

are some physiological hindrances that may greatly decrease the drug efficacy and create

the need for using nanomaterials to assist in the delivery of scheduled drugs. Therefore,

first, nanoparticles must have suitable dimensions that allow them to smoothly pass tiny

capillaries with 5-6 microns in diameter. A range of 10-100 nm is required for particles to

proceed through systemic circulation [5]. Then access to various sites inside the body is

available. Secondly, nanoparticles are more easily consumed by cells via internalization

than larger micromolecules, which can help increase drug efficacy. The integrated drug

could be released from the nanoparticles and act more efficiently inside the cytoplasm.

Thirdly, nanoparticles have the potential to be used for targeted drug delivery at the

specific disease area, improving drug efficiency. Fourthly, the controlled release of drugs

from nanoparticles can help lessen undesired side reactions. Therefore, nanomaterials

hold great potential for the improvement of the overall therapeutic index, offering another

option for drug delivery.

Table 2-2: Advantages of nanomaterials in drug delivery.

	Advantages
(1)	Ability to pass through narrow capillaries and accessibility of remote areas
(2)	Easily consumed
(3)	Delivery at specific diseased area via active or passive targeting
(4)	Controlled release

In fact, there has been a long history of applying nanotechnology in drug delivery.

Since liposomes were first introduced as carriers for drugs and proteins in 1960 [6],

nanotechnology has entered the field of nanomedicine, and there have been many

nanotech-based products approved by the FDA or still in clinical trials (**Figure 2-1**) [7-9].
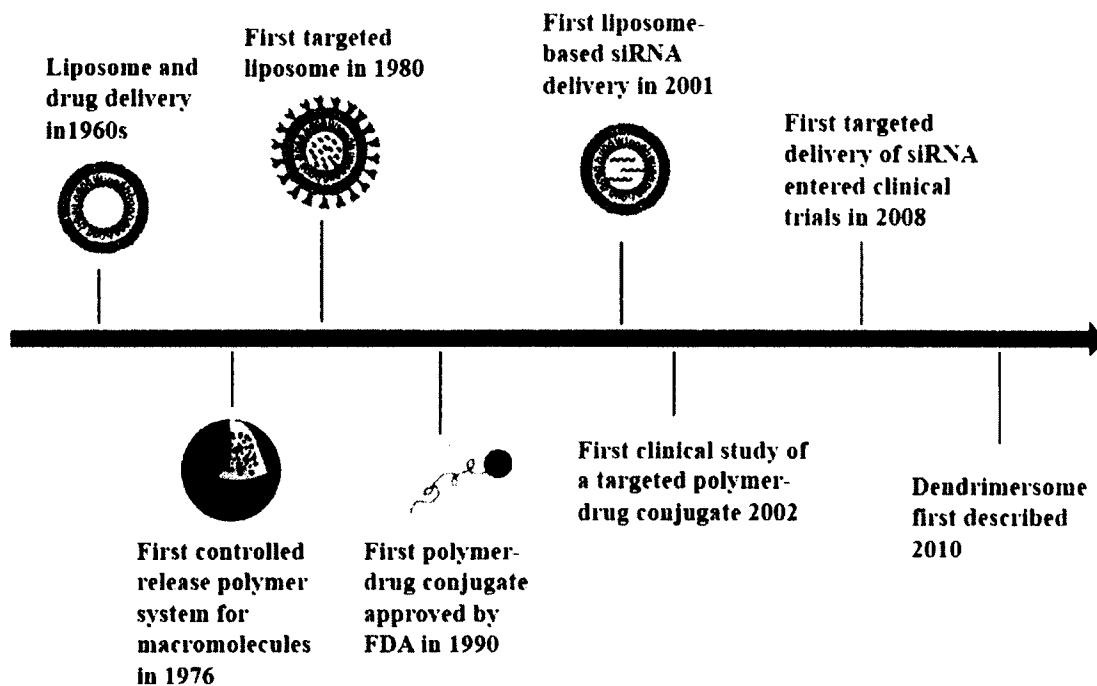
Figure 2-1: Timeline of nanotechnology-based drug delivery systems. Here, we highlight some delivery systems that serve as important milestones throughout the history of drug delivery. Adapted from "Nanotechnology in Drug Delivery and Tissue Engineering: From Discovery to Applications" by Jinjun Shi, et al, 2010, Nano Letters, 10(9), p. 3223-3230.

The main purposes of using nanotechnology in drug delivery applications are (1) to improve the delivery of water insoluble drugs [7]; (2) to deliver large macromolecule drugs into intracellular sites of action; (3) to co-deliver two or more drugs or therapeutic agents for combination treatment; (4) to transport drugs across tight epithelial and endothelial barriers [8]; (5) targeted delivery of drugs in a cell- or tissue-specific manner; (6) real-time read on the *in vivo* efficacy of a therapeutic agent, and (7) visualization of sites of drug delivery by combining therapeutic agents with imaging probes [9].

2.2.2   Classification of Drug Delivery

According to the mechanism of how the drugs are delivered to action sites, drug delivery can be classified as two types: passive and active delivery (Table 2-3).

Table 2-3: Drug delivery: passive targeting versus active targeting [10].

	Passive Targeting	Active Targeting
(1)	Utilizes special deviated conditions prevailing in the diseased area	Depends on targeting ligands and corresponding biomarkers that are overexpressed in diseased cells or tissues
(2)	Less selective	Highly selective
(3)	Restricted in use	Very versatile
(4)	More likely to produce side effects	Less likely to induce side effects

Passive delivery facilitates the deposition of nanoparticles incorporated with drugs in their action sites by taking advantage of certain biophysical properties. The most common examples are direct drug injection and catheterization. Spontaneous drug accumulation in a diseased area with leaky vasculature is another form of passive delivery. This approach is based on the preparation of a drug carrier complex that can avoid removal through the body mechanisms (like metabolism, excretion, opsonisation, and phagocytosis) and stay in the blood circulation allowing its transmission to targeted disease areas. An important application of this mechanism is the delivery of chemotherapeutics in the treatment of cancer, where a special phenomenon called enhanced permeability and retention (EPR) could be well utilized. In oncology, there are some unique structural features shared by many solid tumors, including hypervasculature, defective vascular architecture, and impaired lymphatic drainage leading to the well-characterized EPR effect [10]. These distinctive characteristics are inherent to the tumor milieu, but are not normally present in healthy tissues [11]. Besides, properties of the nanoparticles which include molecular size, shape, and surface charge could also affect the delivery. [11]. For example, previous studies have confirmed that macromolecules

with a molecular weight higher than the renal threshold (40 kDa) tend to accumulate preferentially in neoplastic tissues upon intravenous administration [17-18]. The normal vasculature endowed with tight junctions is impermeable to molecules sized over 2-4 nm, and can keep the nanoparticles within the circulation; however, the leaky vasculature of neoplastic tissue allows macromolecules with a diameter under 600 nm to extravasate into the neoplastic tissues [12]. Additionally, most tumors only have a poorly-developed lymphatic system, which would help these extravasated nanoparticles stagnate within the neoplastic tissue [20-21]. Another example comes from the surface property. Nanoparticles coated with polyethylene glycol (PEG) and sized between 200 nm and 500 nm could slip through a barrier of human mucus lining organs such as lungs, gastrointestinal tract, and cervicovaginal tract [5]. In this way, it is possible to deliver chemotherapeutics to tumors within the aforementioned organs.

Different from the passive approach, active delivery uses targeting ligands that can interact with some degree of exclusivity with specific biomarkers overexpressed on targeted cells or tissues. These common ligands include sugars, folic acid, peptides, and explicitly engineered antibodies [5]. They are connected with the drug loaded nanoparticles and direct them to targets in the body such as receptors, lipids, antigens, and proteins. For example, in Miao's study [13], functionalizing hydroxypropyl-b-cyclodextrin copolymer nanoparticles were developed for targeting delivery of paclitaxel to integrin $\alpha_v\beta_3$-rich tumor cells. In another study, Tomoki Sugiyama *et al* [14] used VEGFR (vascular endothelial growth factor receptor)-1-targeted peptide APRPG and integrin $\alpha_v\beta_3$-targeted peptide GRGDS to decorate liposomes synergistically and tested them on proliferative HUVECs (human umbilical vein endothelial cells). Results showed

that these dual-targeting liposomes could highly accumulate in tumor tissues of tumor-bearing mice, and intratumoral distribution study indicated that they could also localize on angiogenic vessels as well as distribute around these vessels. Although more complicated than the passive approach, active delivery offers the widest opportunities and alternatives.

2.2.3   Current Status and Challenges

Ideally, a drug administered should reach the diseased site in the human body without affecting the healthy tissues and organs *en route*. After reaching the target, it can release the ingredients at the scheduled time in the appropriate dosage to heal. Further, after the diseased part is cured, the remnant drug could be expelled from the body to avoid any side effects. Especially in the treatment of cancer, drugs with high efficacy and little side effect are always the first-line option. Additional delivery vehicles are developed to help achieve that ideal goal. For example, some common nanosystems include liposomes [24-26], polymeric micelles [27-30], polymer-drug conjugates [15], and dendrimers [16]. There are also some newer types developed or still under research, which include nanocages, nanogels, nanofibers, nanoshells, nanorods, and nanocontainers [5].

However, there is still a long way to go from the current nanoproducts to the ideally expected one. The translation of active delivery from laboratory to clinical application is not as smooth as people expect. One possible reason is the complicated manufacturing process, which includes biomaterial assembly, ligand coupling/insertion, and purification [4]. Another one is targeting ligands. Besides, there are some other considerable variables, such as ligand biocompatibility, cell specificity, binding affinity,

mass production, purity, ligand surface density and arrangement, spacer type and length

dividing ligand molecules and nanoparticles [33-34]. In fact, of the current

nanotechnology-based drug delivery systems that are in the market or still under clinical

trials, the majority are passive delivery. Obviously, compared to the active approach, it is

relatively simple and the requirement is not that harsh. The drug loaded nanosystems

would accumulate at the diseased area by utilizing unique characteristics inherent to the

disease. Therefore, a thorough understanding of biological features is necessary for

designing and preparing drug loaded nanosystems.

In this dissertation, an HNT based drug delivery nanosystem was built using the

passive approach. The specific expected result of using this tool was based on some

characteristics of biological environment inherent to the disease. In other words, the

biological characteristics of the diseased area were utilized to enhance the efficacy as

well as to reduce side effects of the scheduled drugs, leading to improvement of the

overall therapeutic result.

2.3 Halloysite Nanotubes

2.3.1 General Information and Structure

Halloysite nanotubes (HNTs) are naturally occurred alumino-silicate clay, and can

be mined from natural deposits in many countries like America, Brazil, China, France,

South Korea and Turkey [17]. They have a chemically similar composition as kaolinite

$Al_2Si_2O_5(OH) \cdot 4nH_2O$ but with a difference being they have a hollow tubular structure.

HNTs are formed by multiple bilayers of silicon dioxide and aluminum oxide. Most

commercially available HNTs share a typical three-dimension structure: the inner

diameter is between 10 and 20 nm, the external diameter ranges from 50 to 100 nm, and

the length of these tubes varies from 500 to 2000 nm [18]. Their wall is composed of 10 to 15 bilayers of aluminum and silicon oxide [18]. These structural features render halloysite a potential for drug delivery.

2.3.2   Current Application

Recently, halloysite nanotubes have attracted more and more researchers' attention, and many papers have been published to report their achievements. In Ravindra's review paper [19], some advantages of applying halloysite nanotubes were pointed out, such as (1) natural, nontoxic, biocompatible; (2) fine particle size, high surface area and superb dispersion; (3) high cation exchange capacity; (4) maintains uniform, sustained release rates and no initial overdose; (5) capable of prohibiting release unless triggered and tunable release rates; (6) protects active agent within its lumen during harsh material processing; (7) capable of loading multiple active agents simultaneously; (8) reduces the volume of costly active agents; (9) implementable in many forms such as powders, creams, gels, lotions and sprays; (10) high aspect ratio, high porosity and non-swelling; (11) superior loading rates to other carriers, fast adsorption rate and high adsorption capacity; (12) regeneration ability and increased efficacy. Because of these versatile properties, HNTs can be used in many biological and non-biological applications. In another paper, Rawtani and Agrawal [20] introduced multifarious applications of halloysite nanotubes, like corrosion prevention, thermal resistance, fillers for various nanocomposites, cellular response, polymerization reactions, drug delivery, immobilization matrixes, and remediation.

In this dissertation, we will explore the potential of HNTs in the field of drug delivery.

2.4   Layer-by-Layer Assembly

2.4.1   Definition and Developmental History

Layer-by-layer (LbL) assembly is defined as the use of oppositely charged

materials with wash steps on a charged surface to build controlled architecture of a

multilayer polymer film (**Figure 2-2**).
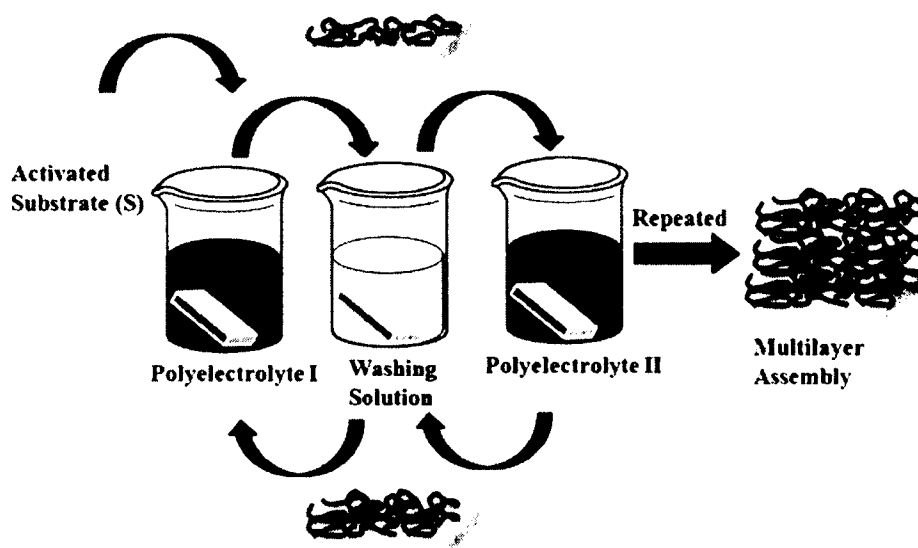
Figure 2-2: An example of layer-by-layer process through immersion.

This can be accomplished by using many techniques such as immersion. spin,

spray, electromagnetism, or fluidics as reviewed by Richardson *et al* [21]. The first

implementation of this technique is attributed to Kirkland and Iler, who carried it out

using microparticles in 1966 [22]. Later this method was revitalized by Gero Decher

because of the discovery of its applicability to a wide range of polyelectrolytes (PEs)

[23].

2.4.2   Mechanism

By definition, one may believe LbL multilayer build-up results solely from electrostatic attraction. Actually, many other attractive forces are also involved cooperatively; this is typical for high-molecular weight building blocks, while electrostatic repulsion provides self-limitation of the absorption of individual layers. This involvement and interactions of multiple forces make it possible to extend the LbL technique to similarly charged polymers, hydrogen-bonded films [24], nanoparticles [25], hydrophobic solvents [26], and other unusual systems [27]. With improvement in techniques, the deposition and wash steps can be performed in many different ways including dip coating, spin-coating, spray-coating, flow based and electro-magnetic techniques [21].The methods used to prepare the multilayer can distinctly impact the properties of the products and allow their applications in various fields.

2.4.3   Advantages and Applications

The LbL technique offers several advantages over other thin film deposition methods, such as (1) the process is simple and can be inexpensive; (2) a wide range of materials like polyions, metals, ceramics, nanoparticles, and biological molecules can be applied in LbL; (3) a high degree of control over the structure and thickness of the multilayer films; (4) a resolution of 1 nm by the fact that each bilayer can be as thin as 1 nm. Because of these properties, LbL has been used in many applications [21] including corrosion control, biomedical applications [28], ultrastrong materials [29], and many more [30].

2.5   Osteosarcoma

2.5.1   Epidemiology

It is estimated by the American Cancer Society that there are about 800 new cases of osteosarcoma every year in the United States. However, osteosarcoma is the most common primary malignancy of bone in children and adolescents [31]. It usually occurs in the metaphysis of long bones like the distal femur, proximal tibia, and proximal humerus during the second decade of life. Another small peak lies in between 60 to 80 years [32]. Overall, it has a moderate incidence rate, with 10 to 26 new cases per million worldwide each year [33].

2.5.2   Treatment and Prognosis

Since first being introduced by Boyer in 1805 [34], osteosarcoma has been recognized for more than 200 years. However, the progress in prevention, diagnosis, and treatment of this tumor is still very limited. It is pointed out by the American Cancer Society that there is no way to protect against osteosarcoma, and there are no special tests to find this tumor in people without symptoms or strong risk factors. The best way is to come to a doctor when any symptom of this disease is noticed. What's worse, pulmonary micrometastasis could occur in at least 80% of patients at diagnosis [35]. These metastases could not be found through conventional image tests. They can continue their growth and spread 8 to 12 months after the surgical removal of the primary tumor mass, and become the main cause of patients' death within 12 to 24 months of their appearance [35]. The current standard treatment options include surgery, chemotherapy, and radiation. Surgical intervention can remove all the detectable tumor mass, while chemotherapeutics can kill the invisible micrometastasis around the whole body.

Radiation is applied when patients cannot bear the severe side reactions of the surgery and chemotherapeutics. In most cases, an effective treatment result requires the combination of both surgery and chemotherapeutics.

2.5.3 Current Challenge and Novel Approaches

The 5-year survival rate in osteosarcoma in the first half of the 20th century was less than 20% [36].These patients were treated mainly with limb amputation and most of them died of lung metastasis [37]. In the 1970s, the application of multi-chemotherapeutics, together with the gradually improved surgical techniques, helped to improve the 5-year survival rate to around 60% in localized osteosarcoma (**Figure 2-3**) [31].
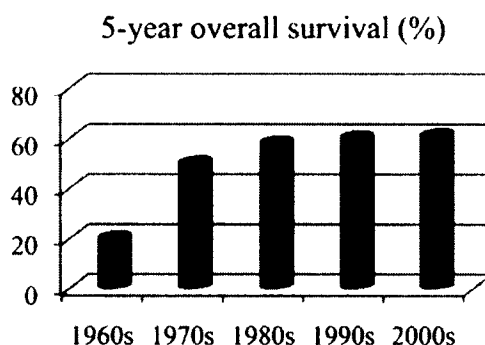
Figure 2-3: Five-year overall survival of localized osteosarcoma [31].

By contrast, the long-term survival of patients with metastatic osteosarcoma still remains at 25-30% [56-58]. The main chemotherapeutic agents used for metastatic osteosarcoma have not changed much during the past decades [38]. Therefore, new chemotherapeutic agents, technologies, and strategies are urgently needed to improve the outcome of treatment for patients with osteosarcoma.

2.6   Surgical Site Infection

2.6.1   Epidemiology

Surgical site infection (SSI) is a common healthcare-associated infection (HCAI), which is estimated to account for 16% of the total HCAI [39]. In the United States, approximately five million cases of SSI occur every year, leading to an average of 7.3 extra days in the hospital, and over 1.6 billion dollars of additional hospital charges [40]. Some studies showed that around 5% of all surgical operations were carried out with complications of infection in hospitals in developed countries [41]. The situation in developing countries is significantly worse, and some studies pointed out that the infection rate may be twenty times higher than that in developed countries [42]. In a word, SSI has become a serious cause of morbidity, emotional stress, and financial cost to the affected patients and health care institutions [43].

2.6.2   Prevention

A good understanding of the SSI can be of great assistance while a full clinical assessment is required to identify risk factors followed by measures to modify these factors. The Department of Health (2007) and NICE (2013) recommend some measures [39] as follows:

1) Patients should stop smoking at least four weeks before surgery.

2) Pre-operative showering to reduce bacterial load on the skin

3) Antibiotic prophylaxis

4) Hair removal when required

5) Blood glucose should be controlled below 11 mmol/L

6) Body temperature should be maintained above 36 °C within the perioperative period to prevent vasoconstriction

7) Skin and hands preparation of those present in the operating room

8) SSI surveillance should be completed.

In daily routine, the application of antibiotics is an indispensable part of the treatment of SSI. Efficient agents with fewer side reactions are always needed. Compared to conventional treatment, new nanotechnology-based drug delivery systems may offer some other options to patients and physicians.

2.7   Surgical Sutures

Sutures are routinely used in surgeries for the fixation of tissue. Since they are in direct contact with the wound, they have excellent potential to be used for local delivery of active molecules or cells to improve wound healing. In one recent study, adipose-derived stem cells were filled into surgical sutures to secrete cytokines and promote wound healing [44]. In another paper, an anti-infective coating of surgical sutures were developed with a combination of antiseptics and fatty acids [45]. An *in vitro* study was carried out and the result showed that a sustained release was observed, and *Staphylococcus aureus* could be efficiently killed. However, there are limited papers about using sutures as a carrier to deliver active molecules and cells to target sites. Plenty of room is left for research regarding effective use of sutures for drug delivery.

CHAPTER 3

METHODS AND INSTRUMENTATION FOR EXPERIMENTATION AND ANALYSIS

3.1   Benchtop Vacuum Pump

Vacuum loading, as one method to be tested, was used to load drug molecules into halloysite nanotubes. **Figure 3-1** shows the equipment required for the drug loading process. The drug solution was made at controlled concentration. Then halloysite powder was added into the solution, followed by full vortex to mix the suspension completely. After that, the suspension was placed under vacuum (-25 in Hg) for 30 minutes. Air bubbles were observed, which may suggest the solution with drug molecules was replenished inside the nanotubes. When no air bubbles come out, the process was stopped and the suspension was stirred completely. Then the vacuum loading was restarted. This process was repeated three times. The final suspension was centrifuged, and the supernatant was collected for absorbance measurement, by which the amount of loaded drug could be calculated indirectly. The sediment was air-dried at room temperature, and crushed into fine powder for later use.

Figure 3-1: Vacuum pump and jar for vacuum loading process.

3.2   Ultraviolet Visible Spectroscopy

Ultraviolet visible spectroscopy was used to measure the absorbance of sample solution that contains target drug molecules. **Figure 3-2** shows the Nanodrop 2000c that was used in the absorbance measurement. A standard calibration curve should be built first through measuring several absorbance values of target solutions with known concentrations. Then a linear relationship could be built between the absorbance value and concentration of drug solution. By comparison with the standard curve, the concentration of the test solution can be calculated. This method was used in the release studies where the released methotrexate and nitrofurantoin from the HNTs based drug delivery system could be calculated.
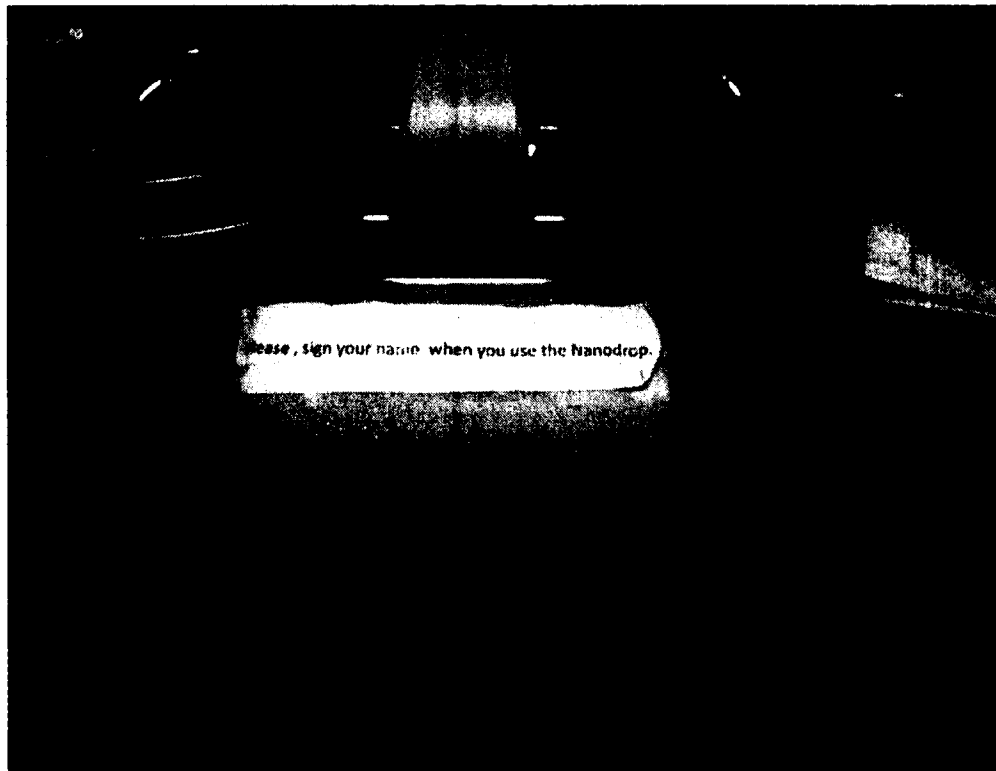
Figure 3-2: Nanodrop 2000c was used for UV-Vis absorbance measurement.

3.3 Scanning Electron Microscope

Figure 3-3 shows the scanning electron microscope (SEM) Hitachi S-4800 used

in this project. It uses an electron beam to collect sample information and form images.

The electron beam is produced from an electron gun at the top of the microscope. It

passes through the electromagnetic fields and lenses to focus on the sample. Once the

sample receives the beam, it will emit X-rays and electrons that are collected by detectors

as signals. These signals are then used to form images on the monitor screen. In this

dissertation, the SEM was used to examine morphology of halloysite nanotubes and

halloysite/drug composites.

Figure 3-3: Scanning electron microscope was used to image visual changes of halloysite particles.

3.4   Inverted System Microscope

Figure 3-4 shows the inverted microscope system of Olympus IX51 that was designed for practical convenience and cost-effective performance for live cell study, *in vitro* fertilization and other cellular injection applications. In this dissertation, a live/dead kit was used to test the cytotoxicity of halloysite-based composites to osteosarcoma cells. The Olympus IX51 was used to record the cellular response on the exposure of test nanoparticles.

Figure 3-4: Inverted system microscope (OLYMPUS IX51).

3.5   Microplate Reader LT-4000

Microplate readers are widely used in research, drug discovery, bioassay

validation, quality control and manufacturing processes in the pharmaceutical and

biotechnological industries and in academic organizations. In this dissertation, a kit called

"CellTiter 96 Aqueous One Solution Reagent" (Invitrogen, Carlsbad, CA) was used to

test the response of osteosarcoma cells to the released methotrexate from the HNTs based

drug delivery system. **Figure 3-5** shows the microplate reader LT-4000 (Phenix Systems,

La Jolla, CA) used to read the results.
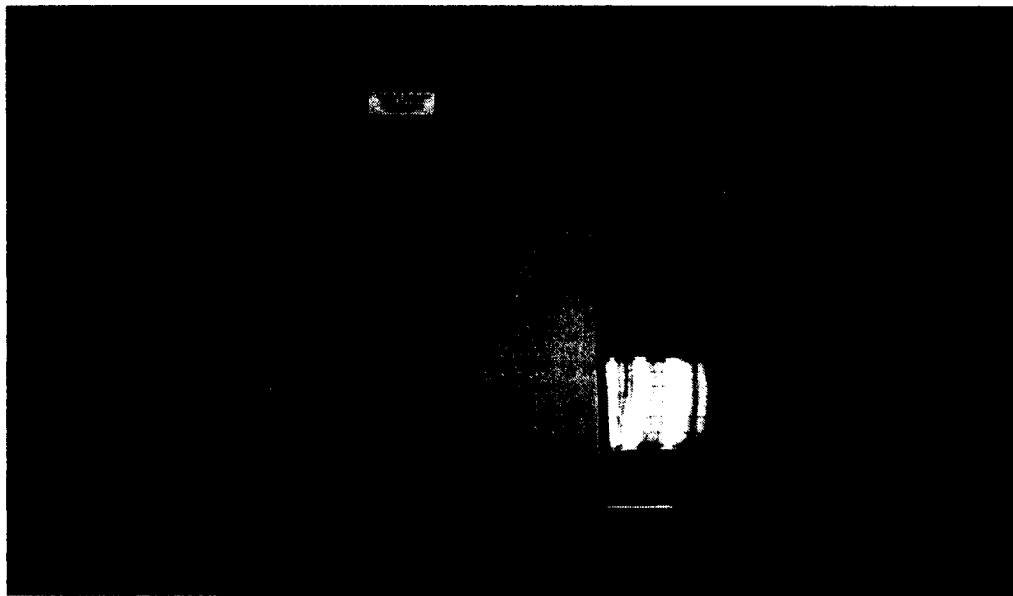
Figure 3-5: Microplate reader LT-4000. A 96-well plate was used for the assay.

3.6   Thermo Scientific GENESYS 20

The Thermo Scientific GENESYS 20 (Houston, TX) (**Figure 3-6**) is a low-cost, easy-to-use, and reliable visible spectrophotometer designed for routine laboratories. In this dissertation, it was used to test the optical density (OD 600 nm) of the test bacteria, which is directly related to cellular density. In this way, the effect of the released drug could be indirectly reflected via the values.
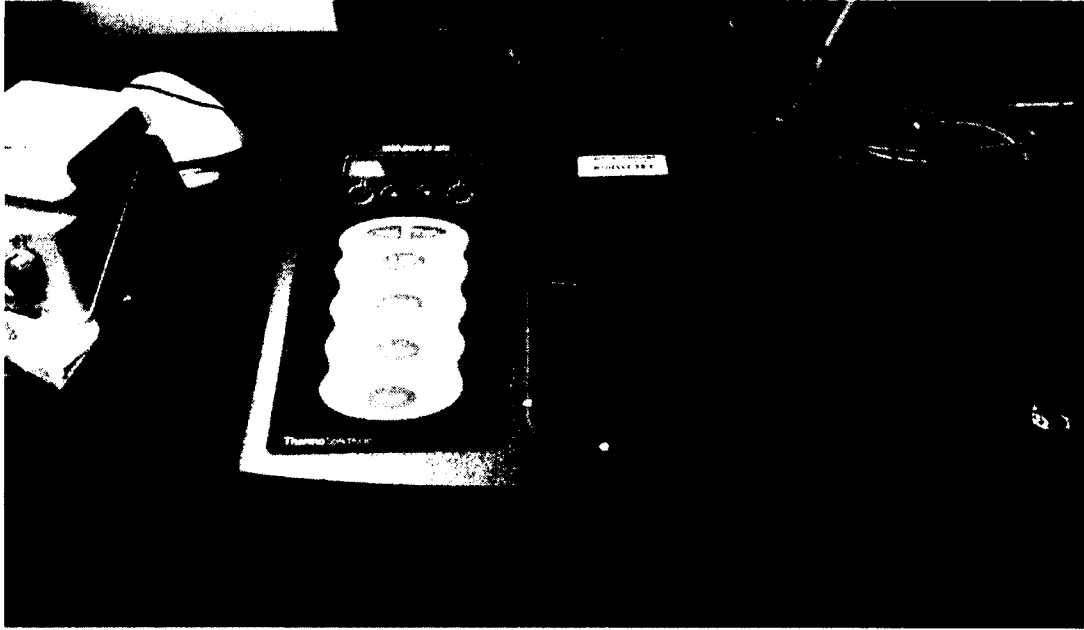
Figure 3-6: Thermo Scientific GENESYS 20.

CHAPTER 4

FABRICATION METHODS OF LOADING HALLOYSITE NANOTUBES WITH DRUGS

4.1   Introduction

4.1.1   Background

Ideally, an agent should have content efficacy of the desired biological function with few unexpected side effects. However, most currently available agents in the pharmaceutical market have more or less side effects, and their efficacy becomes lower and lower because of drug tolerance from long term use. Especially in the treatment of cancer, which is still the most common cause of mortality in humans, huge amounts of chemotherapeutics are used to eliminate malignant cells. Meanwhile, normal cells and tissues are also attacked, and patients suffer from all kinds of side effects, which can equally threaten their lives. Therefore, novel agents, technologies, and strategies are needed to improve medical treatment for patients.

4.1.2   Drug Delivery

It is currently estimated to take a decade and cost over 120 million dollars to bring a new drug through discovery, clinical testing, development, and regulatory approval [46]. Another strategy is to improve the safety and efficacy of current drugs by delivering drugs at a controlled rate, slow and targeted delivery. Compared to conventional drug administration methods, the newly formed and nanotechnology-based drug delivery

systems have several advantages in their inherent ability to overcome solubility and stability issues, localize drug delivery, and diagnose via *in vivo* image [1]. Theoretically, these systems can improve the stability, absorption, and therapeutic concentration of drugs within the target tissue. They can also provide a sustained or controlled release at the target site. In the pharmaceutical industry, the research on drug delivery has become a strategy tool to expand drug markets through repackaging classic drugs in new delivery technologies. It is estimated that about 13% of the currently global pharmaceutical market is related to the sale of products based on drug delivery systems [3].

According to the mechanism of how drugs are sent to the target sites, drug delivery systems can be divided into two types, active and passive delivery. In the active approach, biorecognition molecules are attached to the surface of the nanovehicles to target specific biomarkers overexpressed by cells or tissues. In the passive approach, the goal is to facilitate deposition of nanocarriers within target sites, where some distinctive characteristics are present only in the target sites rather than normally healthy tissues. Take cancer as an example, the phenomenon of enhanced permeability and retention is utilized to facilitate deposition of nanoparticles loaded with chemotherapeutics within the tumor microenvironment. Although active targeting delivery is an ultimately ideal model, its transmission from theory to practice and from laboratory to clinical practice did not occur as smoothly as people expected. Compared to passive delivery, the requirement for active targeting is more rigorous such as higher exclusivity and longer stability in the blood circulation. Therefore, most of the currently available drug delivery systems belong to the passive category. In this project, HNTs based drug delivery systems were built via

three different methods. These methods were compared through their performance in both loading and release processes.

4.1.3   Halloysite Nanotubes

Halloysite is a naturally occurring alumino-silicate clay and can be mined from natural deposits in many countries such as America, Brazil, China, France, Japan, South Korea and Turkey [17]. It has a similar chemical composition with kaolin, but differs in having a hollow tubular structure. Most of commercially available HNTs share a typical three dimension structure: the inner diameter is between 10 and 20 nm, the external diameter ranges from 50 to 100 nm, and the length of these tubes varies from 500 to 2000 nm [18]. Their wall is composed of 10 to 15 bilayers of aluminum and silicon oxide [18]. They have a huge surface area around 65 m^2/g and a big pore volume of 1.25 ml/g [19]. All of the above characteristics make HNTs a good alternative for drug delivery. In this chapter, we will discuss some common fabrication methods used for drug loading with HNTs, to show the potential of using HNTs in drug delivery.

4.2   Materials and Methods

4.2.1   Materials

Halloysite nanoclay, methotrexate, sodium hydroxide solution (1 mol/l), hydrochloric acid solution, polyvinylpyrrolidone (Molecular Weight~1,3000,000; 1 mg/ml in DI water), and poly(acrylic acid) solution (Molecular Weight~250,000, 3 ml/100 ml in DI water) were obtained from Sigma Aldrich, St. Louis MO.

4.2.2   Standard Calibration Curve and Light Sensitivity Test

As it is said in the product instruction that methotrexate (MTX) is sensitive to light, the impact of light exposure on MTX needs to be examined first. A premade MTX

solution with known concentration (1 mg/ml, pH=11) was kept without light protection in a regular laboratory environment. Samples of the MTX solution were collected and measured by UV-Vis every 24 hours for one week. The values were compared with that of the original MTX solution, and results were analyzed with one-way ANOVA (IBM SPSS 22.0). To establish a standard calibration curve for the relationship between MTX concentration and absorbance value, several MTX solutions with different known concentrations were used. Then, the standard calibration curve for MTX was made from Excel.

4.2.3   Fabrication Methods

Three fabrication methods were used in this project, and they were physical adsorption, vacuum loading, and layer-by-layer (LbL) coating. The detailed process was described as follows.

4.2.3.1   *Physical Adsorption*

One hundred milligram HNTs powders were immersed into 1 ml MTX solution with controlled concentration at 1 mg/ml. A metal stir bar was added to keep stirring the suspension for 24 hours, which may help increase the contact between HNTs and MTX molecules. After that, the suspension was centrifuged and the supernatant was collected for UV-Vis absorbance measurement. The sediment was air-dried under regular room temperature, and was then crushed into fine powders for later use.

4.2.3.2   *Vacuum Loading*

One hundred milligram HNTs powders were immersed into 1 ml MTX solution with controlled concentration at 1 mg/ml. Then the suspension was placed into a jar that was connected with a vacuum pump. A metal stir bar was added to keep stirring the suspension while loading, which may help increase the contact between HNTs and MTX

molecules. Once the negative pressure inside the jar reached the pump limit (-25 in Hg), the vacuum pump was turned off and the jar was sealed. After 24 hours, the jar was opened and the suspension was centrifuged. The supernatant was collected for UV-Vis absorbance measurement, and the sediment was air-dried under regular room temperature as well as crushed into fine powders for later use. To avoid potential loss of MTX molecules from HNTs, the wash step was not included. Theoretically, the HNT/MTX composite was a combinational result from physical adsorption and vacuum loading. Through comparison with the result of physical adsorption, the pure amount of MTX loaded inside the lumen of HNTs could be indirectly obtained.

4.2.3.3   *Layer-by-Layer Coating*

As pH and the number of coated bilayers of polymers (PVP/PAA) may have an impact on the drug loading property, different pH (3, 5, and 7) with different numbers of bilayers (3, 6, and 9) were used for LbL coating. To make the whole process simple, the HNT/polymer composite was premade first. One gram HNT powders were immersed into 30 ml Polyvinylpyrrolidone (PVP) solution (0.1 mg/ml). Then the suspension was kept being shaken for 15 minutes and then centrifuged and the supernatant was removed. Deionized (DI) water was used to wash the sediment for 5 minutes, and was removed after centrifuge. The same procedure was repeated with poly(acrylic acid) (PAA) solution (0.1 mg/ml) to build the second layer. In this way, one bilayer was completed. The HNT/polymer composites were made according to the predetermined groups. Then, 100 mg of the HNT/polymer composites were immersed into 1 ml MTX solution with controlled concentration at 1 mg/ml and controlled pH correspondingly. All the

supernatants were collected for UV-Vis absorbance measurement, and the sediments were air-dried and crushed into fine powders for later use.

4.2.4   SEM Scanning

The samples including HNTs, HNT/MTX composite, and HNT/polymers/MTX composite were examined by SEM for any sign of visible change.

4.2.5   Drug Release Test

HNT/MTX or HNT/polymer/MTX composites (25 mg/sample) were immersed into 5 ml DI water, and the suspensions were placed on a shaker kept being shaken for 10 minutes. Then the suspensions were centrifuged, the supernatants were collected for UV-Vis absorbance measurement, and 5 ml fresh DI water was replenished for continuous release. The process was repeated until only slight release of MTX could be detected in the supernatant. Then, sodium hydroxide water (pH=11) was used subsequently to trigger extra release.

4.3   Results and Discussion

4.3.1   Standard Calibration Curve

As the Nanodrop 2000c only has reliable accuracy when the absorbance value lies between 0 and 1, samples with high concentrations were approximately diluted before absorbance measurement. For the standard calibration curve, the results are shown in **Table 4-1** and **Figure 4-1**. The linear relation between MTX concentration and absorbance value is strong and reliable within the absorbance value range between 0 and 1, which can be used to calculate the concentrations of MTX sample solutions.

Table 4-1: Standard calibration curve for MTX (wavelength: 300 nm).

Concentration (ug/ml)	2	4	6	8	10	12	14	16	18	20
Absorbance Value	.101	.203	.302	.401	.494	.586	.681	.774	.865	.956
Standard Curve	$y = 0.047x + 0.015$ ($R^2 = 0.999$, y-absorbance value, x-MTX concentration (ug/ml))									
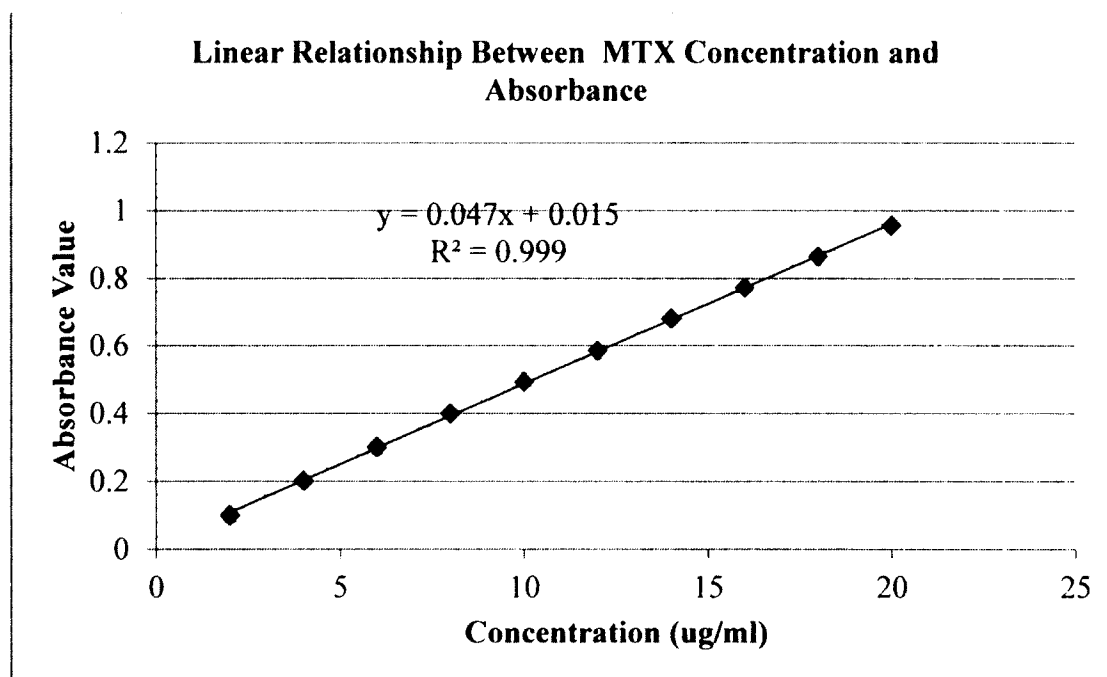
Figure 4-1: Standard calibration curve for MTX made with Excel 2007.

4.3.2 Light Sensitivity Test of MTX

Table 4-2 and **Figure 4-2** show the results of the light sensitivity test of MTX. SPSS (22.0) was applied to analyze whether a significant change occurred during a 7-day period of light sensitivity test. A Shapiro-Wilk's test (P>.05) showed that the UV-Vis absorbance values were approximately normally distributed for all of the samples, and a Levene's test verified the equality of variances in the samples (homogeneity of variance)

(P>.05). Then, the one-way ANOVA test (P>.05) showed that there was no significant difference among all these groups, which means the impact of light exposure on the MTX could be ignored during a seven day period.

Table 4-2: Light sensitivity test for MTX (wavelength: 300 nm).

	UV-Vis Absorbance Value						
	Day-1	Day-2	Day-3	Day-4	Day-5	Day-6	Day-7
Sample 1	.526	.532	.530	.529	.536	.542	.538
Sample 2	.535	.523	.523	.522	.532	.552	.542
Sample 3	.527	.516	.527	.532	.538	.523	.544
Mean	.529	.524	.527	.528	.535	.539	.541
SD	.005	.008	.004	.005	.003	.015	.003
P Value	N/A	.967	.993	1.000	.955	.678	.437

(1) One-way ANOVA (IBM SPSS 22.0) was used to analyze the statistical difference among these data.
(2) SD stands for standard deviation.
(3) All the samples of MTX solution were diluted 100 time fold.
P value shows the result comparison with Day-0.
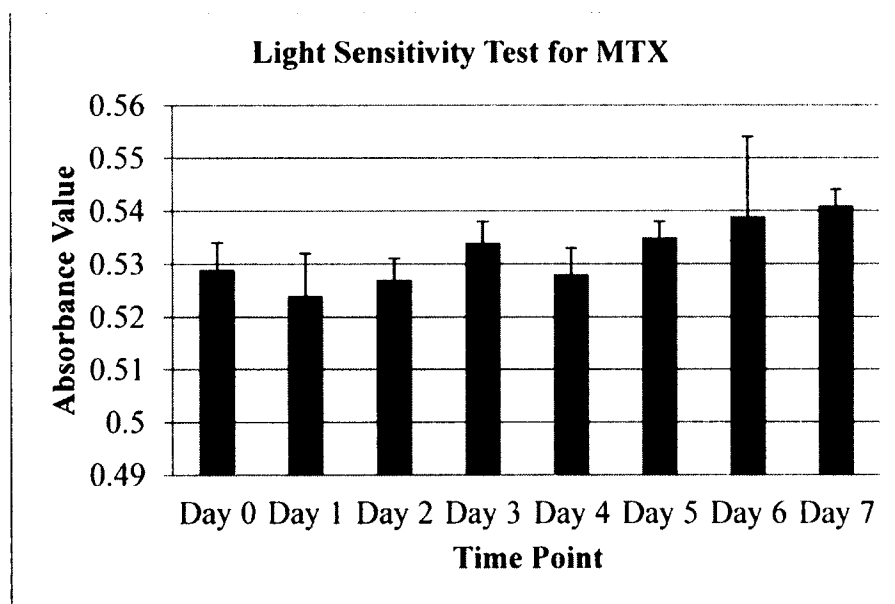
Figure 4-2: Result of light sensitivity test for MTX during a 7-day period.

4.3.3   SEM Scanning of HNT/MTX Composites

As we see in the SEM images (**Figure 4-3**), pure HNTs showed very smooth outside surfaces. The products from both physical adsorption and vacuum loading shared the same appearance as the arrow pointed in **Figure 4-3** (B), and a bright layer could be seen on the outside of HNTs. In fact, in the process of vacuum loading, MTX molecules could also be physically adsorbed to the wall of HNT. In other words, physical adsorption was partially included in vacuum loading. **Figure 4-3** (C) and (D) show the images of HNT/polymer composites from LbL fabrication, and a bright layer on the outside surface could also be seen. There is an obvious limit of the SEM that the differences in LbL structures with different numbers of layers could not be observed, and they may present a similar appearance with the results from physical adsorption and vacuum loading. However, in **Figure 4-3** (E) the uncoated portion of HNT was clearly seen as the arrow pointed, and the bright layer of LbL structure was also clearly pointed out in **Figure 4-3** (F).
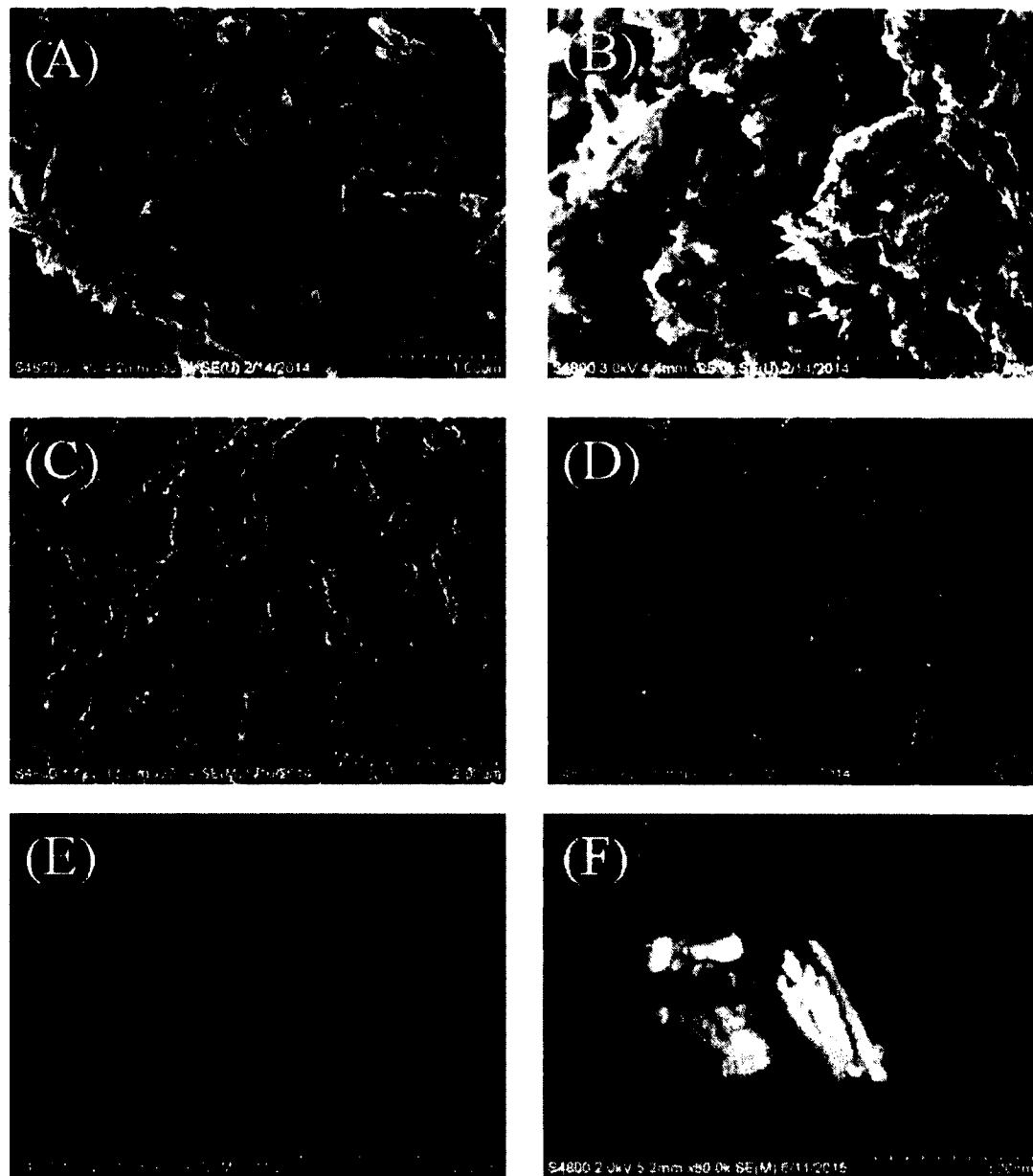
Figure 4-3: SEM images of HNTs and HNT/MTX composites. (A) Pure HNTs particles; (B) MTX attached on the outside surface of HNTs; (C) and (D) show clumped HNT/polymer composite from LbL fabrication; (E) and (F) LbL structure was built on the outside surface.

4.3.4   Fabrication of HNT/MTX Composites

Three methods were used to fabricate the HNT/MTX composites, and they were physical adsorption, vacuum loading and LbL coating. A general statistical description of the fabrication results is shown in **Table 4-3**.

Table 4-3: MTX loading within HNTs or HNTs/polymer composites.

		HNTs/Polymer (mg)	MTX to load (ug)	MTX loaded (ug)	Efficiency (%)
Physical Adsorption (PA)		100±0.2	1047.6	530.96±3.40	50.70±0.30
Vacuum Loading (VL)		100±0.2	1047.6	515.28±11.02	49.20±1.04
LbL Coating pH=3	3 bilayers (3--3)	100±0.2	1046.5	928.55±4.05	88.73±0.40
	6 bilayers (3--6)	100±0.2	1046.5	979.04±0.77	93.53± 0.06
	9 bilayers (3--9)	100±0.2	1046.5	996.77± 0.96	95.23± 0.06
LbL Coating pH=5	3 bilayers (5--3)	100±0.2	1046.5	752.02±2.98	71.90±0.30
	6 bilayers (5--6)	100±0.2	1046.5	789.33±0.89	75.43± 0.06
	9 bilayers (5--9)	100±0.2	1046.5	796.42±2.83	76.10± 0.26
LbL Coating pH=7	3 bilayers (7--3)	100±0.2	1046.5	476.84±4.37	45.57± 0.42
	6 bilayers (7--6)	100±0.2	1046.5	487.06±10.26	46.57±1.01
	9 bilayers (7--9)	100±0.2	1046.5	510.60±3.54	48.80±0.36
Instruction: 1. There were 3 samples in each group.					

In each test group, a certain amount of MTX was successfully loaded within HNTs or HNT/polymer composites. Groups of physical adsorption and vacuum loading had a similar result, which was also close to the group of LbL coated under pH 7, but significantly lower than those coated under pH 5 and pH 3. Among all the groups, the one coated with nine bilayers under pH 3 had the highest loading of MTX, while the one with three bilayers under pH 7 was the lowest (**Figure 4-4**).

MTX Loading Efficiency
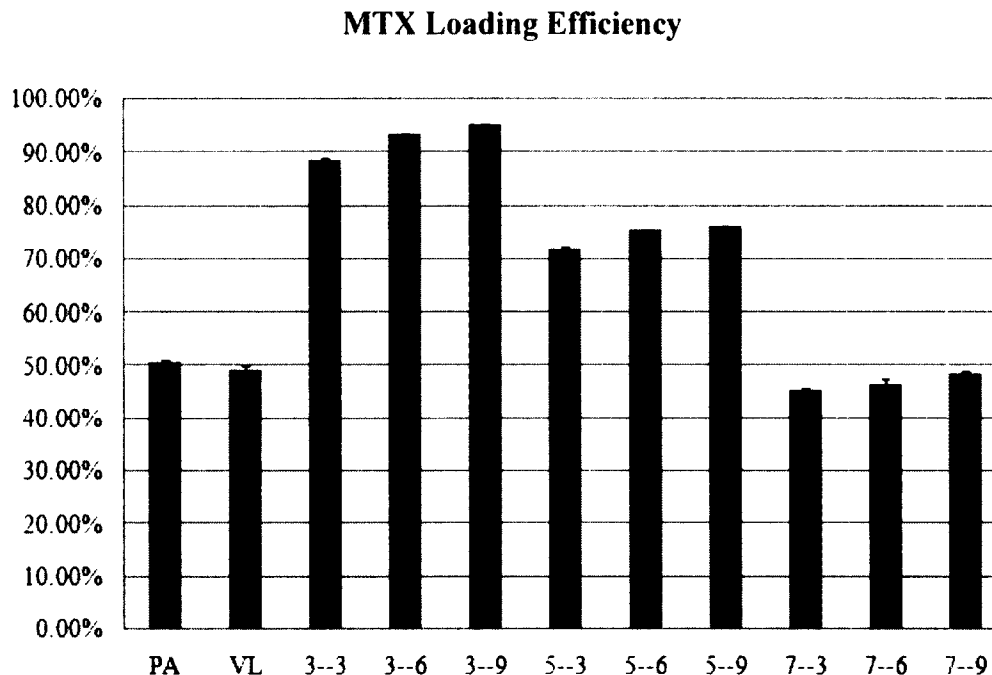
Figure 4-4: MTX loading efficiencies among all test groups.

As a nanocontainer, HNTs have a natural lumen which can be used to load small molecules. They also have a huge surface area of 65 m^2/g and a big pore volume of 1.25 mL/g [19], and can physically adsorb molecules on the surface or trap them in the pores inside their structure. Therefore, a certain amount of MTX could be adsorbed physically within HNTs.

The vacuum loading procedure used in this project was, in fact, a combination of physical adsorption on the outside surface and vacuum loading inside the lumen. In practice, it is impossible to send MTX molecules into the lumen with no contact between MTX molecules and the outside surface of HNTs. Theoretically, the result of vacuum loading should be higher than that of physical adsorption. However, the results in both

groups were almost the same. One possible explanation is the amount of MTX loaded inside HNTs lumen could be statistically ignored. Or MTX molecules could not be loaded within the lumen.

The LbL structure built on the outside surface of HNTs obviously increased the surface area and the porosity volume of the nanoparticle, which can be utilized to attach more MTX molecules. As seen in the results, LbL structures with different numbers of layers under different pH did impact the loading ability of MTX. It suggested that lower pH and more layers could help increase the capacity of MTX loading. Still, statistical analysis is required to make a firm conclusion.

4.3.5   Statistical Characteristics of Samples

Before the statistical comparison of the three methods, it is necessary to figure out the impact of LbL layers and pH on the HNTs' fabrication within the LbL groups, and to select the best combination of LbL structure and pH. **Table 4-4** shows the statistical analysis of the difference of MTX loading with different numbers of LbL layers when pH was controlled. The result of MTX loading within the HNT/polymer composites was used as the parameter for comparison. A Shapiro-Wilk's test (P>.05) showed that the results of MTX loading were approximately normally distributed for all of the samples, and a Levene's test verified the equality of variances in the samples (homogeneity of variance) (P>.05). Then, one-way ANOVA with Post Hoc test was applied for the analysis (**Table 4-4**).

Table 4-4: Statistical analysis of the impact of LbL layers on MTX loading.

	pH=3	pH=5	pH=7
One-way ANOVA P Value	.000	.000	.002

Post Hoc Test within Each Groups								
pH=3			pH=5			pH=7		
3 bilayers	6 bilayers	9 bilayers	3 bilayers	6 bilayers	9 bilayers	3 bilayers	6 bilayers	9 bilayers
3 bilayers N/A	.000	.000	N/A	.000	.000	N/A	.232	.002
6 bilayers .000	N/A	.000	.000	N/A	.027	.232	N/A	.012
9 bilayers .000	.000	N/A	.000	.027	N/A	.002	.012	N/A

In the groups of pH 3 and pH 5, the number of layers did play a role in the performance of MTX loading. Given the results of MTX loading in **Table 4-3**, a hypothesis could be made that more layers can help increase the MTX loading under pH of 3 and 5. In the groups of pH 7, there was no statistical difference between groups of three bilayers and six bilayers. However, both of them were significantly different from groups of nine bilayers. Therefore, the trend that more layers could increase loaded MTX under pH 7 was not as strong as that under pH 3 and 5.

On the other hand, when the number of layers was controlled, the impact of pH on the MTX loading was shown in **Table 4-5**. Similarly, a Shapiro-Wilk's test ($P>.05$) showed that the results of MTX loading were approximately normally distributed for all of the samples, and a Levene's test verified the equality of variances in the samples (homogeneity of variance) ($P>.05$). Then, one-way ANOVA with Post Hoc test was applied for the analysis (**Table 4-5**).

tubular structure inside where small molecules could be stored. They also have a huge surface area and porosity volume that could be utilized to adsorb or trap target molecules. The LbL structure built on the outside surface can further increase the surface area and pore volume, which accounts for the higher capacity of MTX loading. Theoretically, unlimited layers could be added continuously, which may suggest ideal capacity for drug loading. However, abundant clumps of HNT/polymer composites (Figure 4-3 C and D) formed during the LbL coating process, and the number of layers was greatly limited.

The pH could indirectly affect the capacity of MTX loading in HNT/polymer through its important role in the LbL structure. As seen in the polyelectrolyte pair of PVP and PAA, a lower pH could help increase the MTX loading.

Some other factors like the drug solubility, size, and charge also have some influence on the loading process with the HNTs based drug delivery system. Obviously, a higher concentration of loading solution could have more MTX attached or trapped within HNTs or HNT/polymer composites when the final balance arrives.

4.3.7   Drug Release

As pH and the number of layers within the LbL structure play a role in the process of MTX loading, groups of samples with LbL structure were compared among themselves. Figure 4-5, Figure 4-6, and Figure 4-7 show the results of MTX release where pH was controlled to show the impact of number of layers on the release.
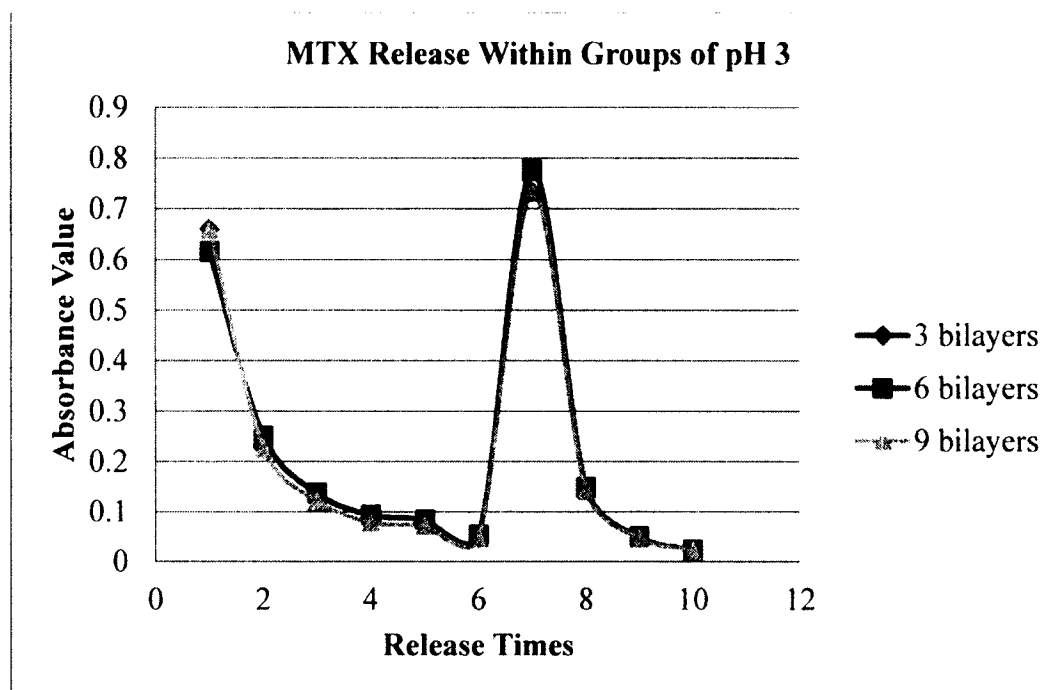
Figure 4-5: UV-Vis absorbance measurement result of MTX release within groups where MTX was loaded under pH 3. DI water was used for the first six times, and sodium hydroxide (pH 11) was used for the rest.
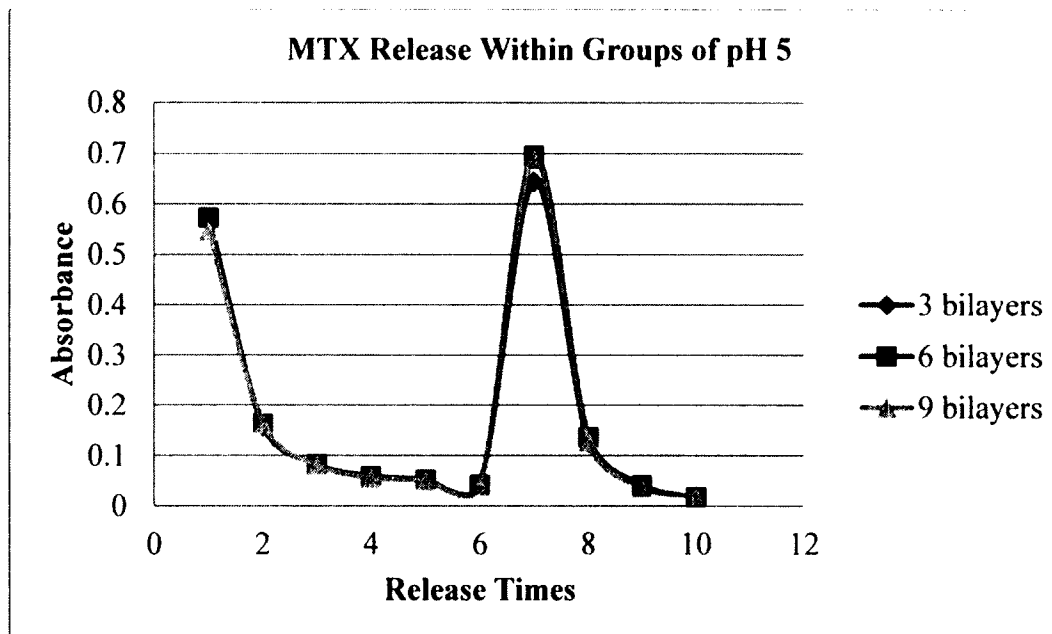
Figure 4-6: UV-Vis absorbance measurement result of MTX release within groups where MTX was loaded under pH 5. DI water was used for the first six times, and sodium hydroxide (pH 11) was used for the rest.
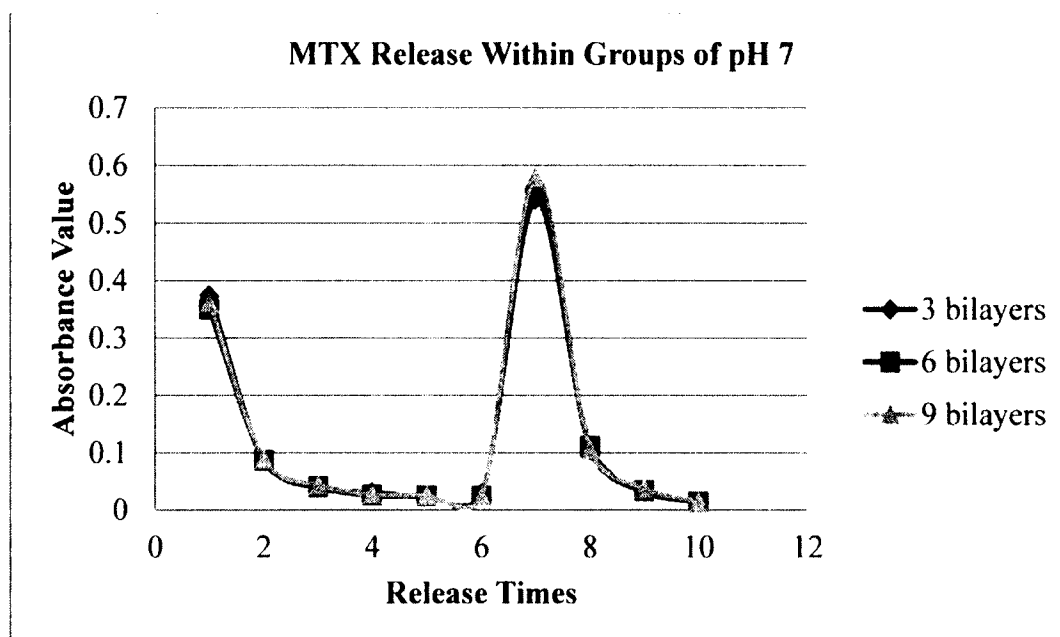
Figure 4-7: UV-Vis absorbance measurement result of MTX release within groups where MTX was loaded under pH 7. DI water was used for the first six times, and sodium hydroxide (pH 11) was used for the rest.

It is clear that when pH was controlled, the number of LbL layers did not have a significant impact on the release profile. Within each pH group, the results looked the same. In all these groups, a burst release was seen the first time, and subsequent lower and lower releases continued until the second peak of MTX release, where sodium hydroxide was used to trigger extra release.

Figure 4-8, **Figure 4-9**, and **Figure 4-10** show the results of MTX release where LbL structure was controlled to expose the impact of pH on the MTX release profile.
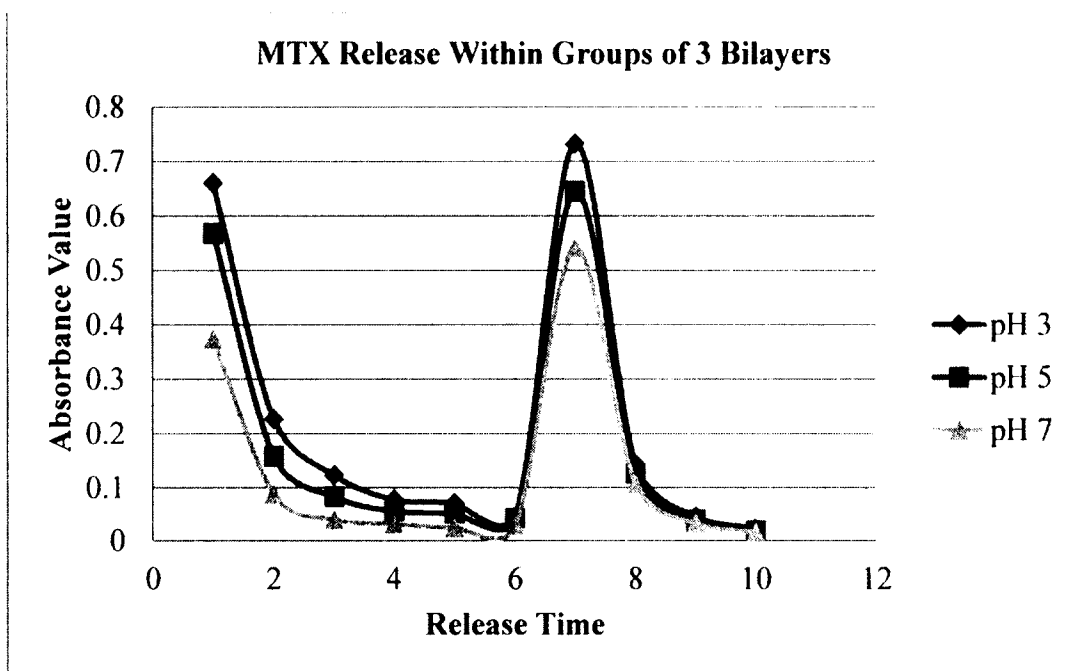
Figure 4-8: UV-Vis absorbance measurement result of MTX release within groups where MTX was loaded with three bilayers of (PVP/PAA). DI water was used for the first six times, and sodium hydroxide (pH 11) was used for the rest.
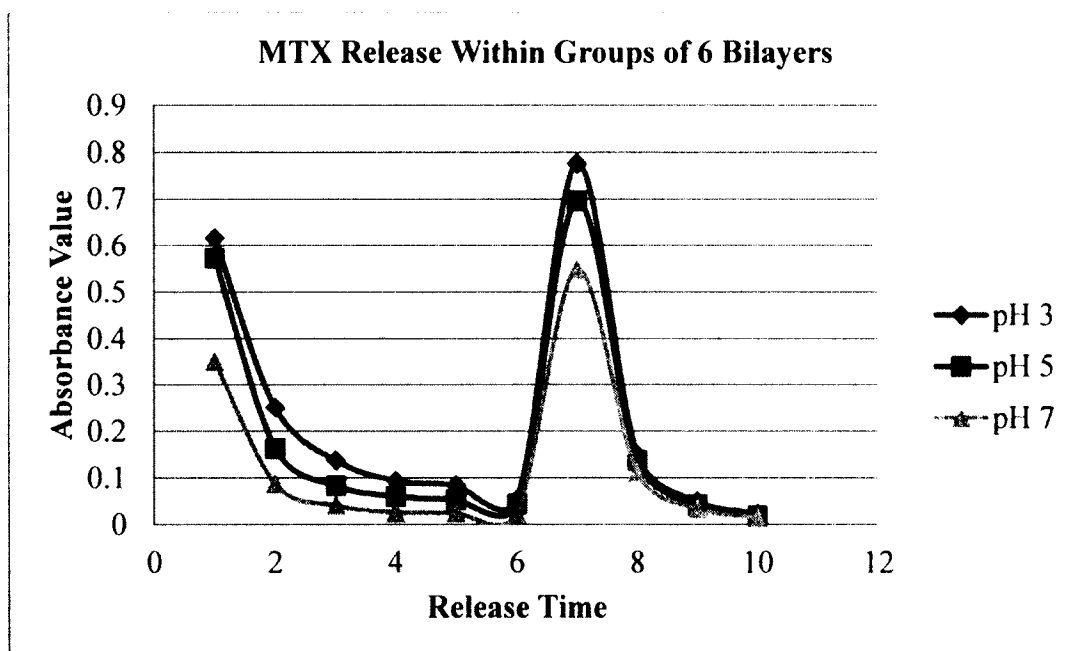
Figure 4-9: UV-Vis absorbance measurement result of MTX release within groups where MTX was loaded with six bilayers of (PVP/PAA). DI water was used for the first six times, and sodium hydroxide (pH 11) was used for the rest.
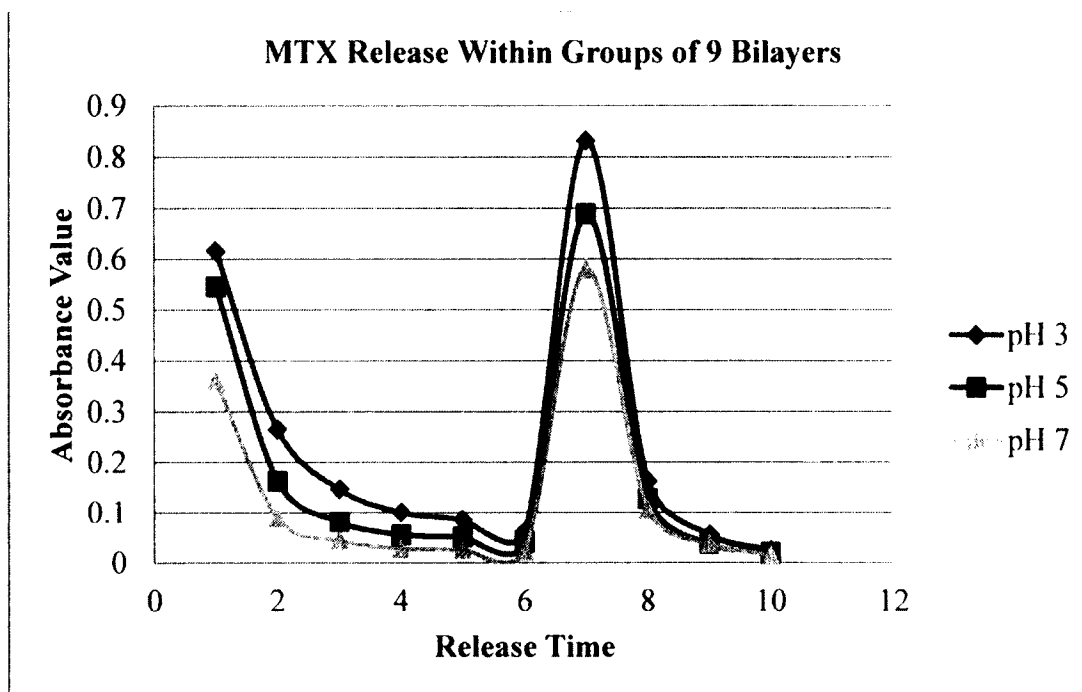
Figure 4-10: UV-Vis absorbance measurement result of MTX release within groups where MTX was loaded with nine bilayers of (PVP/PAA). DI water was used for the first six times, and sodium hydroxide (pH 11) was used for the rest.

Still, a burst release was seen the first time, and subsequent lower releases went on until the second peak where sodium hydroxide was used for extra MTX release. Although the shape of the release profile in each group was the same, the groups of pH 3 had the highest release almost every time while the groups of pH 7 had the lowest. Unlike the number of bilayers in the LbL structure, pH showed a significant impact on the release results, which suggests that a lower pH may help increase the release of MTX.

Therefore, within the LbL coated HNTs groups, the one with nine bilayers under pH 3 was selected to represent the LbL coating fabrication for comparison with the other two methods. **Figure 4-11** shows the results of MTX release among the three fabrication methods.

MTX Release Comparison
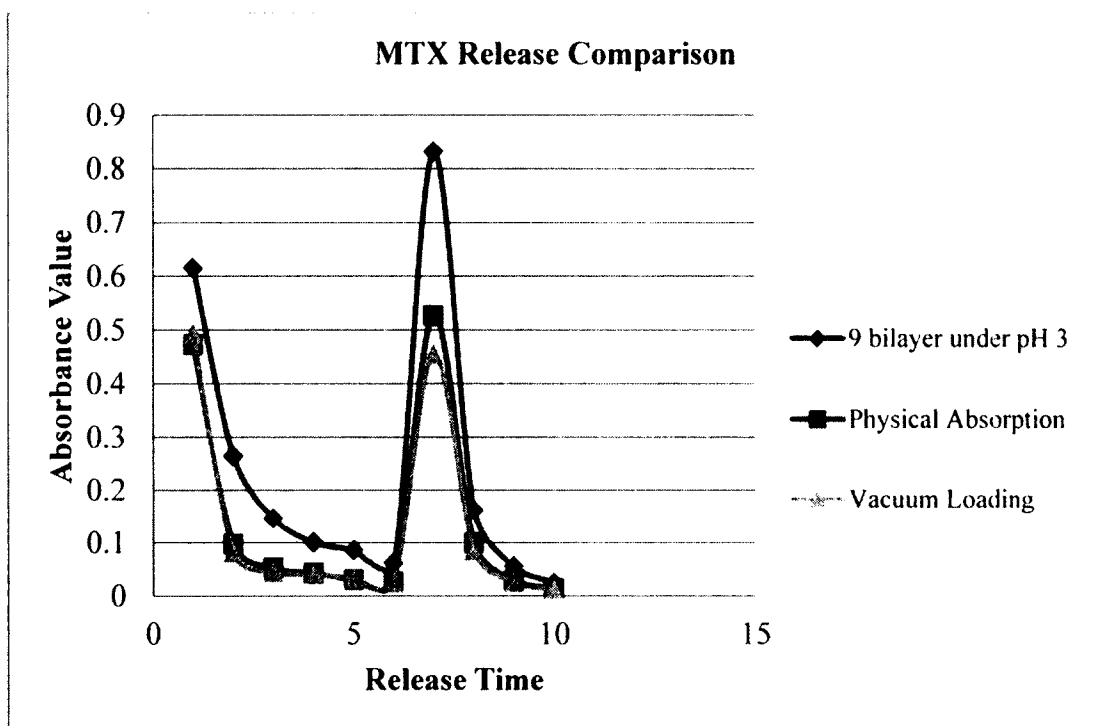
Figure 4-11: UV-Vis absorbance measurement result of MTX release among groups with different fabrication methods. DI water was used for the first six times, and sodium hydroxide (pH 11) was used for the rest.

Still, the shapes of the release profile were the same. However, the group with LbL structure had the highest release while the other two shared the same performance. Additionally, the ratio between test particles and water could also affect the release profile. In this project, the ratio was controlled at 5mg/ml, and the release process was repeated ten times.

4.3.8   Process of Drug Release

The main factor that drives loaded MTX to be released in surrounding solution is the concentration gradient, which is also the same mechanism used in the drug loading process. All the dissolved MTX molecules keep moving around in the solution all the time. Some moved from HNTs to surrounding solution, while others moved from solution to HNTs, which means both the loading and releasing processes were occurring

at the same time. However, the net moving direction of the total molecules was consistent with the concentration gradient between the solution and the HNT/MTX nanoparticles. Once a new balance was reached, the net moving stopped. When fresh DI water was replaced, a new concentration gradient formed, and the net moving of MTX molecules towards a lower concentration restarted, which would continue until the next balance occurred.

The burst release of MTX on the first time could be explained by the theory of concentration gradient, as it had the biggest value on the first time. When sodium hydroxide was replenished instead of DI water, all of the test groups showed a second peak of release. The reason is the basic environment can increase the solubility of MTX in water, and increase the net movement of MTX molecules from HNTs to solution. It well explains the second peak in the groups of physical adsorption and vacuum loading.

In the groups of LbL coating, not only did the higher pH increase the solubility of MTX, it also changed the LbL structure leading to more MTX molecules releasing from HNTs. The best evidence is the superimposed release of MTX in the LbL coating group, which was higher than that in both groups of the others. Therefore, the LbL structure could help carry more MTX molecules than pure HNTs. In this style, the loaded MTX molecules would continuously be released into the surrounding environment, and the period for this release process would be partially determined by the rate of MTX consumption by the circumambient tissue.

4.4   Conclusions

In this chapter, MTX was successfully loaded within HNTs or HNT/polymer composites through three methods including physical adsorption, vacuum loading, and

LbL coating. HNTs coated with the LbL structure had a significantly higher ability than the other two methods in MTX loading, and there was no statistical difference between physical adsorption and vacuum loading in the performance of MTX loading and releasing, which may suggest that little or slight MTX was loaded within the HNTs lumen. Although it has already been reported that HNTs could be used to load resveratrol within their lumen space [47], the same method was not well applied with MTX. pH had a very important role in the MTX loading, while the number of coated layers could only slightly increase the loaded MTX under lower pH. In the release process, a burst release was seen in all the test groups, and subsequent lower releases continued until a second peak occurred by the usage of sodium hydroxide. Compared with pure HNTs, the LbL coated HNTs had higher release of MTX, which may show a potential of longer release period. Besides the properties of HNTs or HNT/polymer composites, the consumption rate of MTX by the surrounding environment could partially determine the length of the release period, too. As a natural nanomaterial, HNTs showed great potential of loading and releasing target molecules, and offered another option for drug delivery.

CHAPTER 5

POTENTIAL APPLICATION OF USING HALLOYSITE NANOTUBES BASED DRUG DELIVERY IN THE TREATMENT OF OSTEOSARCOMA

5.1   Introduction

This chapter is based on my published manuscript titled *"Drug Coated Clay Nanoparticles for Delivery of Chemotherapeutics," Current Nanoscience,* 2016, 12(2) [48]. I am the author of this paper, and its content is used only in my dissertation. In this chapter, an *in vitro* cellular test with osteosarcoma is used to show the potential of using HNTs as a tool to deliver chemotherapeutics in the treatment of cancer.

5.1.1   Halloysite Nanotubes

Halloysite nanotubes (HNTs) are naturally formed alumino-silicate clay tubules that are chemically similar to kaolin clay [70-72]. HNTs occur abundantly in nature and can be readily mined and sorted, making them an economically viable nanomaterial [49]. HNTs are routinely used as a functional filler to improve the mechanical performance of cements and polymers [74-76]. The geometrical structure and surface charges of HNTs make the material a viable nanocontainer for drugs, bioactive macromolecules, and polymers, for sustained and extended releases [77-79].

Recently, a publication reported the application of using HNTs to deliver resveratrol to cancer cells [47]. Their inner luminal space was used for loading resveratrol

and an additional coating of poly(sodium 4-styrene-sulfonate) and poly(allylamine

hydrochloride), or protamine salt and dextransulfate sodium salt was coated on HNTs to

slow the drug release. With a negatively charged outer surface, HNTs can be effectively

coated by sequential adsorption of positively and negatively charged polyelectrolytes

(layer-by-layer (LbL) nano-assembly). LbL nano-assembly of multiple polyelectrolyte

nano-films has been shown as a potential multifunctional carrier system for drugs,

enzymes, and cells [80-82]. Recent studies have also shown that HNTs display non-

cytotoxic effects on several cell types such as mesenchymal stem cells,

fibrochondrocytes, osteoblasts and human dermal fibroblasts (up to concentrations of .1

mg/ml) [83-84]. The biocompatible and drug release properties of HNTs make them an

ideal candidate for new drug delivery systems.

5.1.2   Methotrexate

Methotrexate (MTX) is commonly used in the treatment of cancer, autoimmune

diseases, ectopic pregnancy, and for the induction of medical abortions. Since being

discovered in the early 1970s, MTX has become one of the four major classes of

chemotherapeutic agents with established efficacy in the treatment of osteosarcoma [50] .

MTX is an antimetabolite and antifolate drug that inhibits dihydrofolatereductase, an

enzyme involved in cellular DNA synthesis. It is generally considered that a serum

concentration of MTX greater than 1,000 μmol/l administered as an infusion over four to

six hours is required for successful therapy [85-86].

5.1.3   Osteosarcoma

Osteosarcoma (OSA) is the most common malignancy of bone in children and

adolescents, and is characterized histologically by the production of an extracellular

osteoid-like matrix. It represents about 3.4% of all childhood tumors and 56% of

malignant bone tumors [51]. Standard treatments include adjuvant chemotherapy,

radiotherapy, hormone or biological therapy, and if OSA is refractory, surgical ablation of

the primary tumor is needed. Advancements in treatment modalities have led to increased

rates of 'limb-sparing' surgeries, but patients are still threatened with the risk of

recurrence. Tumor recurrence is greater than 90% for the patients without clinically

diagnosed metastasis who receive surgical resection of the primary malignancy and do

not continue with adjuvant chemotherapy [50]. Surgical abscission can remove all sites of

clinically detectable tumor mass physically and systemic chemotherapy can inhibit

micrometastasis before and/or after surgery. Other patients with similar disease

conditions who are administered chemotherapeutic agents alone will suffer a 100%

probability of local recurrence without surgical excision of the primary tumor [52].

Significant advances have been made in the treatment of osteosarcoma over time;

however, new treatment and prevention strategies are still needed.

In this chapter, we demonstrate that polyelectrolyte coated HNTs loaded with

MTX can be easily fabricated and that MTX coated HNTs can be embedded into nylon-6.

HNT nanocomposites were tested for their cytotoxic and anti-proliferative effects against

osteosarcoma cells. HNT/MTX doped composites were shown to alter osteosarcoma cell

morphology and behavior and inhibit cell proliferation. Data support the potential for

using doped HNT/polymer composites as a delivery tool for chemotherapeutic agents

capable of delivering a focal and sustained concentration of drugs.

5.2   Materials and Methods

5.2.1   Materials

Osteosarcoma cells (OC, UMR-106) were obtained from ATCC, Manassas, VA.

Halloysite nanoclay, methotrexate, sodium hydroxide solution (1 mol/l), hydrochloric

acid solution (pH=2), Polyvinylpyrrolidone (Molecular Weight~1,3000,000; 1 mg/ml in

DI water), poly(acrylic acid) solution (Molecular Weight~250,000, 3 ml/100 ml in DI

water), nylon-6, and formic acid solution were obtained from Sigma Aldrich, St. Louis,

MO. 96-well plates and other lab plastics were purchased from MidSci, St. Louis, MO.

Dulbecco's Phosphate Buffered Saline (DPBS), Dulbecco's Modified Eagle's Medium

(DMEM), fetal bovine serum (FBS), Live/Dead Viability/Cytotoxicity kit and penicillin-

streptomycin-amphotericin (PSA) antibiotics were obtained from Life Technologies,

Carlsbad, CA. CellTiter 96 Aqueous One solution reagent was purchased from Promega,

Madison, WI.

5.2.2   Composite Fabrication

Two hundred milligram HNTs were immersed in 1 ml of polyvinylpyrrolidone

solution (1 mg/ml, pH=2) and mixed for ten minutes. The mixture was then centrifuged

at 13.4×1000 R.P.M. for three minutes and the supernatant was removed. The process

was repeated with poly-acrylic acid solution (1 mg/ml, pH=2) and the alternating of PVP

and PAA was repeated. A total of six layers were deposited (HNT/(PVP/PAA)$_3$). After

the sixth layer, 1 ml of methotrexate solution (1000 μg/ml, pH=2) was added and mixed

for ten minutes, and centrifuged. The composites were dried and crushed into fine

powder for later use. To avoid any potential loss of MTX, the coating process ceased

after the drug layer was added. The final structure was HNT/(PVP/PAA)$_3$/MTX (see

Figure 5-1). The HNT/(PVP/PAA)₃/MTX composites were also examined as a functional

filler for nylon-6. Nylon-6 solution (20% w/w) was prepared by dissolving with formic

acid. HNT/(PVP/PAA)₃/MTX (3% w/w) was mixed into the nylon-6 solution

homogeneously, then poured into a 24-well plate, and was air-dried for 24 hours. The

final product was nylon-6 loaded with HNT/(PVP/PAA)₃/MTX. **Figure 5-1** details the

coating architecture of control and experimental groups.
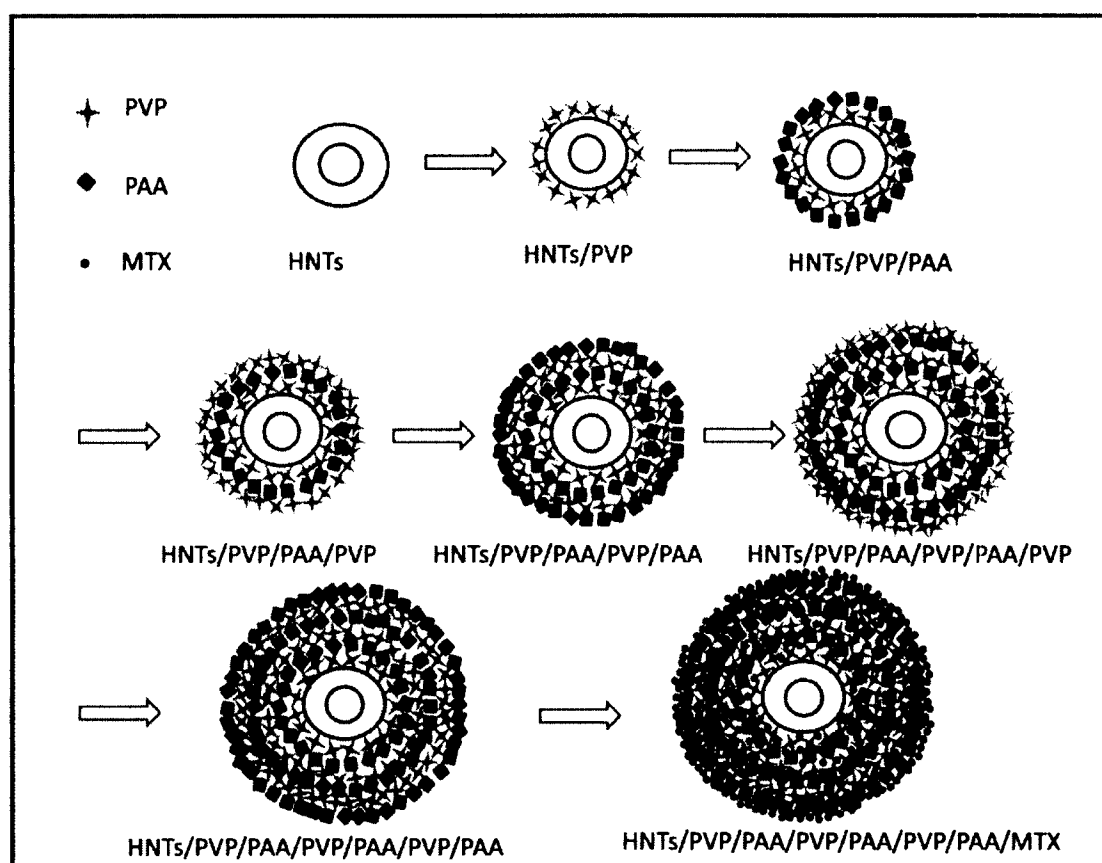
Figure 5-1: Graphic illustration depicting the assembly of the polyelectrolyte coatings and drug infusion process on the surface of a halloysite nanotube. The assembly process begins at top left with specific steps proceeding from left to right and top to bottom. The fabrication is based on electrostatic interactions between all materials (Halloysite nanotubes (HNTs), polyvinylpyrrolidone(PVP), Poly (acrylic acid) (PAA), methotrexate(MTX)). This graphic depicts the process and is not meant to suggest the final coating structure.

5.2.3   Scanning Electron Microscopy

Coated HNT samples were coated with $(PVP/PAA)_3/MTX$ and imaged with a

Hitachi Field Emission Scanning Electron Microscope. Demonstration of the coated

HNTs and surface features were observed.

5.2.4   Drug Release Tests

First, a calibration curve was created for MTX to compare with the drug elution

profiles of the $HNT/(PVP/PAA)_3/MTX$ composites. Three sample sets, each with 20 mg.

of $HNT/(PVP/PAA)_3/MTX$, were immersed in deionized water (1 ml, pH=7.0) and mixed

for ten minutes. Samples were centrifuged and the supernatants were collected for UV-

vis. analysis (Nanodrop 2000c, ABS wavelength 300 nm). Samples were replenished

with fresh DI water and the process was repeated 15 more times (total time=160

minutes).

5.2.5   Cell Culture

Osteosarcoma cells were plated in 25 cm^2 tissue culture flasks, and incubated at

37 °C under humidified 5% CO_2 and 95% air in complete DMEM containing 10% FBS

and 1% PSA. Subconfluent cells were passaged with 0.25% trypsin, collected by

centrifugation, suspended in complete DMEM and cultured at a 3:1 split into 25 cm^2

tissue culture flasks. These cultures were used for viability and proliferation tests.

5.2.6   Viability and Proliferation Tests

Subconfluent osteosarcoma cells were released with 0.25% trypsin, collected by

centrifugation, re-suspended in complete DMEM, and seeded in a 96-well plate. After 24

hours, culture wells were then washed with DPBS. The cells were next exposed to

DMEM alone, DMEM/HNT, $DMEM/HNT/(PVP/PAA)_3$,

DMEM/HNT/(PVP/PAA)₃/MTX, DMEM/HNT/(PVP/PAA)₃/nylon, and

DMEM/HNT/(PVP/PAA)$_3$/MTX/nylon. The cell density was controlled at 10,000 per

well. Other parameters included: HNT (2000 μg/ml), HNT/(PVP/PAA)$_3$ (2000 μg/ml),

HNT/(PVP/PAA)$_3$/MTX (2000 μg/ml), HNT/(PVP/PAA)$_3$/nylon (10 mg/ml),

HNT/(PVP/PAA)$_3$/MTX/nylon (10 mg/ml). After 72 hours, the Live/Dead

viability/cytotoxicity kit was applied for viability test, and the CellTiter 96 aqueous

solution reagent was applied for proliferation test.

5.3   Experimental Results

5.3.1   Drug Coating

Under SEM microscopy uncoated HNTs displayed a tubular structure with

smooth surfaces while coated HNTs (+/- MTX) have a thin coating as seen in **Figure 5-2**.

HNTs often stacked together, with small clusters and aggregated clumps that may have

resulted due to the drying preparation step required for electron microscopy.
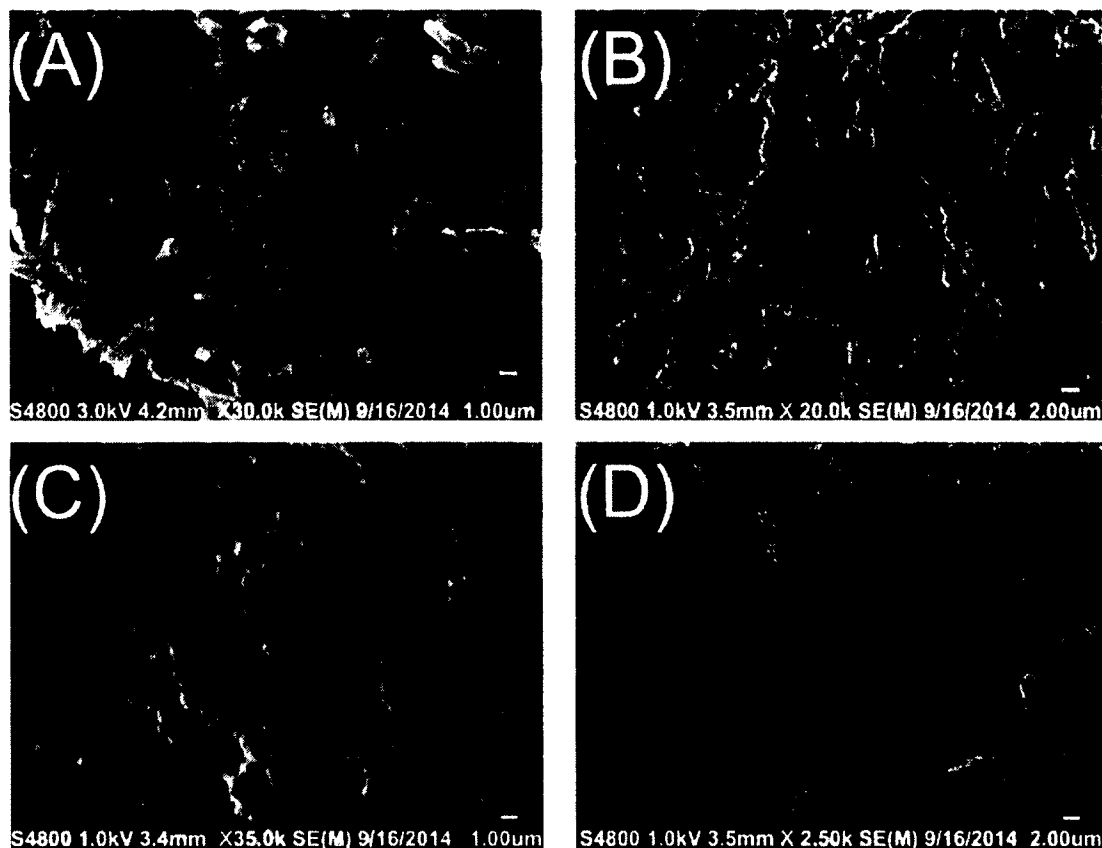
Figure 5-2: Scanning electron microscopic images of uncoated HNTs (A) and HNTs that have been coated HNT/(PVP/PAA)₃/MTX)(B), (C), and (D). Coated HNTs are visible in Figure (B) and (C) (arrows). Clusters of coated HNTs were seen in figure (C) and larger aggregate clumps (D) were observed and may have formed during processing for SEM.

Visual confirmation that coated and drug coated HNTs were successfully mixed into nylon-6 is clearly visible in **Figure 5-3**. There were noticeable changes in contrast and color of the coated HNT/nylon composites after being air-dried overnight, the formic acid evaporated completely leaving only the complex of HNT/(PVP/PAA)₃/nylon and HNT/(PVP/PAA)₃/MTX/nylon (**Figure 5-3**). Compared to HNT/(PVP/PAA)₃/nylon, the yellow color of the HNT/(PVP/PAA)₃/MTX/nylon suggests that MTX had been released. Results from the Live/Dead cytotoxicity and cell proliferation tests support this observation.
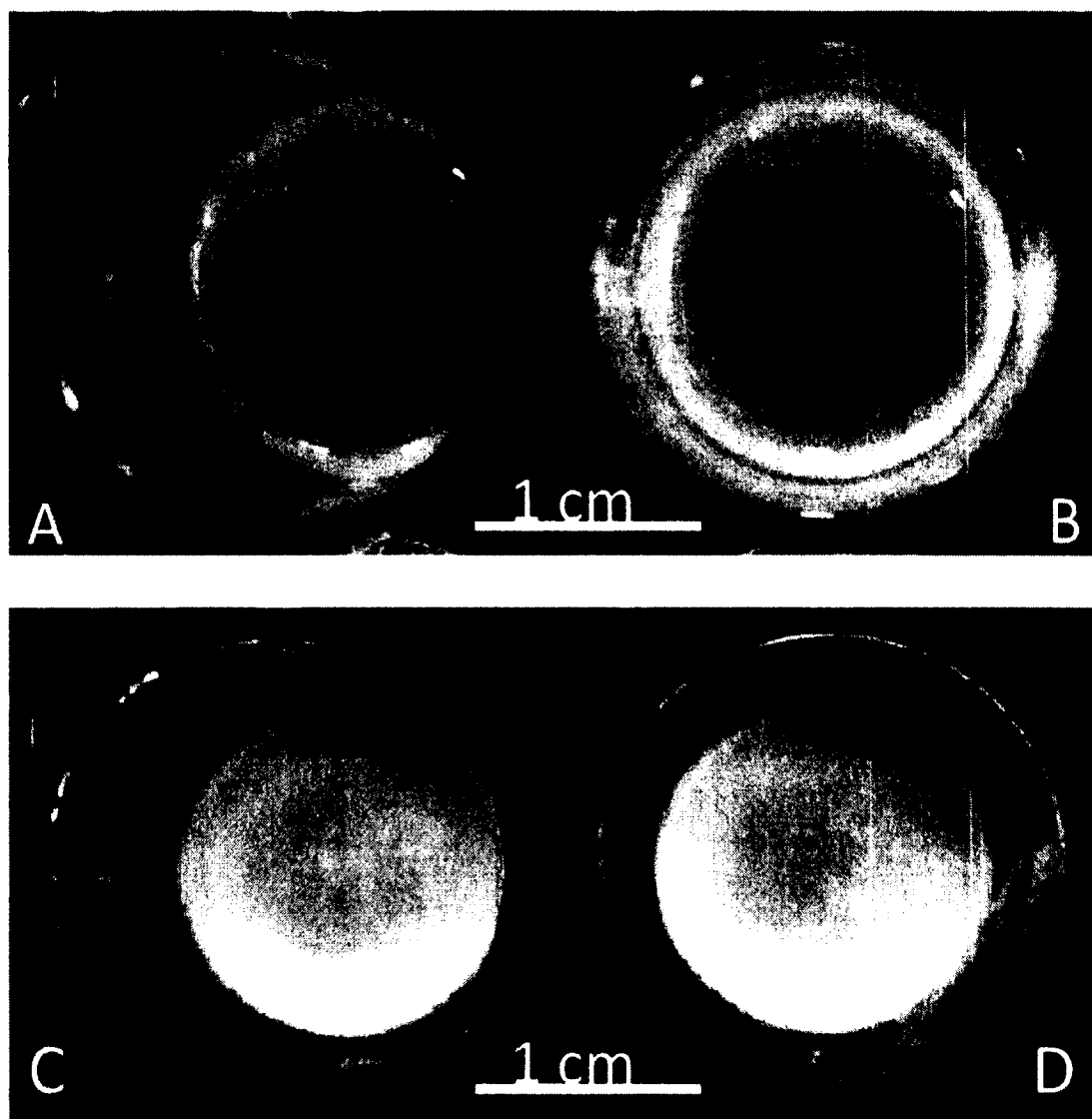
Figure 5-3: Time-lapse images of the air-dried coated HNT composites (A, C). HNT/(PVP/PAA)₃ (white disks) vs. (B, D) HNT/(PVP/PAA)₃/MTX (yellowish tint).Nylon-6 solution (20% w/w) was treated with formic acid. HNT/(PVP&PAA)₃ and HNT/(PVP/PAA)₃/MTX (3% w/w) were then thoroughly mixed into the nylon-6solution, then poured into a 24-well plate, and air-dried and observed after a 24 hours period.

5.3.2   Drug Release from HNTs

During drug elution monitoring, the HNT/(PVP/PAA)₃/MTX samples showed a

burst release during the first 10 minutes and continued with a steady release that slowly

decreased until a second release peak after 130 minutes, with MTX released at reduced

levels through 160 minutes (**Figure 5-4**). The first release may be from a layer of drugs

positioned on the very outer surfaces of the composites. The second burst release may be

due to the pH of the immersing solution, which can affect the degradation rate of the PEs.

Also, some of the drug molecules may have seeped out from the porous PE structures.

The release study was terminated after 160 minutes, as very little amount of MTX was

being released. DI water, with a neutral pH, was used as the elution medium during the

release test. MTX concentration gradient and the pH of immersing solution are presumed

to have determined the release profile of MTX. Overall, the PE coatings appeared to have

effectively trapped MTX.
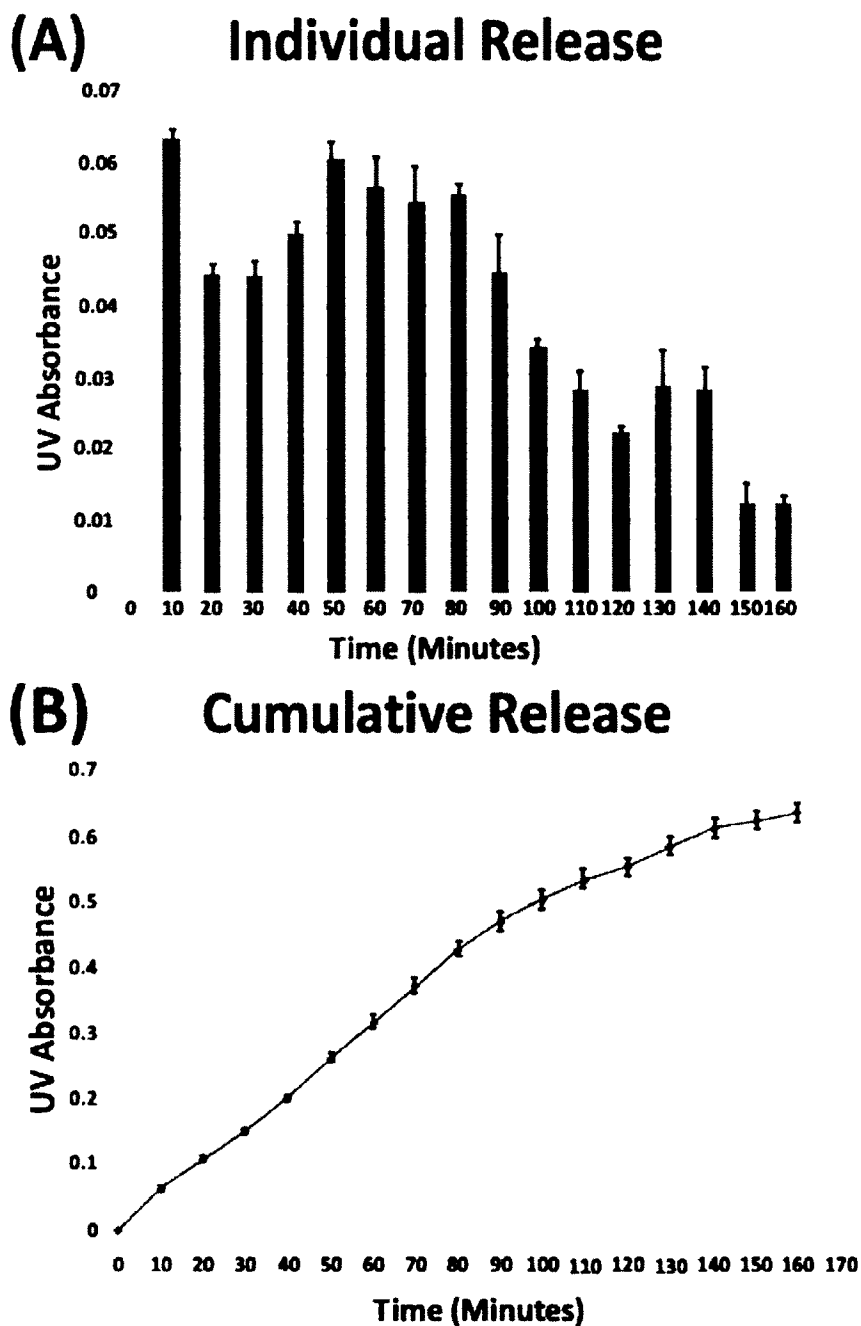
Figure 5-4: Drug release for MTX from HNT/(PVP/PAA)₃/MTX in DI water (pH 7) over 160 minutes. The UV absorbance represents the concentration of MTX in the samples. Figure A displays the amount of drug released at each time point. Figure B shows the cumulative release of all the samples by time point.

5.3.3   Live/Dead Cytotoxicity

Osteosarcoma cells in monolayer culture proliferated and obtained confluence within 2-3

days with little cell death observed (**Figure 5-5** A-C). Osteosarcoma cells were also unaffected by

the addition of HNTs (**Figure 5-5** D-F). Cells proliferated and achieved confluence comparable to

normal, untreated cells (compare **Figure 5-5** B and C with **Figure 5-5** E and F).
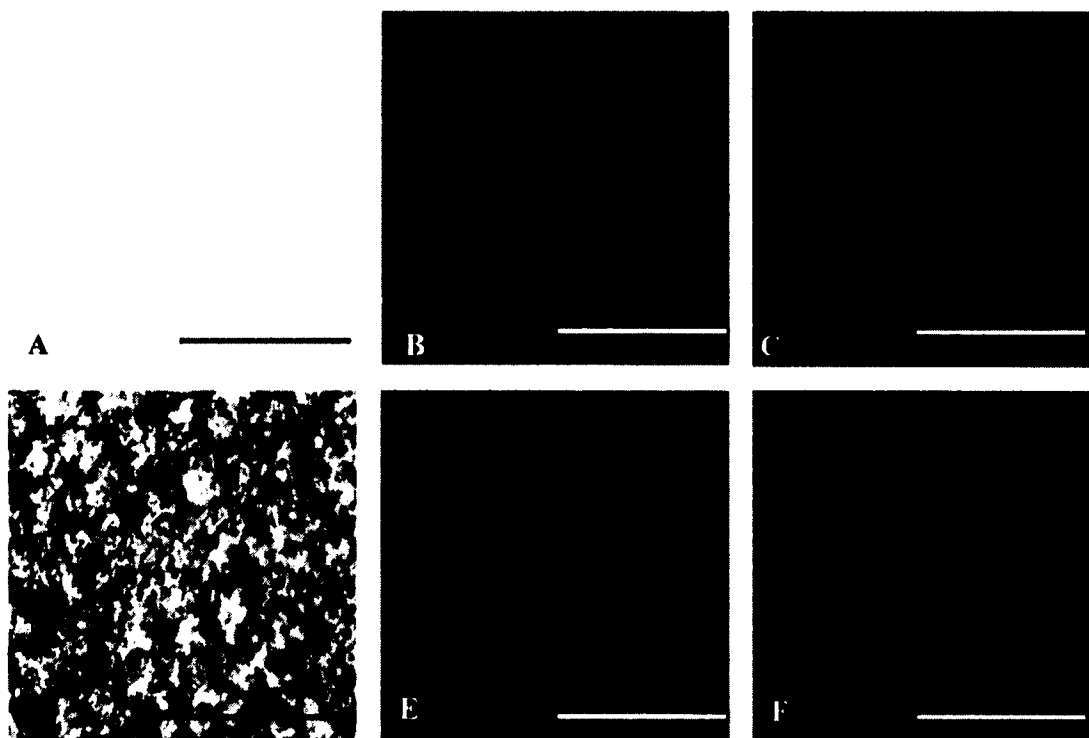
Figure 5-5: Cytotoxic response to HNTS. (A-C) Group 1:Osteosarcoma cell cultures with no HNT addition. (D-F) Group 2: Osteosarcoma cells exposed to HNTs at a concentration of 2000 ug/ml). A, D = Phase contrast, B,E = Live Dead assay showing live cells (green), C, F = Dead assay showing dead cells (red). The brown coloration in figure 5-5D is due the high concentration of HNTs. Bar = 200 microns.

Coated HNTs (without MTX, control Group 3), HNT/(PVP/PAA)$_3$ coated nanoparticles

could be seen clearly as particulate material (**Figure 5-6** A). Although osteosarcoma cells were

not as confluent as seen in groups 1 and 2, the majority of the cells were observed growing and

proliferating with few cell deaths (**Figure 5-6** A-C). In MTX treated groups, the cellular response

was very different (**Figure 5-6** D-F). In group 4, osteosarcoma cells exposed to HNTs with a

(PVP/PAA)₃/MTX coating showed a marked reduction in cell growth as compared to controls

(Group 3). However, only a few dead cells were observed (**Figure 5-6** F).
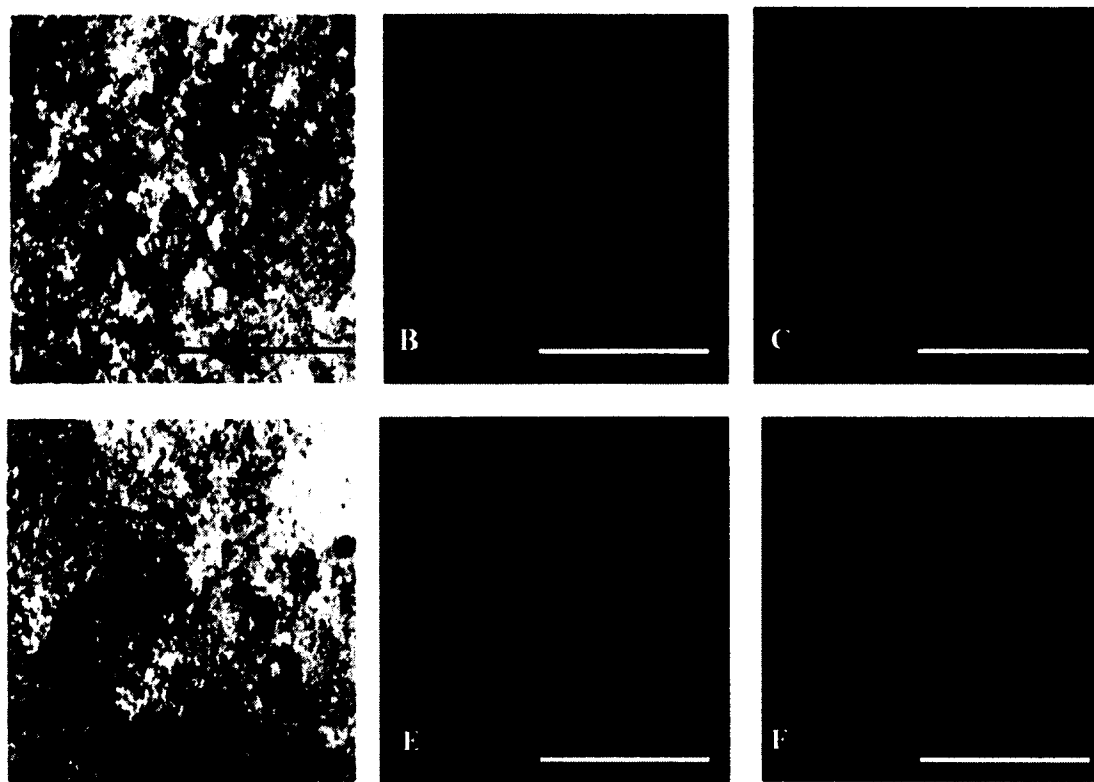
Figure 5-6: Cellular response to PE coated HNTs and HNTs coated with PEs and MTX. (A-C) Group 3: Osteosarcoma cells were exposed to HNT/(PVP/PAA)₃ (2000 ug/ml). (D-F) Group 4: Osteosarcoma cells were exposed to HNT/(PVP/PAA)₃/MTX (2000 ug/ml). A, D = Phase contrast, B, E = Live/Dead assay showing live cells (green), C, F = Live/Dead assay showing dead cells (red). Bar = 200 microns.

When HNTs coated with (PVP/PAA)₃ were embedded in nylon-6, results also

showed a low cytotoxic effect, as cells grew to confluence with little cell death (**Figure**

5-7 A-C). In contrast, cells exposed to HNT/(PVP/PAA)₃/MTX/nylon grew but

proliferation was inhibited with only a few dead cells observed (**Figure 5-7** D-F).
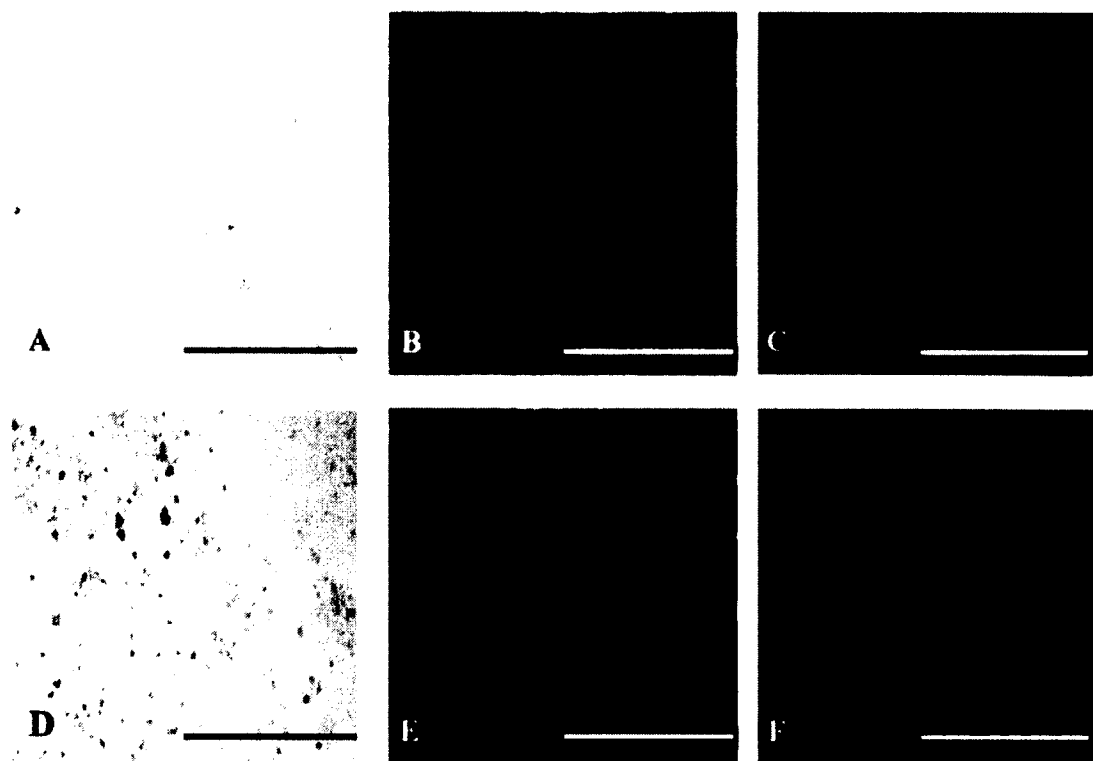
Figure 5-7: Cellular response to coated HNTs embedded in nylon. (A-C) Group 5: Osteosarcoma cells were exposed to HNT/(PVP&PAA)$_3$/nylon (10 mg/ml)). (D-F) Group 6: Osteosarcoma cell were exposed to HNTs/(PVP&PAA)$_3$/MTX/nylon (10 mg/ml). A, D = Phase contrast, B, E = Live/Dead assay showing live cells (green), C, F = Live/Dead assay showing dead cells (red). Bar = 200 microns.

5.3.4   Cell Proliferation Assay

The result of the cell proliferation assay is shown in **Table 5-1**. The values of Groups 1, 2 and 5 were very similar suggesting that HNTs and HNT/(PVP/PAA)$_3$/nylon did not provoke an anti-proliferative response. Groups 3, 4 and 6 showed a reduction in cell proliferation, which can be attributed to the degraded polyelectrolyte layers (in Groups 3 and 4) and MTX released from the drug coated HNTs composites (in Groups 4 and 6).

Table 5-1: Control and experimental groups and their coating architecture with results of the cellular proliferation assays.

Group	Treatment	Value
Control	(DMEM only)	0.290 ± 0.000
Group 1	Normal cells	1.987 ± 0.074
Group 2	HNTs only	2.118 ± 0.154
Group 3	HNTs/(PVP&PAA)$_3$	1.114 ± 0.097
Group 4	HNTs/(PVP&PAA)$_3$/MTX	0.924 ± 0.103
Group 5	HNTs/(PVP&PAA)$_3$/nylon-6	1.895 ± 0.288
Group 6	HNTs/(PVP&PAA)$_3$/MTX/nylon-6	1.162 ± 0.120
Sixteen samples were used in each of the group (except group 2 which has 14 cases as two outliers were removed) for the cellular proliferation tests. The absorbance value is directly related to the number of viable cells.		

As shown in **Figure 5-8**, when exposed to uncoated HNTs and coated HNTs (+/-MTX), cellular response among these groups was significantly different. Compared with the group of normal cells, cell proliferation was higher in the group of HNTs and stayed the same in the group of HNT/(PVP/PAA)$_3$/nylon, whereas it became lower in the other groups. A significant reduction was shown in the group of HNT/(PVP/PAA)$_3$/MTX/nylon, and a further reduction was seen in both groups of HNT/(PVP/PAA)$_3$ and HNT/(PVP/PAA)$_3$/MTX. The result of statistical analysis is shown in **Table 5-1**. SPSS (22.0) was applied with one-way ANOVA, and the normality ($P>.05$) and homogeneity ($P=.044$) were checked. Significant differences ($P=.000$) were seen among the groups, and subsequent Post Hoc tests were used to show the specific difference among the groups (**Table 5-2**). Overall, the pattern in cell proliferation mirrors that observed in the cytotoxicity analyses.

Results of The Cellular Proliferation Assays
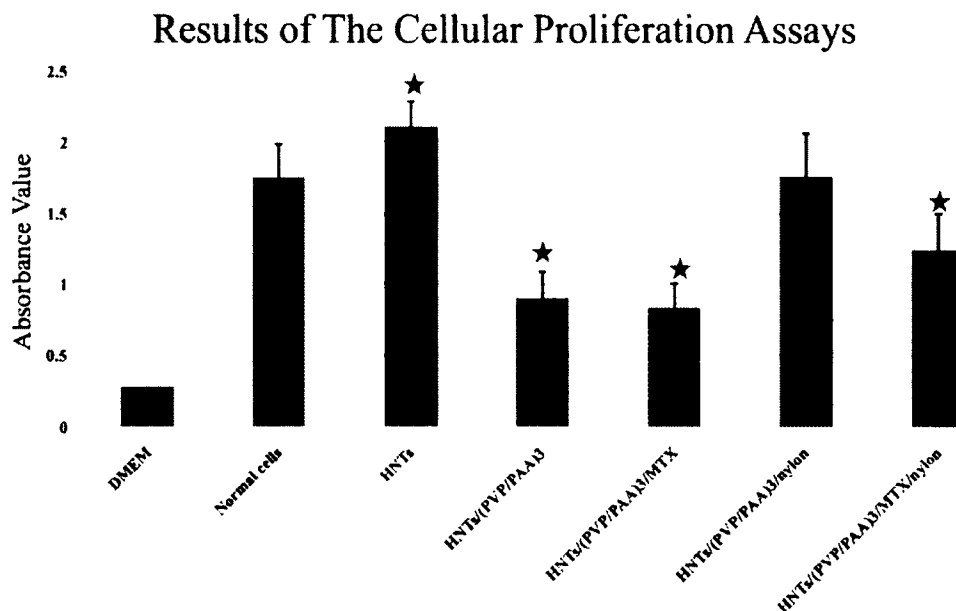
Figure 5-8: Sixteen samples were used in each group (except Group 2 which has 14 cases as two outliers were removed) for the cellular proliferation tests. The absorbance value is directly related to the number of viable cells. From left to right, the groups are: DMEM Control, Group 1 (Normal cells), Group 2 (HNTs), Group 3 (HNT/(PVP/PAA)$_3$), Group 4 (HNT/(PVP/PAA)$_3$/MTX), Group 5 (HNT/(PVP/PAA)$_3$/nylon), and Group 6 (HNT/(PVP/PAA)$_3$/MTX/nylon). Statistical analysis was applied with IBM SPSS 22.0, and the stars indicate a significant difference exists when compared with Group 1.

Table 5-2: Template for inserting tables.

Comparison	Significant Difference (P value)
Group 1 Vs. Group 2	P = .000
Group 1 Vs. Group 3	P = .000
Group 1 Vs. Group 4	P = .000
Group 1 Vs. Group 5	P = .803
Group 1 Vs. Group 6	P = .000
Group 3 Vs. Group 4	P = .409
Group 3 Vs. Group 5	P = .000
Group 4 Vs. Group 6	P = .000
Group 5 Vs. Group 6	P = .000
IBM SPSS (22.0) and one-way ANOVA were used for the statistical analysis.	

5.4 Discussion

In previous papers, the luminal porosity of HNTs has been estimated to be around

0.25 ml/g, while the outside surface area of HNTs has been shown to be about 57 m^2/g

[53]. It is apparent that the HNT lumen has space limits for drug loading. Attempts have

been made to enlarge the HNT lumen to increase drug loading by acid etching, and while

increases in drug loading capacity were observed, there are limits to how much drug may

be loaded with this technique [54]. The outer HNT surface provides significantly more

potential surface area for drug loading, especially if the surface has been modified or

coatings have been applied onto (or around) the outer surface. In HNTs, silica is mainly

distributed on the outer surfaces, whereas alumina is mainly positioned on the inner

surface and edges of the tubule. Upon exposure to water, the outer surface will have a

negative charge over a wide range of pH (2~10), so at an appropriate pH above 2,

halloysites' negatively charged outer surface permits sequential adsorption of positive

and negative charged polyelectrolytes [53].

When immersed in water, PVP is positively charged [55] and PAA is negatively

charged [56]. Accordingly, we used the outer HNTs surface rather than the inner luminal

space of HNTs to load and release MTX using a scheme for coating HNTs with

sequential layers of positively charged PVP and negatively charged PAA [57]. In this

way, the PE coatings provide a means for controlling both the location of the drug and

the pattern of drug release. The data showed high concentrations of MTX were absorbed

during the coating process, as little MTX was discernable in the acidic loading solution

(pH=2) after coating process. This supports the conclusion that the majority of the MTX

molecules had been attached to the PE layers or trapped within the pore spaces. The two

different burst releases seen in the UV-vis release data, suggests that the PE layers may have become more porous during fabrication. The first burst release of MTX may have come from the MTX molecules attached to the outside surface of the clumped material. The second burst release might have occurred because of slow degradation of the PE layers, which liberated more MTX molecules subsequently. Another important factor to consider is the rate of MTX that is consumed by the environment, which may affect the length of drug release.

Cytotoxicity assays showed that osteosarcoma cells proliferated in the presence of untreated HNTs and few cells died even after exposure to a very high concentration of HNTs (2 mg/ml). This is consistent with previous studies where halloysite nanotube exposure had little negative impact on cell growth or functionality [83-84]. Furthermore, HNTs coated with PVP and PAA which was further mixed within nylon-6 (HNT/(PVP/PAA)$_3$/nylon) also showed little to no cytotoxic effect. In the other groups, HNT/(PVP/PAA)$_3$, HNT/(PVP/PAA)$_3$/MTX, and HNT/(PVP/PAA)$_3$/MTX/nylon showed little cytotoxicity, with only a few dead cells observed with the Live/Dead cytotoxicity assay. However, their cellular proliferation was significantly reduced.

Statistical analysis showed that Group 2 (HNTs, P=.000), Group 3 (HNT/(PVP/PAA)$_3$, P =.000), Group 4 (HNT/(PVP/PAA)$_3$/MTX, P =.000), and Group 6 (HNT/(PVP/PAA)$_3$/MTX/nylon, P =.000) are significantly different from Group 1 (Normal cells), which means the cell proliferation was significantly higher in Group 2 and reduced in Groups 3, 4, and 6. In Group 2, it seems that HNTs had a stimulant effect on the cells, as the mean was higher than that in Group 1. Although there was no MTX in Group 3, the reduction of cell proliferation might be caused by the interaction between

hydrolyzed polymers and amino acids in the medium which led to a subsequent failure of cell proliferation. In Group 4, besides the effect of hydrolyzed polymers, the release of MTX further reduced the cell proliferation, but did not kill the cells. As there was no difference between Groups 1 and 5 (P=.803) which means the composites of HNT/(PVP/PAA)$_3$/nylon had no effect on the cells, the reduction of cell proliferation in Group 6 could only be explained as the release of MTX. The same principle could be used to explain the difference between Groups 5 and 6 (P=.000). No difference was shown between Groups 3 and 4 (P=.409), as both hydrolyzed polymers and MTX could only stop cell proliferation but not kill them. Group 5 was significantly different from Group 3 (P=.000), because the nylon structure could well trap hydrolyzed polymers which prevent their interaction with amino acids inside the medium. But it could not completely restrain the release of MTX into the medium, which caused a limited reduction of cell proliferation in Group 6 when compared with Group 4 (P=.000).

In sum, morphological observations, cytotoxicity and proliferation assays support the conclusion that MTX was released from HNT/(PVP/PAA)$_3$/MTX and HNT/(PVP/PAA)$_3$/MTX/nylon composites and subsequently altered osteosarcoma cell morphology and inhibited cell proliferation, which provided support for its potential use as a drug delivery vehicle. Our drug releasing system offers other advantages, including carrying a higher drug load as compared with using a vacuum to load drugs into the HNT lumen. When drug doped HNTs are added to different polymers there is a point where addition of increased amounts of doped HNTs (to increase drug load) decreases material properties (tensile resistance, adhesion, etc.) [94-95]. Our method has the potential to overcome this by placing the appropriate (required) drug-load on the surface of the

HNT/PEs, thus offering no challenges to material properties. Preliminary experiments with MTX release from nylon-6 are suggestive that this method of drug incorporation may also be applied to other polymers.

Current studies are directed at refining the specific PE shell structure with the intent to increase/decrease the loading ability of HNTs, speed up/down drug release, and enable doping with multiple drugs. As we have shown, chemotherapeutic drugs can be doped into HNT/polymer mixtures such as Nylon-6 and still retain an anti-cancer cell effect. This offers much promise for the incorporation of drug coated HNTs into a variety of medical grade, biocompatible synthetic polymers and/or natural proteins for use in anti-infective, chemotherapeutic or histiogenic catheters, gauze, sponges, and sutures.

5.5 Conclusion

Halloysite nanotubes did not provoke a cytotoxic effect on osteosarcoma cells nor inhibit their proliferation ability up to a concentration of 2000 ug/ml. Methotrexate was incorporated into a PE coating and was observed to be released from the coating. Released MTX resulted in altered cell behavior including morphological changes in osteosarcoma cells and a reduction in cell proliferation. After the MTX-coated HNTs were mixed with nylon-6, the releasing ability of MTX was preserved, and the released MTX also altered osteosarcoma cell behavior and inhibited cell proliferation. As a nanocomposite drug delivery system, MTX coated HNTs show a potential for the delivery of antitumor drugs. While MTX was the drug used in this study, there is also a potential for the system to incorporate other drugs. The system also has the potential to insert drugs at different coating depths that may permit multiple, combinatorial or even sequential release depending on coating architecture and composition.

CHAPTER 6

POTENTIAL APPLICATION OF USING HALLOYSITE NANOTUBES BASED SUTURES IN THE PREVENTION OF SURGICAL SITES INFECTION

6.1   Introduction

In this chapter, another application was used to verify the feasibility of using halloysite nanotubes (HNTs) based drug delivery system in the medical field. The hypothesis was that nitrofurantoin (NFT) coated halloysite composites could release the drug in a sustained manner and efficiently inhibit bacterial proliferation, which showed a potential in the prevention of surgical site infection (SSI).

6.1.1   Surgical Site Infection

Surgical site infection is a postoperative complication feared in surgery, and can lead to considerable consequences for patients and high medical cost for society [96-97]. It is a common healthcare-associated infection (HCAI), and accounts for about 16% of the total HCAI [39]. In the United States, approximately five million cases of SSI occur every year, leading to an average of 7.3 extra days in hospital, and over 1.6 billion dollars of additional hospital charges [40]. A prospective study from Spain [58] showed that SSI happened to 9.02% of the total people who underwent surgery. Their stays were prolonged by 14 days, and the excess hospital costs were $10,232 per patient. What is worse, health costs only accounted for 10% of overall costs, and there was an extra

$97,433 per person from indirect social costs. SSI has become a serious cause of morbidity, emotional stress, and financial cost to the affected patients and health care institutions [43]. Appropriate strategies, technologies, and agents are needed to improve surgical treatment and save unnecessary direct health costs as well as indirect social costs.

6.1.2   Nitrofurantoin and Drug Delivery

One Italian study for epidemiology and microbiology of surgical wound infections included 676 patients with signs and symptoms indicative of infections, and showed common pathogens that included *S. aureus*, *P. aeruginosa*, *E. coli*, *S. epidermidis*, and *E. faecalis* [59]. Nitrofurantoin (NFT) is an antibiotic which has been proven effective against many bacterial pathogens including *E. coli*, *S. aureus*, and *E. faecalis* [60]. Because of low rate of resistance, more and more attention has been focused on NFT. NFT exerts greater effects on bacterial cells than mammalian cells, and the development of resistance to its effects is low because of its involvement in many different processes important to bacterial cells. For example, acquired resistance in *E. coli* continues to be rare [60]. However, it also has some shortcomings, which seriously limit its usage. The peak blood concentration of NFT following an oral dose of 100 mg is less than 1 ug/ml, and tissue penetration is negligible. It can be metabolized by the liver rapidly, and is excreted mainly in urine. Therefore, it is used mostly in urinary tract infections. The application of a newly formed HNTs based drug delivery system could potentially improve this situation. Given its low tissue penetration and broad antibacterial function in the pathogens related to surgical site infection, NTF was used as a model drug loaded in the HNTs system and showed potential against *E. coli* to prevent SSI.

6.1.3   Electrospun Nanofibers and Sutures

Because of the rapid development of nanoscience and nanotechnology over the past decades, there are many advances made not only in preparation and characterization of nanomaterials, but also in their functional applications [61]. One example is the application of nanofibers, which have been widely studied in the biomedical field, including drug delivery. Their advantages are obvious, such as 1) drug loading is easy to implement via electrospinning process; 2) the high applied voltage used in the electrospinning process has negligible influence on drug activity; 3) they have high specific surface area and short diffusion passage length which give the nanofiber drug delivery system higher overall release rate than bulk materials; 4) the release profile can be finely controlled by modulation of nanofiber morphology, porosity and composition [61]. Therefore, electrospun nanofibers containing a HNTs based drug delivery system was used to form a scaffold, which could be potentially developed into sutures and widely used in surgeries. In this way, a local and sustained release of antibiotics is expected to prevent potential SSI after surgery.

6.2   Materials and Methods

6.2.1   Materials

Halloysite nanoclay ($H_4Al_2O_9Si_2 \cdot 2H_2O$, MW 294.19), Nitrofurantoin ($C_8H_5N_4O_5$, MW 238.16 g/mol), Sodium hydroxide solution (1 N), Hydrochloric acid solution (1 N), Polyvinylpyrrolidone ((C_6H_9NO)x, Molecular Weight~1,3000,000), Poly(acrylic acid) solution (Molecular Weight~250,000, 35 wt.% in H2O), Nylon-6 (($C_6H_{11}NO$)n, mp 220 ℃), LB Broth, and E. coli were obtained from Sigma Aldrich, St. Louis, MO.

6.2.2   Light Sensitivity Test and Standard Calibration Curve

According to the product instruction, nitrofurantoin is sensitive to light, and the impact of light exposure on NFT needs to be examined first. Saturated NFT solution was prepared, and its initial UV-Vis absorbance value was measured. Then, the solution was kept under routine laboratory conditions without light protection. Samples of the NFT solution were collected and measured by UV-Vis every 24 hours. The results were analyzed with IBM SPSS 22.0 to find any significant change during the light exposure.

To establish a standard calibration curve for the relationship between NFT concentration and absorbance value, several NFT solutions with different known concentrations were used (**Table 6-1**). Then, the standard calibration curve for NFT was made through Excel (2007 Version).

6.2.3   Composite Fabrication

In Chapter 4, three common fabrication methods were compared, and the LbL coating was proven to be best in performance of both loading and releasing. Therefore, the LbL coating was used to prepare HNTs for NFT loading. Polyvinylpyrrolidone (PVP) and Poly(acrylic acid) (PAA) were used for the initial 18 layers of LbL coating on the outside surface of HNTs. Then the HNT/polymer composites were air dried and crushed into fine powders. Next, 500 mg of HNT/polymer composite was immersed into 5 ml acetone, which contains NFT at the concentration of 4 mg/ml. A stir bar was used to keep stirring the suspension, which could help increase the contact between NFT and HNT/polymer composite. After 24 hours, the suspension was centrifuged, and the supernatant was removed. The sediment was air dried and crushed into fine powders for later use.

6.2.4   Morphological Analysis: SEM

Pure HNTs and coated HNT/NFT composites were examined using a scanning electron microscope (Hitachi S-4800) to show the morphological change on the surface.

6.2.5   Drug Release Test

Twenty five milligram HNT/(PVP/PAA)$_9$/NFT or reformed nylon composite containing 25 mg HNT/(PVP/PAA)$_9$/NFT were immersed into 5 ml DI water. The suspension was kept shaking for 10 minutes, and then centrifuged to collect the supernatant for UV-Vis absorbance measurement. Residual supernatant was removed, and fresh DI water was replenished. The process was repeated until slight amounts of NFT were detected. NFT was assessed by spectroscopic measurement at 370 nm.

6.2.6   Test Bacterium

For *in vitro* studies *E. coli* was used. The test strain was susceptible to NFT (MIC 32 ug/ml). *E. coli* was cultured within LB broth at 37 °C before testing.

6.2.7   Anti-Proliferation Tests

E. coli cells were resuspended in regular LB broth and adjusted to 1×10^8 cfu/ml by OD_{600} measurement. Then bacterial suspensions (3 ml) with regular broth and test samples (Grouping seen in **Table 6-1**) were prepared in sealed plastic capillaries. Samples were incubated for 6 hours at 37 °C, and OD_{600} spectroscopic measurement was used to determine the changes of cellular density in each sample.

77

Table 6-1: Grouping of samples for anti-proliferation test.

Groups	Abbreviation	Standing for
Control	C	Blank Control
Sample 1	H	Pure HNTs
Sample 2	HP	HNT/(PVP/PAA)$_9$
Sample 3	HPN	HNT/(PVP/PAA)$_9$/NFT
Sample 4	N	Nylon-6
Sample 5	HPn	HNT/(PVP/PAA)$_9$/Nylon-6
Sample 6	HPNn	HNT/(PVP/PAA)$_9$/NFT/Nylon-6

6.3   Results

6.3.1   Standard Calibration Curve for NFT

As the nanodrop 2000c only has reliable accuracy when the absorbance value lies between 0 and 1, samples with high concentration were diluted before absorbance measurement. **Table 6-2** and **Figure 6-1** show the results of the standard calibration curve for NFT. A clear linear relation between NFT concentration and absorbance value was built within the spectroscopic range between 0 and 1, which is reliable (R^2=0.999) and was used for other tests.

Table 6-2: Standard calibration curve for NFT (wavelength: 370 nm).

Concentration (ug/ml)	.5	1.0	1.5	2.0	2.5	3.0	3.5	4.0	4.5	5.0
Absorbance Value	.037	.076	.113	.154	.193	.229	.272	.308	.345	.384
Standard Curve	y = .077x - .001 (R^2 = .999, y-absorbance value, x-NFT concentration (ug/ml))									

Standard Calibration Curve of Nitrofurantoin

Chart showing linear calibration line with equation $y = 0.077x - 0.001$ and $R^2 = 0.999$; x-axis "Concentration (ug/ml)" from 0 to 6, y-axis "Absorbance" from 0 to 0.45.
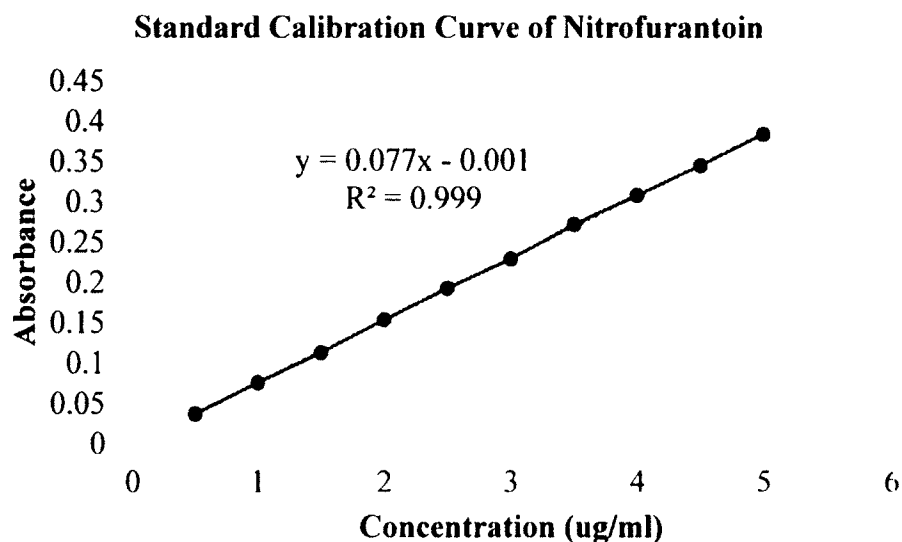
Figure 6-1: Standard Calibration Curve for NFT. A reliable (R^2=.999) linear relation between NFT concentration (ug/ml) and absorbance (370 nm) value showed up within the spectroscopic range of 0 to 1.

6.3.2   Light Sensitivity Test for NFT

The light sensitivity test lasted three days (**Table 6-3**), and a declining trend of absorbance value could be clearly seen (**Figure 6-2**), which means NFT would degrade slowly on light exposure. S analysis was applied, and the result shows that the sample had been statistically different from its original status since the second day. On the other hand, it also shows that NFT could not degrade completely in 24 hours. The majority of NFT molecules stayed in solution (**Table 6-3**). For practical purposes, the degradation could be ignored if all the required processes could be finished in one day.

Table 6-3: Light sensitivity test for NFT (wavelength: 370 nm).

	Day-0	Day-1	Day-2	Day-3
Sample 1	.613	.587	.583	.565
Sample 2	.612	.600	.588	.569
Sample 3	.617	.593	.587	.573
Mean	.614	.593	.586	.569
SD	.003	.007	.003	.004
P	N/A	.002	.000	.000

(1) One-way ANOVA (IBM SPSS 22.0) was used to analyze the statistic difference among these data.
(2) SD stands for standard deviation.
(3) All the samples of NFT solution were 10 times diluted.
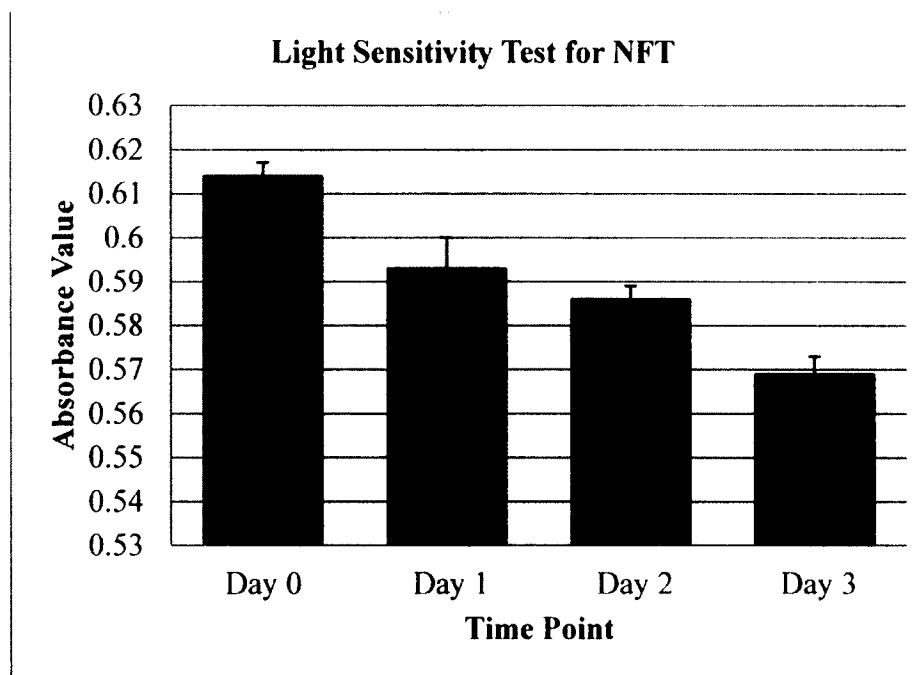
Figure 6-2: Result of light sensitivity test for NFT. A clear declined trend of the absorbance value is seen, which means NFT degraded slowly because of light exposure.

6.3.3   Drug Coating

Electron scanning is a direct way to show the morphological change on the outside surface of HNTs after the fabrication process. Pure HNTs (**Figure 6-3** A and B) showed smooth outside surface, though some tubes had already shown a bright layer because of absorption of water from air which could be seen as kind of contamination. NFT coated HNTs (**Figure 6-3** C and D) also showed a bright layer on the outside as the arrow pointed. The halloysite particle inflated and the tubular structure disappeared. Some tubes clumped together, while the majority stayed uncoated, which suggested huge loading potential for further fabrication.
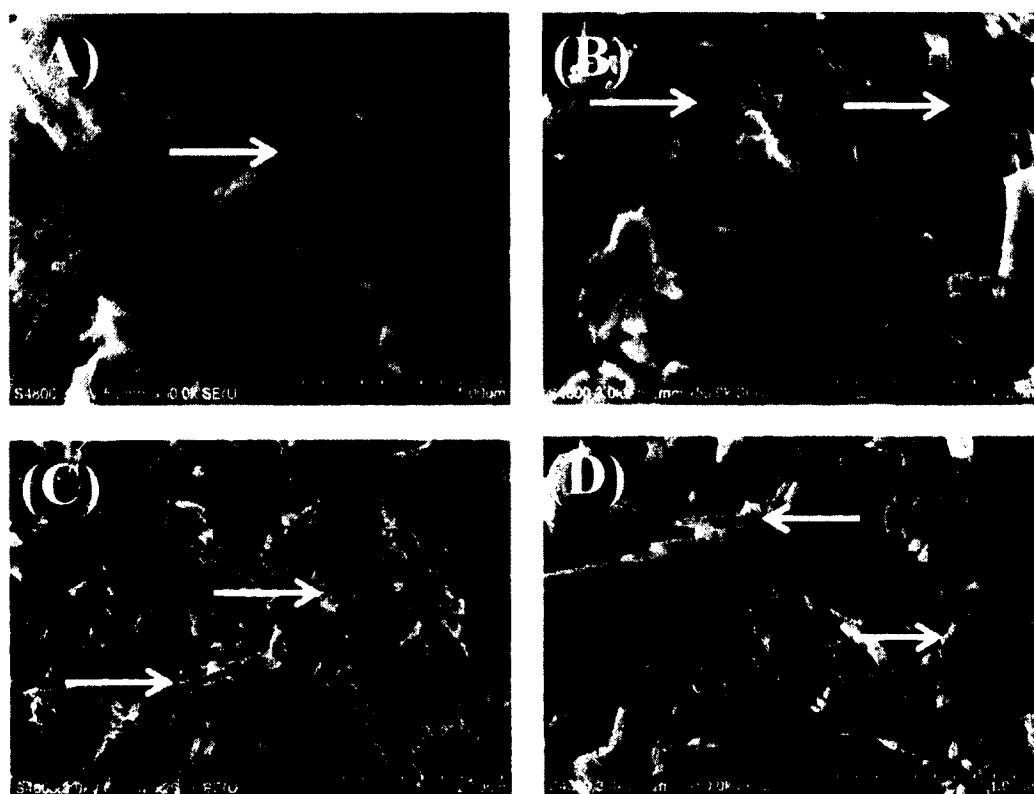
Figure 6-3: Electron scanning images of HNTs and coated HNTs. (A) and (B) are pure HNTs, while (C) and (D) are coated HNTs (HNT/(PVP/PAA)$_9$/NFT).

An indirect method was used to measure the loading amount of NFT on

HNT/(PVP/PAA)$_9$ composites. 25 mg HNT/(PVP/PAA)$_9$/NFT was immersed into 500 ml

DI water for a complete release of NFT. Sample solution was collected, centrifuged, and

measured by UV-Vis spectroscopy. According to the above relationship between the NFT

concentration and absorbance value, the result of .030 could be translated into .403

ug/ml, and the released NFT was 201.3 ug. In this way, 1 mg HNT/(PVP/PAA)$_9$/NFT

was calculated to carry about 8.1 ug NFT.

6.3.4 Drug Release from HNTs

HNT/(PVP/PAA)$_9$ and HNT/(PVP/PAA)$_9$/NFT composites were directly mixed

within nylon-6 solution (formic acid) individually (**Figure 6-4** A). After complete

evaporation of formic acid, sample disks (pure nylon-6, HNT/(PVP/PAA)$_9$/nylon-6, and

HNT/(PVP/PAA)$_9$/NFT/nylon-6) were formed (**Figure 6-4** B). 25 mg

HNT/(PVP/PAA)$_9$/NFT and sample disks which contain 25 mg HNT/(PVP/PAA)$_9$/NFT

were immersed into 5 ml DI water for NFT release test.
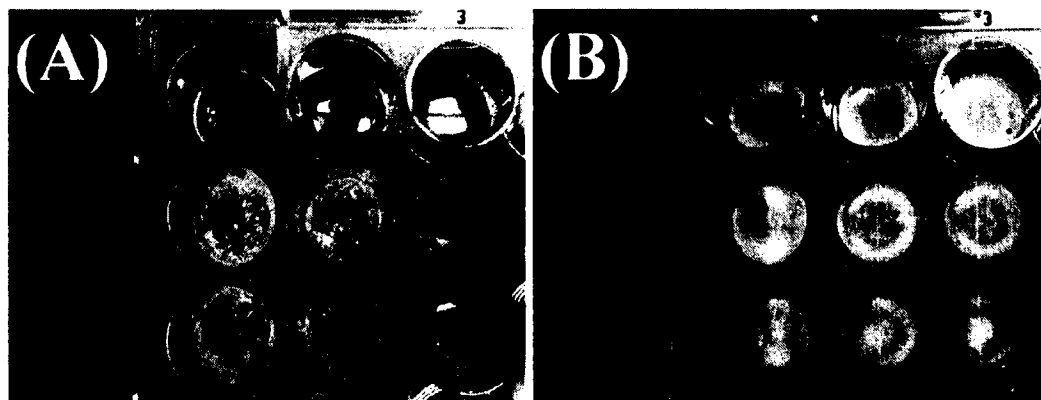
Figure 6-4: Incorporation of nylon-6 with HNT/(PVP/PAA)$_9$ and
HNT/(PVP/PAA)$_9$/NFT composites. Groups: nylon-6 (Row A), HNT/(PVP/PAA)$_9$
(Row B), and HNT/(PVP/PAA)$_9$/NFT (Row C). After the complete evaporation of
formic acid, sample disks formed.

In **Figure 6-5**, the release cycles for both HNT/(PVP/PAA)$_9$/NFT and

HNT/(PVP/PAA)$_9$/NFT/nylon-6 ran 14 times as no more released NFT could be detected

by the nanodrop. There was a burst release in both of groups, and the one of

HNT/(PVP/PAA)$_9$/NFT was much higher than the other (**Figure 6-5** A). Then the release

decreased sharply at the second and third cycle, after which it went mildly until the end.
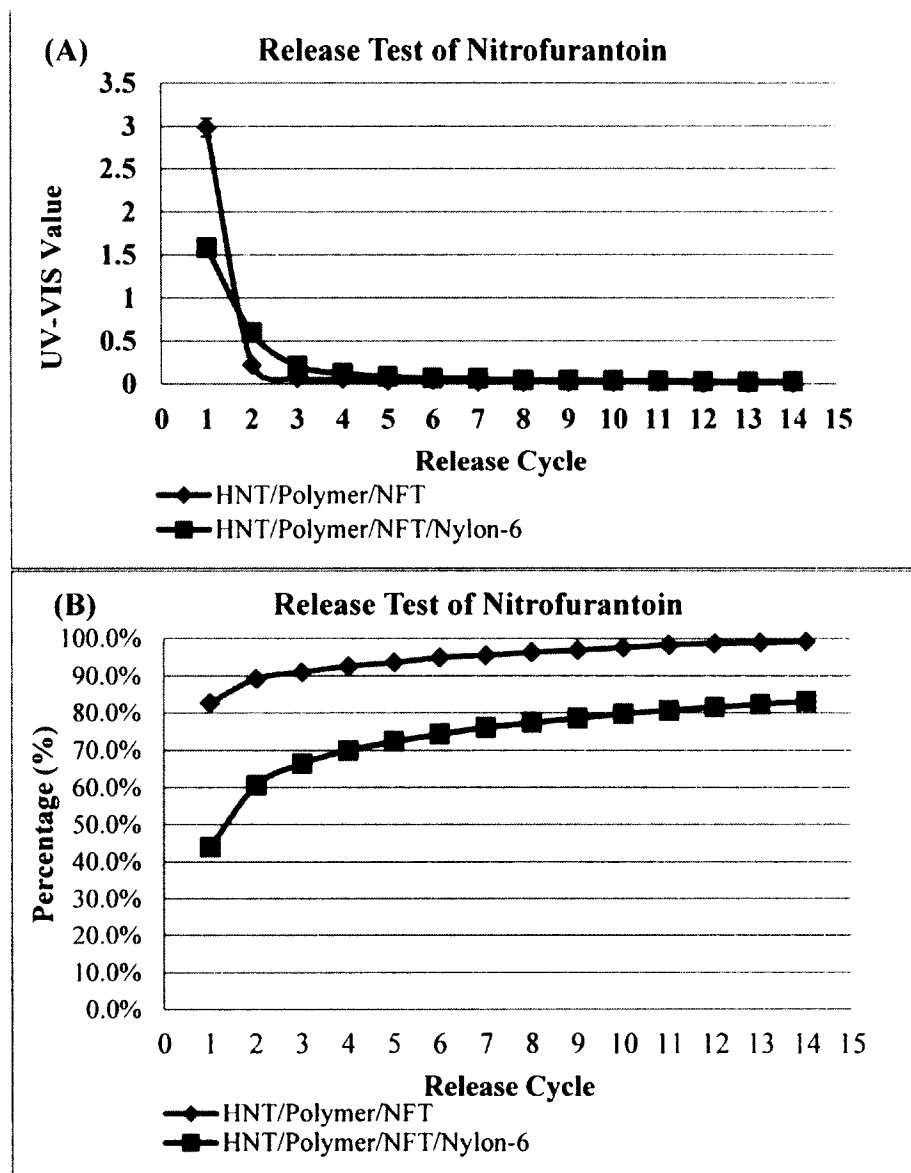
Figure 6-5: Release test of NFT. The total release cycle ran 14 times. (A) shows the individual release for each cycle, and (B) shows the total percentage of release by each cycle.

In **Figure 6-5** (B), HNT/(PVP/PAA)$_9$/NFT composites had a higher release percentage than its nylon-6 counterpart, which means by the end of the test, there was still some NFT not released from HNT/(PVP/PAA)$_9$/NFT/Nylon-6, which may help increase the release period.

6.3.5 Bacterial Anti-Proliferation Test

In **Figure 6-6**, (A) and (C) show the initial images of the *E. coli* culture in each group. In the groups of HNT, HNT/(PVP/PAA)$_9$ and HNT/(PVP/PAA)$_9$/NFT, the broths were a little turbid because of the suspension of sample powders. While in the other groups, the broths were relatively clear. Sample powders and disks were clearly seen in the broths.
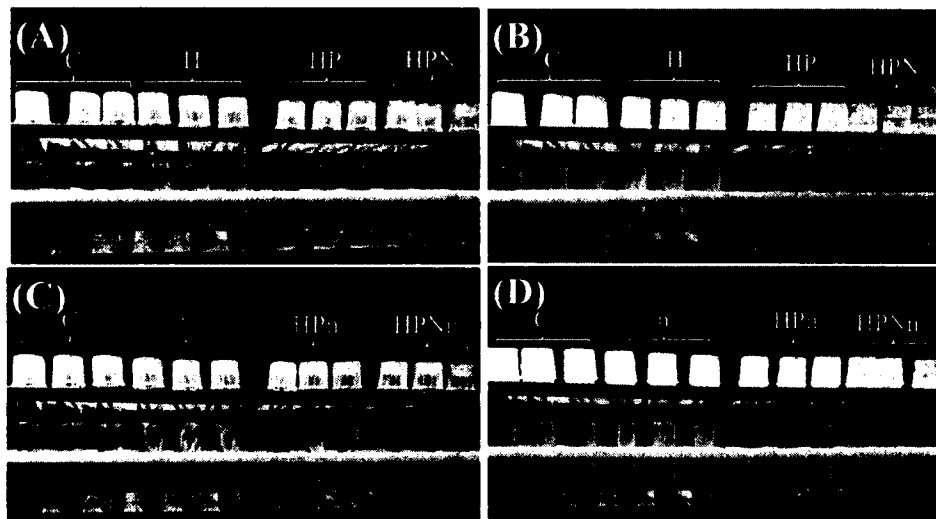
Figure 6-6: Anti-proliferation test of NFT with *E. coli*. Group description: C=Control, H=HNTs, HP=HNT/(PVP/PAA)$_9$, HPN= HNT/(PVP/PAA)$_9$/NFT, N= Nylon-6, HPn= HNT/(PVP/PAA)$_9$/Nylon-6, HPNn= HNT/(PVP/PAA)$_9$/NFT/Nylon-6. (A) and (C) show the initial images of bacterial culture, while (B) and (D) show their images after 6 hours.

Figure 6-6 (B) and (D) show the images of *E. coli* culture of six hours. Except for the groups of HNT/(PVP/PAA)$_9$/NFT and HNT/(PVP/PAA)$_9$/NFT/Nylon-6, all the other

groups present oyster white turbidity, which made them look the same. In group of

HNT/(PVP/PAA)$_9$/NFT, the sample powders were seen in the bottom as sediment. It is

the same with the group of HNT/(PVP/PAA)$_9$/NFT/Nylon-6 where sample disks stayed

intact within the broth.

Table 6-4 and Figure 6-7 show the result of spectroscopic measurement of the

broth in each group at 600 nm. After 6 hours, E. coli proliferated very well in the control

group with a much higher spectroscopic value. In the groups containing tested powders,

the values in both groups of HNT and HNT/(PVP/PAA)$_9$ were higher than that in fhs

control group, while it became very low in the group of HNT/(PVP/PAA)$_9$/NFT. In the

other three groups with tested disks, the values in groups of Nylon-6 and

HNT/(PVP/PAA)$_9$/Nylon-6 were a little lower than the control, and the one in the

HNT/(PVP/PAA)$_9$/NFT/Nylon-6 was much lower, which was also very close to that in

the initial group.

Table 6-4: Result of anti-proliferation test of nitrofurantoin with E. coli.

	E. coli (Control)	HNT	HNT Polymer	HNT Polymer NFT	Nylon-6	HNT Polymer Nylon-6	HNT Polymer NFT Nylon-6
Sample 1	.918	.686	1.236	.131	.906	.853	.045
Sample 2	.914	.681	1.215	.129	.891	.858	.044
Sample 3	.935	.661	1.222	.123	.912	.864	.048
Mean	.922	.676	1.224	.128	.903	.858	.046
SD	.011	.013	.011	.004	.011	.006	.002

(1). OD$_{600}$ value is directly related to the cellular density of E. coli in broth.
(2). The spectroscopic measurement of the initial E. coli was .040.
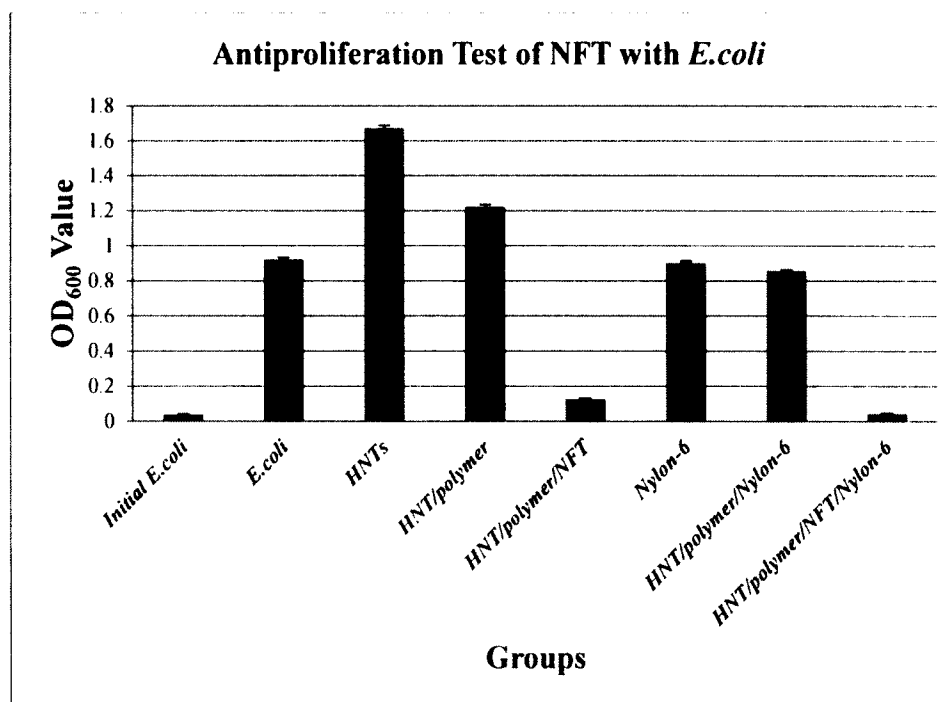
Figure 6-7: Anti-proliferation test of NFT with *E. coli*.

Statistical analysis was applied with one-way ANOVA (IBM SPSS Statistics 22). The initial group was not included in the results as it is not normally distributed. A Shapiro-Wilk's test (P>.05) showed that the spectroscopic values were approximately normally distributed for all the groups. A Levene's test verified the equality of variances in the samples (homogeneity of variance) (P>.05). In **Table 6-5:** Statistical analysis of anti-proliferation test., only the groups of control and Nylon-6 were statistically same, while all the others were different. Additionally, the spectroscopic value in the group of HNT/(PVP/PAA)$_9$/NFT/Nylon-6 was very close to that of the initial, which suggested the bacterial proliferation was completely inhibited.

Table 6-5: Statistical analysis of anti-proliferation test.

	C	H	HP	HPN	N	HPn	HPNn
C	N/A	.000	.000	.000	.199	.000	.000
H	.000	N/A	.000	.000	.000	.000	.000
HP	.000	.000	N/A	.000	.000	.000	.000
HPN	.000	.000	.000	N/A	.000	.000	.000
N	.199	.000	.000	.000	N/A	.001	.000
HPn	.000	.000	.000	.000	.001	N/A	.000
HPNn	.000	.000	.000	.000	.000	.000	N/A
Sample size n=3							

6.4   Discussion

6.4.1   Strategy Novelty

Surgical site infection (SSI) is a common postoperative complication in surgery, which may cause serious consequent to patients in both finance and health. A routine and efficient way to prevent SSI is the application of antibiotics during the perioperative period, which mainly includes enteral administration and parenteral route. In the former class, there are three methods of administration including oral, sublingual, and rectal. Drugs given by enteral administration (except rectal way) are subjected to significant first pass metabolism through the liver, and the amount of drug entering the systemic circulation would vary significantly for different individuals and drugs [62]. In the parenteral course, drugs can be given through veins, arteries, muscles, spinal canal, and skins. After entering the systemic circulation, drugs will be distributed evenly in the blood stream around the whole body. Only a small fraction of drug molecules are delivered to sites where their actions are expected, and the rest can expose normal tissues to risk of side reactions.

The application of HNTs based drug delivery system can change this situation. Nitrofurantoin was used in this project as an example. On the one hand, NFT could be directly released from temporary body implants (like sutures, staples, glues and tapes) to sites of action, which can greatly improve drug efficiency. On the other hand, unnecessary exposure of NFT to regular tissues can be avoided, and patients will not suffer from any side reaction.

Another benefit of this strategy comes from the extension of drug application. In this project, NFT has good activity against many bacteria including *E. coli*, *S. aureus*, and *E. faecalis*, which are also included in the list of common pathogens for surgical site infection. Besides, NFT has a preference of bacterial cells over mammalian cells, and acquired resistance in sensitive bacteria is relatively rare. However, its clinical application is limited to urinary tract infection because of some limitations like low bioavailability, poor tissue penetration, and fast metabolism by liver [60]. By applying the strategy of directly delivering NFT to sites of action, all the above problems disappeared and NFT became a good alternative for the prevention of SSI.

6.4.2   Advantage of Layer-by-Layer Coating

In Chapter 4, three common methods have been compared, and the layer-by-layer technique showed better performance in both drug loading and releasing than the other two. Therefore, the LbL technique was used for the fabrication of HNT based drug delivery vehicle in this experiment. Theoretically, the built LbL structure on the outside surface of HNTs could be used to trap NFT molecules, and the more layers there were, the more molecules would be held inside the LbL base. Meanwhile, the release period would be extended correspondingly with the increased layers.

The LbL technique is an easy and cheap process with no specially required equipment. The drug layer could be placed anywhere inside the LbL structure according to the application goal. In this preliminary experiment, as NFT was the only tested drug, it was placed on the most outside layer to 1) achieve a burst release at the start of the release process and reach the required drug concentration for NFT's antibiotic action (MIC90 for *E. coli* is 32 ug/ml [63]), 2) avoid unnecessary loss of NFT in process of adding extra layers. What's more, one drug could be theoretically incorporated multiple times during the fabrication process, and more than one drug could be included in the LbL design.

6.4.3   Release Properties

An ideal drug delivery system should not release drugs too fast or too slow. Released drugs need to stay above a required concentration to take action, and the status should continue until achievement of the expected result. The HNTs based drug delivery system showed a potential for such properties in release tests. The main driving force for the NFT release was the concentration gradient between DI water and HNT/polymer nanoparticles. Once entering aqueous solution, NFT molecules started to move, and the net direction was from HNT to DI water, which was opposite to that in the fabrication process. This trend lasted until a balance was reached, where the net moving of NFT molecules stopped. After the replenishment with fresh DI water, a new concentration gradient, which was smaller than the prior one, formed between HNT and DI water leading to another cycle of NFT release. In this way, the release period was partially determined by the consuming rate of drugs by surrounding environment. The concentration gradient also determined the release rate, which could well explain the fast

release at the initial stage and slow release at the end. Besides, the LbL structure could

also affect the release process, as NFT molecules trapped between different layers might

present different release spans. Finally, by comparing the release results of

HNT/(PVP/PAA)$_9$/NFT and HNT/(PVP/PAA)$_9$/NFT/Nylon-6, the filling of coated HNT

into nylon-6 could help slow down rather than inhibit the release process. This property

enabled the HNT delivery system have more potential in nylon-6 based applications.

6.4.4   Anti-Proliferation Test with *E. coli*

In **Figure 6-7**, the increased OD$_{600}$ value in the control group, compared with the

initial, showed the bacterial growth during the past 6 hours. To avoid the sediment of

bacterial cells, no centrifuge operation was done with the samples. Although left standing

for a while, there were still some HNTs or coated HNTs suspending in the broth which

may affect the spectroscopic measurement of the bacterial density.

In the groups of HNTs and coated HNTs, their OD$_{600}$ values represented the

absorbance of both *E. coli* and HNTs or coated HNTs. Fortunately, in the group of

HNT/(PVP/PAA)$_9$/NFT whose OD$_{600}$ values was .128 ± .004, it suggested that the

increased OD$_{600}$ values caused by HNTs or coated HNTs should be smaller than .128.

Given the values in the group of HNTs (1.676 ± .013) and HNT/(PVP/PAA)$_9$ (1.224 ±

.011), the bacterial growth should not have been inhibit. Instead, the bacterial growth was

stimulated to increase to some degree. At least, both HNT and HNT/(PVP/PAA)$_9$were

not harmful to *E. coli*. Compared with the control group of *E. coli*, the decreased value in

group of HNT/(PVP/PAA)$_9$/NFT was caused only by the release of NFT. There was also

a significant decrease in the group of HNT/(PVP/PAA)$_9$ when compared with group of

HNT. The reason could be the pH change caused by polymer layers because they were

fabricated in a strong acid environment (pH=3), which compromised the stimulant effect of HNT on E. coli.

In the rest groups of nylon-6, HNT/(PVP/PAA)$_9$/Nylon-6, and HNT/(PVP/PAA)$_9$/NFT/Nylon-6, the values only represented the growth of bacteria as the coated HNT powders were filled in the nylon-6 matrices rather than suspended in the broth. The values in the group of nylon-6 were statistically the same as that of the control group, which proved that the nylon-6 disks in the broth did not affect the bacterial growth in the past six hours. Although formic acid has been reported to be very efficient in reducing the population of E. coli [64] and it was used to prepare the solution of nylon-6, the result in Group nylon-6 could well confirm the complete evaporation of formic acid during fabrication process.

On this basis, the slight decrease in the group of HNT/(PVP/PAA)$_9$/Nylon-6 could be due to the pH change caused by the coated polymers, and the huge difference between the group of HNT/(PVP/PAA)$_9$/NFT/Nylon-6 and the control was only caused by the released NFT. To be more specific, the spectroscopic value in the group of HNT/(PVP/PAA)$_9$/NFT/Nylon-6 (.046 ± .002) was just slightly higher than that of initial E. coli (.040) as NFT could well inhibit bacterial proliferation but not kill them.

6.4.5   Challenge

During the fabrication of layer-by-layer structure, the coated HNT particles could easily clump together, which may stop further coating of more layers. As seen in **Figure 6-3** (C) and (D), even after the process there were still a lot of HNTs staying uncoated. Therefore, more study is required to increase the ratio of coated HNT versus uncoated ones, which reserves a huge room for the drug loading improvement.

6.5   Conclusions

Halloysite nanotubes did not provoke a cytotoxic effect on *E. coli* cells nor inhibit their proliferation ability. Nitrofurantoin was incorporated into a PE coating and observed released from the coating. Released NFT resulted in a reduction in bacterial proliferation. After the NFT-coated HNTs were mixed with Nylon-6, the releasing ability of NFT was preserved, and the released NFT also inhibited bacterial proliferation. As a nanocomposite drug delivery system, NFT coated HNTs show a potential for the delivery of antibiotic drugs. While NFT was the drug used in this study, there is also a potential for the system to incorporate other drugs. The system also has the potential to insert drugs at different coating depths that may permit multiple, combinatorial or even sequential release depending on coating architecture and composition.

CHAPTER 7

CONCLUSIONS AND FUTURE WORK

7.1   Conclusions

In this dissertation, halloysite nanotubes were studied as nano-carriers to load and

release drugs (methotrexate and nitrofurantoin) for potential clinical applications. Three

common fabrication methods were compared including physical adsorption, vacuum

loading, and layer-by-layer coating. The drug loaded halloysite composites were filled

within nylon-6, and continuously provided a sustained release of loaded drugs. *In vitro*

osteosarcoma cell test and *in vitro E. coli* test confirmed the intact biological functions of

released drugs. In this way, the halloysite based drug delivery system showed a potential

medical application and provided another option for drug delivery.

Physical adsorption and vacuum loading are common methods used for HNT

fabrication, while layer-by-layer coating was studied as a novel method to prepare the

HNT based drug delivery vehicle. Methotrexate was used as the model drug to be

delivered, and the LbL coating method had better performance than the other two in both

loading and releasing. Therefore, LbL coating was used for drug loading in subsequent

experiments.

Osteosarcoma is the most common malignant bone cancer in children and

adolescents, and local relapse was a main cause of death after surgical remove of the

primary tumor mass. One important strategy is to prevent postoperative recurrence, which is the main target of the newly formed HNT-based drug delivery system. LbL technique was applied, and MTX was loaded within the LbL layers. Then the MTX coated HNTs composites were added within nylon-6 as fillers. Pure HNTs and HNT/PE/nylon composites did not provoke a cytotoxic effect on osteosarcoma cell nor inhibit their proliferation ability, but the released MTX caused significant decrease in cell proliferation. Even after the MTX coated HNTs were mixed within nylon-6, the releasing ability of MTX was preserved, and its anti-proliferation function was kept intact. As a nanocomposite drug delivery system, MTX coated HNTs showed a potential to deliver antitumor drugs directly to sites of action to prevent future relapse. The system also holds a potential to incorporate other drugs at different coating depths that may permit multiple, combinatorial, or even sequential release depending on coating architecture and composition.

Surgical site infection is a common and feared complication. It can cause considerable consequences for patients and high medical costs for society. One potential strategy to improve the current treatment result is to enhance the efficacy of routine antibiotics. The nitrofurantoin coated HNTs drug delivery system provides such an option. NFT coated HNTs presented a burst initial release followed by sustained mild drug liberations in DI water. After being filled in nylon-6, the releasing ability was preserved and the release became milder and longer. In the *in vitro* bacterial anti-proliferation test, the NFT coated HNT showed efficient inhibition on the bacterial growth, suggesting a potential in the prevention of SSI.

7.2 Future Work

7.2.1 Improving Loading Efficiency

Under routine laboratory condition, one hard challenge with the HNT fabrication is to improve the loading efficiency. In both **Figure 4-2** and **Figure 6-4**, it clearly showed that a big ratio of HNTs stayed uncoated after fabrication. Regular vortex machine and shaker cannot completely separate the nanoparticles after centrifuge, leaving them in clumps. Therefore, there is still a huge space for further coating, which holds a potential for increasing the drug loading ability. Maybe a high frequency sonicater is a possible solution? However, its impact on the layer-by-layer structure needs to be considered as well.

7.2.2 Tunable Layer-by-layer Fabrication

The layer-by-layer fabrication method is an easily controllable process, as each layer's coating is an independent process. Factors like polyelectrolytes, concentration, pH, and solvent can greatly impact the properties of the built layer-by-layer structure. It is potential to endow the LbL structure different properties by tuning these factors.

7.2.3 Multiple and Sequential Drug Delivery

Theoretically, there is little limitation in the layer-by-layer coating. The target drug could be coated at any depth within the LbL structure, and multiple drugs could be coated at different depths. Therefore, there is a potential for multiple and sequential drug delivery with the HNT based system. Further studies of the release profile for the sequential drug release will continue in Dr. Mills' lab.

7.2.4 *In Vivo* Animal Test

Preliminary *in vitro* tests with both osteosarcoma cells and *E. coli* have individually confirmed the feasibility of applying HNTs based drug delivery system in the treatment of cancer and surgical site infection. To further verify the hypothesis about the practical potential of HNT based drug delivery system, animal test is required. Potentially target medical supplies like bone cement, sutures, and tissue scaffold could be made through technologies including electrospinning, electrospray, and 3-D printing. Chemotherapeutics, antibiotics, and hormones could be loaded with HNT based system and then filled within aforementioned medical products. Animal models are planned to test the feasibility of drug delivery through HNT based systems.

This dissertation presents three simple methods for drug delivery with halloysite nanotubes. Two preliminary *in vitro* tests were showed to foresee potentially future application in medical field. I hope these studies could provide another option for the research in drug delivery.

REFERENCES

[1] Y. S. Chaudhari, "Nanoparticles-A paradigm for topical drug delivery," *Chronicles of Young Scientists*, vol. 3, no. 1, pp. 82-85, 2012.

[2] M. M. Amiji, "Nanotechnology-improving targeted delivery," *Drug Delivery*, vol. 17, pp. 53-56, 2007.

[3] S. K. Sahoo, S. Parveen and J. J. Panda, "The present and future of nanotechnology in human health care," *Nanomedicine: Nanotechnology, Biology and Medicine*, vol. 3, no. 1, pp. 20-31, 2007.

[4] J. Shi, A. R. Votruba, O. C. Farokhzad and R. Langer, "Nanotechnology in drug delivery and tissue engineering: from discovery to applications," *Nano Letters*, vol. 10, no. 9, pp. 3223-3230, 2010.

[5] V. K. Khanna , "Targeted delivery of nanomedicines," *ISRN Pharmacology*, vol. 2012, 2012.

[6] A. D. Bangham and R. W. Horne, "Negative staining of phospholipids and their structural modification by surface-active agents as observed in the electron microscope," *Journal of Molecular Biology*, vol. 8, no. 5, pp. 660IN2-668IN10, 1964.

[7] X. Cao, W. Deng, M. Fu, Y. Zhu , H. Liu, L. Wang, J. Zeng, Y. Wei, X. Xu and J. Yu, "Seventy-two-hour release formulation of the poorly soluble drug silybin based on porous silica nanoparticles: in vitro release kinetics and in vitro/in vivo correlations in beagle dogs," *European Journal of Pharmaceutical Sciences*, vol. 48, no. 1, pp. 64-71, 2013.

[8] R. Ghaffarian, T. Bhowmick and S. Muro, "Transport of nanocarriers across gastrointestinal epithelial cells by a new transcellular route induced by targeting ICAM-1," *Journal of Controlled Release*, vol. 163, no. 1, pp. 25-33, 2012.

[9] L. Zhang, H. Xue, Z. Cao, A. Keefe, J. Wang and S. Jiang, "Multifunctional and degradable zwitterionic nanogels for targeted delivery, enhanced MR imaging, reduction-sensitive drug release, and renal clearance," *Biomaterials*, vol. 32, no. 20, pp. 4604-4608, 2011.

[10] U. Prabhakar, H. Maeda, R. K. Jain, E. M. Sevick-Muraca, W. Zamboni, O. C. Farokhazd, S. T. Barry, A. Gabizon, P. Grodzinski and D. C. Blakey, "Challenges and key considerations of the enhanced permeability and retention effect for nanomedicine drug delivery in oncology," *Cancer Research*, vol. 73, no. 8, pp. 2412-2417, 2013.

[11] J. Kreuter, "Nanoparticles – a historical perspective," *International Journal of Pharmaceutics*, vol. 331, no. 1, pp. 1-10, 2007.

[12] R. Bazak, M. Houri, S. El Achy, W. Hussein and T. Refaat, "Passive targeting of nanoparticles to cancer: a comprehensive review of the literature," *Molecular and Clinical Oncology*, vol. 2, no. 6, pp. 904-908, 2014.

[13] Q. Miao, S. Li, S. Han, Z. Wang, Y. Wu and G. Nie, "Construction of hydroxypropyl-β-cyclodextrin copolymer nanoparticles and targeting delivery of paclitaxel," *Journal of Nanoparticle Research*, vol. 14, no. 8, pp. 1-14, 2012.

[14] T. Sugiyama, T. Asai, Y. M. Nedachi, Y. Katanasaka, K. Shimizu, N. Maeda and N. Oku, "Enhanced active targeting via cooperative binding of ligands on liposomes to target receptors," *PLOS One*, vol. 8, no. 6, p. e67550, 2013.

[15] R. Duncan, "Polymer conjugates as anticancer nanomedicines," *Nature Reviews Cancer*, vol. 6, no. 9, pp. 688-701, 2006.

[16] S. Bai, C. Thomas, A. Rawat and F. Ahsan, "Recent progress indendrimer-based nanocarriers," *Therapeutic Drug Carrier Systems*, vol. 23, no. 6, 2006.

[17] A. Ghebaur, S. A. Garea and H. Lovu, "New polymer–halloysite hybrid materials—potential controlled drug release system," *International Journal of Pharmaceutics*, vol. 436, no. 1-2, pp. 568-573, 2012.

[18] E. Abdullayev and Y. Lvov, "Halloysite clay nanotubes as a ceramic "skeleton" for functional biopolymer composites with sustained drug release," *Journal of Materials Chemistry B*, vol. 1, no. 23, pp. 2894-2903, 2013.

[19] R. Kamble, M. Ghag, S. Gaikawad and B. K. Panda, "Halloysite nanotubes and applications: a review," *Journal of Advance Scientific Research*, vol. 3, no. 2, 2012.

[20] D. Rawtani and Y. K. Agrawal, "Multifarious applications of halloysite nanotubes: a review," *Rev.Adv.Mater.Sci*, vol. 30, pp. 282-295, 2012.

[21] J. J. Richardson, M. Bjommalm and F. Caruso, "Technology-driven layer-by-layer assembly of nanofilms," *Science*, vol. 348, no. 6233, p. aaa2491, 2015.

[22] R. K. Iler, "Multilayers of colloidal particles," *Journal of Colloid and Interface Science*, vol. 21, no. 6, pp. 569-594, 1966.

[23] G. Decher and J.-D. Hong, "Buildup of ultrathin multilayer films by a self-assembly process, consecutive adsorption of anionic and cationic bipolar amphiphiles on charged surfaces," *Makromolekulare Chemiem. Macromolecular Symposia*, vol. 46, no. 1, pp. 321-327, 1991.

[24] A. Laschewsky, E. Wischerhoff, S. Denzinger, H. Ringsdorf, A. Declorte and P. Bertrand, "Molecular recognition by hydrogen bonding in polyelectrolyte multilayers," *Chemistry-A European Journal*, vol. 3, no. 1, pp. 34-38, 1997.

[25] N. A. Kotov, I. Dekany and J. H. Fendler, "Layer-by-layer self-assembly of polyelectrolyte-semiconductor nanoparticle composite films," *The Journal of Physical Chemistry*, vol. 99, no. 35, pp. 13065-13069, 1995.

[26] Y. Shimazaki, M. Mitsuishi, S. Ito and M. Yamamoto, "Preparation of the layer-by-layer deposited ultrathin film based on the charge-transfer interaction," *Langmuir*, vol. 13, no. 6, pp. 1385-1387, 1997.

[27] N. Cini, T. Tulun, G. Decher and V. Ball, "Step-by-step assembly of self-patterning polyelectrolyte films violating (almost) all rules of layer-by-layer deposition," *Journal of the American Chemical Society*, vol. 132, no. 24, pp. 8264-8265, 2010.

[28] H. Ai, S. A. Jones and Y. M. Lvov, "Biomedical applications of electrostatic layer-by-layer nano-assembly of polymers, enzymes, and nanoparticles," *Cell Biochemistry and Biophysics*, vol. 39, no. 1, pp. 23-43, 2003.

[29] Z. Tang, N. A. Kotov, S. Magonov and B. Ozturk, "Nanostructured artificial nacre," *Nature Materials*, vol. 2, no. 6, pp. 413-418, 2003.

[30] G. Decher and J. B. Schlenoff, Multilayer thin films - sequential assembly of nanocomposite materials, *John Wiley & Sons*, 2006.

[31] K. Ando, M.-F. Heymann, V. Stresing, k. Mori, F. Redini and D. Heymann, "Current therapeutic strategies and novel approaches in osteosarcoma,"

Cancers, vol. 5, no. 2, pp. 591-616, 2013.

[32] P. A. Meyers and R. Gorlick, "Osteosarcoma," *Pediatric Clinics of North America*, vol. 44, no. 4, pp. 973-989, 1997.

[33] C. A. Stiller, "International patterns of cancer incidence in adolescents," *Cancer Treatment Reviews*, vol. 33, no. 7, pp. 631-645, 2007.

[34] A. B. Boyer, The Lectures of Boyer Upon Diseases of the Bone, James Humphreys, 1805.

[35] N. Jaffe, A. Puri and H. Gelderblom, "Osteosarcoma: evolution of treatment paradigms," *Sarcoma*, 2013.

[36] D. C. Dahlin and M. B. coventry, "Osteogenic sarcoma," *J Bone Joint Surg Am*, vol. 49, no. 1, pp. 101-110, 1967.

[37] R. C. Marcove, V. Mike, J. V. Hajek, A. G. Levin and R. V. Hutter, "Osteogenic sarcoma under the age of twenty-one," *J bone Joint Surg Am*, vol. 52, no. 3, pp. 411-423, 1970.

[38] D. C. Allison, S. C. Carney, E. R. Ahlmann, A. Hendifar, S. Chawla, A. Fedenko , C. Angeles and L. R. Menendez, "A meta-analysis of osteosarcoma outcomes in the modern medical era," *Sarcoma*, 2012.

[39] P. Harrington, "Prevention of surgical site infection.," *Nursing JStandard*, vol. 28, no. 48, pp. 50-58, 2014.

[40] W. J. Martone, W. R. Jarvis , D. H. Culver and R. W. Haley, "Incidence and nature of endemic and epidemic nosocomial infections," *Hospital Infections*, Vols. 3rd ed Boston: Little, Brown and Co, pp. 577-596, 1992.

[41] G. de Lissovoy, K. Fraeman, V. Hutchins, D. Murphy, D. Song and B. B. Vaughn, "Surgical site infection: Incidence and impact on utilization and treatment costs," *American Journal of Infection Control*, vol. 37, no. 5, pp. 387-397, 2009.

[42] B. Allegranzi, S. B. Nejad, c. Combescure, W. Graafmans, H. Attar, L. Donaldson and D. Pittet, "Burden of endemic healthcare associated infection in developing countries: systematic review and meta-analysis," *The Lancet*, vol. 377, no. 9761, pp. 228-241, 2011.

[43] G. Ducel, J. Fabry and L. Nicolle, "Prevention of hospital-acquired infections: A practical guide," *Prevention of Hospital Acquired Infections a Practical*

Guide, vol. Ed 2, 2002.

[44] A. K. Reckhenrich, B. M. Kirsch, E. A. Wahl, T. L. Schenck, F. Rezaeian, Y. Harder, P. Foehr, H.-G. Machens and J. T. Egana, "Surgical sutures filled with adipose-derived stem cells promote wound healing," *Plos One*, vol. 9, no. 3, p. e91169, 2014.

[45] F. D. Matl, J. Zlotnyk, A. Obermeier, W. Friess, S. Vogt, H. Buchner, H. Schnabelrauch, A. Stemberger, A. Stemberger and K.-D. Kuhn, "New anti-infective coatings of surgical sutures based on a combination of antiseptics and fatty acids," *Journal of Biomaterials Science, Polymer Edition*, vol. 20, no. 10, pp. 1439-1449, 2009.

[46] G. Tiwari, R. Tiwari, B. Sriwastawa, L. Bhati, S. Pandey, P. Pandey and S. K. Bannerjee, "Drug delivery systems: An updated review," *International Journal of Pharmaceutical Investigation*, vol. 2, no. 1, pp. 2, 2012.

[47] V. Vergaro, Y. M. Lvov and S. Leporatti, "Halloysite clay nanotubes for resveratrol delivery to cancer cells," *Macromolecular bioscience*, vol. 12, no. 9, pp. 1265-1271, 2012.

[48] L. Sun, C. Boyer, R. Grimes and D. K. Mills, "Drug coated clay nanoparticles for delivery of chemotherapeutics," *Current Nanoscience*, vol. 12, no. 2, pp. 207-214, 2016.

[49] D. G. Shchukin and H. Mohwald, "Surface-engineered nanocontainers for entrapment of corrosion inhibitors," *Advanced functional Materials*, vol. 17, no. 9, pp. 1451-1458, 2007.

[50] N. Jaffe, "Osteosarcoma: review of the past, impact on the future," *Pediatric and Adolescent Osteosarcoma*, pp. 239-262, 2009.

[51] R. J. McKenna , C. P. Schwinn, K. Y. Soong and N. L. Higinbotham, "Sarcomata of the osteogenic series (osteosarcoma, fibrosarcoma, chondrosarcoma, parosteal osteogenic sarcoma, and sarcomata arising in abnormal bone)," *The Journal of Bone & Joint Surgery*, vol. 48, no. 1, pp. 1-26, 1966.

[52] M. P. Link, A. M. Goorin, A. W. Miser, A. A. Green, C. B. Pratt, J. B. Belasco, J. Pritchard, j. S. Malpas, A. R. Baker, J. A. Kirkpatrick and A. G. Ayala, "The effect of adjuvant chemotherapy on relapse-free survival in patients with osteosarcoma of the extremity," *New England Journal of Medicine*, vol. 314, no. 25, pp. 1600-1606, 1986.

[53] G. Tari, L. Bobos, C. S. Gomes and J. M. Ferreira, "Modification of surface charge

properties during kaolinate to halloysite-7A transformation," *Journal of colloid and Interface Sciences*, vol. 210, no. 2, pp. 360-366, 1999.

[54] E. Abdullayev, A. Joshi, W. Wei, Y. Zhao and Y. M. Lvov, "Enlargement of halloysite clay nanotube lumen by selective etching of aluminum oxide," *ACS Nano*, vol. 6, no. 8, pp. 7216-7226, 2012.

[55] N. G. Veerabadran, P. L. Goli, S. S. Stewart-Clark, Y. M. Lvov and D. K. Mills, "Nanoencapsulation of stem cells within polyelectrolyte multilayer shells. Macromol," *Macromolecular Bioscience*, vol. 7, no. 7, pp. 877-882, 2007.

[56] H. J. McDonald and R. H. Spitzer, "Polyvinylpyrrolidone: The electromigration characteristics of the blood plasma expander," *Circulation Research*, vol. 1, no. 5, pp. 396-404, 1953.

[57] A. Seehuber, D. Schmidt and R. Dahint, "Poly(acrylic acid)-poly(ethylene glycol) layers on positively charged surface coatings: molecular structure, protein resistance, and application to single protein deposition." *Langmuir*, vol. 28, no. 23, pp. 8700-8710, 2012.

[58] J. L. Alfonso, S. B. Pereperez, J. M. Canoves, M. M. Martinez, I. M. Martinez and J. m. Martin-Moreno, "Are we really seeing the total costs of surgical site infection? A Spanish study," *Wound Repair and Regeneration*, vol. 15, no. 4, pp. 474-481, 2007.

[59] A. Giacometti, O. Cirioni, A. M. Schimizzi, D. Prete, M. S, F. Barchiesi and M. M. Derrico, "Epidemiology and Microbiology of Surgical Wound Infections. Journal of Clinical Microbiology," *Journal of Clinical Microbiology*, vol. 38, no. 2, pp. 918-922, 2000.

[60] "Nitrofurantoin," Wikipedia, [Online]. Available: https://en.wikipedia.org/wiki/Nitrofurantoin.

[61] J. Fang, X. Wang and T. Lin, "Functional applications of electrospun nanofibers," *InTech-Open Access Publisher*, 2011.

[62] "Enteral Administration," Wikipedia, [Online]. Available: https://en.wikipedia.org/wiki/Enteral_administration.

[63] M. Maaland and L. Guardabassi, "In vitro antimicrobial activity of nitrofurantoin against Escherichia coli and Staphylococcus pseudintermedius isolated from dogs and cats," *Veterinary Microbiology*, vol. 151, no. 3, pp. 396-

399, 2011.

[64] M. Raftari, F. Jalilian, A. S. Abdulamir, R. Son, Z. Sekawi and A. B. Fatimah, "Effect of organic acids on Escherichia coli o157:h7 and staphylococcus aureus contaminated meat," *Open Microbiology Journal,* vol. 3, pp. 121-127, 2009.

[65] K. K. Jain, The handbook of nanomedicine, *Springer Science & Business Media,* 2012.

[66] "Report: nanomedicine market to surpass $160 billion by 2015," Occupational Health & Safety , 29 6 2009. [Online]. Available: http://ohsonline.com/articles/2009/06/29/report-on-nanomedicine-market.aspx . [Accessed 1 6 2010].

[67] V. Wagner, A. Dullaart, A.-K. Bock and A. Zweck, "The emerging nanomedicine landscape," *Nature Biotechnology,* vol. 24, no. 10, pp. 1211-1217, 2006.

[68] L. Zhang, F. X. Gu, J. M. Chan, A. Z. Wang, R. S. Langer and O. C. Farokhzad, "Nanoparticles in medicine: therapeutic applications and developments," *Clinical Pharmacology and therapeutics,* vol. 83, no. 5, pp. 761-769, 2008.

[69] M. E. Davis and D. M. Shin, "Nanoparticle therapeutics: an emerging treatment modality for cancer," *Nature Reviews Drug Discovery,* vol. 7, no. 9, pp. 771-782, 2008.

[70] K. Greish, "Enhanced permeability and retention of macromolecular drugs in solid tumors: a royal gate for targeted anticancer nanomedicines," *Journal of Drug Targeting,* vol. 15, no. 7-8, pp. 457-464, 2007.

[71] H. Maeda, "Vascular permeability in cancer and infection as related to macromolecular drug delivery, with emphasis on the EPR effect for tumor-selective drug targeting," *Proceedings of the Japan Academy, Series B,* vol. 88, no. 3, pp. 53-71, 2012.

[72] K. Cho, X. Wang, S. Nie, Z. Chen and D. M. Shin, "Therapeutic nanoparticles for drug delivery in cancer," *Clinical Cancer Research,* vol. 14, no. 5, pp. 1310-1316, 2008.

[73] M. Talekar, J. Kendall, W. Denny and S. Garg, "Targeting of nanoparticles in cancer: drug delivery and diagnostics," *Anti-Cancer Drugs,* vol. 22, no. 10, pp. 949-962, 2011.

[74] V. P. Torchilin, "Recent advances with liposomes as pharmaceutical carriers," *Nature Reviews Drug Discovery*, vol. 4, no. 2, pp. 145-160, 2005.

[75] R. M. Schiffelers, M. Banciu, J. M. Metselaar and G. Storm, "Therapeutic application of long-circulating liposomal glucocorticoids in auto-immune diseases and cancer," *Journal of Liposome Research*, vol. 16, no. 3, pp. 185-194, 2006.

[76] N. Nishiyama and K. Kataoka, "Current state, achievements,and future prospects of polymeric micelles as nanocarriers fordrug and gene delivery," *Pharmacology & Therapeutics*, vol. 112, no. 3, pp. 630-648, 2006.

[77] S. Shidhaye, V. Lotlikar, S. Malke and V. Kadam, "Nanogel engineered polymeric micelles for drug delivery," *Current Drug Therapy*, vol. 3, no. 3, pp. 209-217, 2008.

[78] M. F. Francis, M. Cristea and F. M. Winnik, "Polymeric micelles for oral drug delivery: why and how," *Pure and Applied Chemistry*, vol. 76, no. 7-8, pp. 1321-1335, 2004.

[79] K. S. Soppimath, T. M. Aminabhavi, A. R. Kulkami and W. E. Rudzinski, "Biodegradable polymeric nanoparticles as drug delivery devices," *Journal of controlled Release*, vol. 70, no. 1, pp. 1-20, 2001.

[80] J. W. Park, C. C. Benz and F. J. Martin, "Future directions of liposome- and immunoliposome-based cancer therapeutics," *Seminars in Oncology*, vol. 31, pp. 196-205, 2004.

[81] T. M. Allen, "Ligand-targeted therapeutics in anticancer therapy," *Nature Review Cancer*, vol. 2, no. 10, pp. 750-763, 2002.

[82] H. Jung, T. Yang, M. D. Lasagna, J. Shi, G. D. Reinhart and P. S. Cremer, "Impact of hapten presentation on antibody binding at lipid membrane interfaces," *Biophysical Journal*, vol. 94, no. 8, pp. 3094-3103, 2008.

[83] G. Bacci, S. Ferrari, F. Bertoni, P. Ruggieri, P. Picci, A. longhi, R. Casadei, N. Fabbri, C. Forni, M. Versari and M. Campanacci, "Long-term outcome for patients with nonmetastatic osteosarcoma of the extremity treated at the istituto ortopedico rizzoli according to the istituto ortopedico rizzoli/osteosarcoma-2 protocol: An updated report," *Journal of Clinical Oncology*, vol. 18, no. 24, pp. 4016-4027, 2000.

[84] L. Kager, A. Zoubek, U. Potschger, U. Kastner, S. Flege, B. Kempf-Bielack, D. Branscheid , R. Kotz, M. Salzer-Kuntschik, W. Winkelmann and G. Jundt, "Primary metastatic osteosarcoma: Presentation and outcome of

patients treated on neoadjuvant cooperative osteosarcoma study group protocols," *Journal of Clinical Oncology*, vol. 21, no. 10, pp. 2011-2018, 2003.

[85] S. Bielack, B. kempf-Bielack, D. Schwenzer, T. Birkfellner, G. Delling, V. Ewerbeck, G. U. Exner, N. Fuchs, U. Gobel, N. Graf and U. Heise , "Results from the cooperative osteosarcoma study group coss of 925 patients," *Klinische Padiatrie*, vol. 211, no. 4, pp. 260-270, 1998.

[86] E. Joussein, S. Petit, J. Churchman, B. Theng, D. Righi and B. Delvaux, "Halloysite clay minerals - a review," *Clay Minerals*, vol. 40, no. 4, pp. 383-426, 2005.

[87] R. Price, B. Gaber and Y. Lvov, "Release characteristics of tetracycline, khellin and nad from halloysite: a cylindrical mineral for delivery of biologically active agents," *J. Microencapsul*, vol. 18, pp. 713-723, 2001.

[88] S. R. Levis and P. B. Deasy, "Characterization of halloysite for use as a microtubular drug delivery system," *International Journal of Pharmaceutics*, vol. 243, no. 1, pp. 125-134, 2002.

[89] Y. Lvov and E. Abdullayev, "Functional polymer-clay nanotube composites with sustained release of bioactive agents," *Progress in Polymer Science*, vol. 38, no. 10, pp. 1690-1719, 2013.

[90] L. Guimaraes, A. N. Enyashin, G. Seifert and H. A. Duarte, "Structural, electronic, and mechanical properties of single-walled halloysite nanotube models," *The Journal of Physical Chemistry*, vol. 114, no. 26, pp. 11358-11363, 2010.

[91] K. Hedicke-Hochstotter, G. T. Lim and V. Altstadt, "Novel polyamide nanocomposites based on silicate nanotubes of the mineral halloysite," *Composites Science and Technology*, vol. 69, no. 3, pp. 330-334, 2009.

[92] D. G. Shchukin, G. B. Sukhorukov, R. R. Price and Y. M. Lvov, "Halloysite nanotubes as biomimetic nanoreactors," *Small*, vol. 1, no. 5, pp. 510-513, 2005.

[93] N. G. Veerabadran, R. R. Price and Y. M. Lvov, "Clay nanotubes for encapsulation and sustained release of drugs," *Nano*, vol. 2, no. 02, pp. 115-120, 2007.

[94] S. Karnik and D. K. Mills, "Clay nanotubes as growth factor delivery vehicle for bone tissue engineering," *J Nanomed Nanotechnol*, vol. 4, p. 104, 2013.

[95] X. Qiu, S. Leporatti, E. Donath and H. Mohwald, "Studies on the drug release properties of resveratrol polysaccharide multilayers encapsulated ibuprofen microparticles," *Langmuir*, vol. 17, no. 17, pp. 5375-5380, 2001.

[96] A. S. Zahr, M. d. Villiers and M. V. Pishko, "Encapsulation of drug nanoparticles in self-assembled macromolecular nanoshells," *Langmuir*, vol. 21, no. 1, pp. 403-410, 2005.

[97] C. Gao, X. Liu, J. Shen and H. Mohwald, "Spontaneous deposition of horseradish peroxidase into polyelectrolyte multilayer capsules to improve its activity and stability," *Chemical Communications*, vol. 17, pp. 1928-1929, 2002.

[98] V. Vergaro, E. Abdullayev, Y. M. Lvov, A. Zeitoun, R. Cingolani, R. Rinaldi and S. Leporatti, "Cytocompatibility and uptake of halloysite clay nanotubes," *Biomacromolecules*, vol. 11, no. 3, pp. 820-826, 2010.

[99] D. S. Kommireddy, I. Ichinose, Y. M. Lvov and D. K. Mills, "Nanoparticle multilayers: surface modification for cell attachment and growth," *Journal of Biomedical Nanotechnology*, vol. 1, no. 3, pp. 286-290, 2005.

[100] N. Jaffe and R. Gorlick, "High-dose methotrexate in osteosarcoma: let the questions surcease—time for final acceptance," *Journal of Clinical Oncology*, vol. 26, no. 27, pp. 4365-4366, 2008.

[101] W. Wei, E. Abdullayev, A. Hollister, D. Mills and Y. M. Lvov, "Clay nanotube/poly(methyl methacrylate) bone cement composite with sustained antibiotic release," *Macromolecular Materials and Engineering*, vol. 297, no. 7, pp. 645-653, 2012.

[102] M. Liu, B. Guo, M. Du, X. Cai and D. Jia, "Properties of halloysite nanotube–epoxy resin hybrids and the interfacial reactions in the systems," *Nanotechnology*, vol. 18, no. 45, p. 455703, 2007.

[103] T. E. Barnett, "The cot-so-hidden costs of surgical site infections," *AORN Journal*, vol. 86, no. 2, pp. 249-258, 2007.